Ryerson University
Digital Commons @ Ryerson

Theses and dissertations

1-1-2005

Liquid distribution and its effect on local mass transfer in a packed column of Pall rings

Yongjia Zhu
Ryerson University

Follow this and additional works at: http://digitalcommons.ryerson.ca/dissertations

 Part of the Chemical Engineering Commons

Recommended Citation
Zhu, Yongjia, "Liquid distribution and its effect on local mass transfer in a packed column of Pall rings" (2005). *Theses and dissertations.* Paper 417.

This Thesis is brought to you for free and open access by Digital Commons @ Ryerson. It has been accepted for inclusion in Theses and dissertations by an authorized administrator of Digital Commons @ Ryerson. For more information, please contact bcameron@ryerson.ca.

LIQUID DISTRIBUTION AND ITS EFFECT ON LOCAL MASS TRANSFER IN A PACKED COLUMN OF PALL RINGS

By

Yongjia Zhu, BSc

Nanjing University of Chemical Technology

Nanjing, China, 1992

A thesis

presented to Ryerson University

in partial fulfillment of the

requirements for the degree of

Master of Applied Science

In the Program of

Chemical Engineering

Toronto, Ontario, Canada, 2005

© Yongjia Zhu 2005

PROPERTY OF
RYERSON UNIVERSITY LIBRARY

UMI Number: EC53791

INFORMATION TO USERS

The quality of this reproduction is dependent upon the quality of the copy submitted. Broken or indistinct print, colored or poor quality illustrations and photographs, print bleed-through, substandard margins, and improper alignment can adversely affect reproduction.

In the unlikely event that the author did not send a complete manuscript and there are missing pages, these will be noted. Also, if unauthorized copyright material had to be removed, a note will indicate the deletion.

UMI®

UMI Microform EC53791
Copyright 2009 by ProQuest LLC
All rights reserved. This microform edition is protected against unauthorized copying under Title 17, United States Code.

ProQuest LLC
789 East Eisenhower Parkway
P.O. Box 1346
Ann Arbor, MI 48106-1346

Author's Declaration

I hereby declare that I am the sole author of this thesis.

I authorize the Ryerson University to lend this thesis to other institutions or individuals for the purpose of scholarly research.

I further authorize Ryerson University to reproduce this thesis by photocopying or by other means, in total or in part, at the request of other institutions or individuals for the purpose of scholarly research.

Abstract

Liquid distribution and its effect on local mass transfer in a packed column of Pall rings

Yongjia Zhu MASc, Chemical Engineering, Ryerson University, 2005

The spatial variations of liquid distribution and local mass transfer coefficient in a 0.30-m column of 25.4-mm Pall rings were investigated. The data of liquid distribution was collected with a 39-cell liquid collector and a wall-flow tube from a doubled-wall section in the column at the packing-support level. The local mass transfer coefficients were measured via the electrochemical technique by individual cathodic nickel-coated Pall rings placed at various spatial positions. Both measurements were conducted at various fluid flow rates with three liquid distributor designs at different bed heights. Liquid distribution and local mass transfer coefficients observed were far from uniform in the column. The wall flow developed along the packed bed until a fully developed flow pattern was reached. With more uniform initial liquid distribution, the less packing height needed to reach the fully developed flow pattern along with higher the mass transfer efficiency in the column. Ladder-type liquid distributor (LLD) showed less angular effect in measurements. Increasing the liquid flow rate slightly improved the uniformity of liquid distribution and enhanced the mass transfer. No influence of gas flow rate on liquid distribution and mass transfer coefficient was found at the range of gas flow rates used. These gas flow rates were much lower than the loading point. Liquid maldistribution factor (M_f) and mass transfer maldistribution factor (MT_{VAR}) decreased with increases in the uniformity of the initial liquid distribution. The values of M_f (MT_{VAR}) were 0.21(0.48), 0.16(0.26) and 0.14(0.22) for single-point liquid distributor (SPLD), cross-type liquid distributor (CLD) and LLD, respectively. By comparison, a good agreement was observed on the relation of M_f and MT_{VAR}.

Acknowledgements

It is difficult to overstate my gratitude to Dr. Huu Doan for his guidance and patience on my thesis during the past years. I would also like to thank Dr. Ali Lohi for serving on the supervision for this thesis.

I am very grateful for the invaluable assistance provided by Peter Scharping and Ali Hemmati during the equipment manufacture and system setup.

I am also indebted to Dr. Dang Vu Trong for some ideas on the data analysis.

Table of Contents

List of Tables

List of Figures

1. Introduction

Inter-phase transport is of fundamental importance in chemical and environmental processes. Among many means available to facilitate inter-phase transport, a random packed column is one of the most common-used devices, especially for mass transport. With the physical simplicity, it has been widely used in many chemical processes such as distillation, absorption and catalytic reaction, etc. Its higher mass transfer efficiency, lower pressure drop, and lower liquid hold-up than a tray column are some of the advantages of the packed column. However, in a packed column the mass transport behavior varies from one location to another due to the complicity of hydrodynamic behavior near the particle-fluid interface. Thus, the study on fluid flow distribution in the column is widely used to predict and evaluate the performance of a packed column. Although the fluid flow distribution inside the packed column can to some extent reflect how the column performs, the performance of the packed column can only be assessed by the final analysis on the mass transfer efficiency.

Many factors may affect liquid distribution including fluid flow patterns, column and packing characteristics, initial fluid distribution, fluid redistribution, fluid physical properties and operational conditions, etc. In practice, these factors interact with each other, and thus, it makes the situation more complicated. In fact, the effects of these parameters on mass transfer coefficients are implicitly included in the experimental data and usually lumped into empirical correlations represented by the dimensionless groups.

Although an overall mass transfer coefficient is widely used in packed column design, it only represents a composite of the distribution of local phenomena. Study on local phenomena is of practical importance because the local mass

transfer distributed within the packings is non-uniform. The knowledge of this non-uniform mass transfer behavior is helpful on fully understanding the mass transfer in packed columns. Although the subject of local phenomenon in a packed bed has received increased attention in recent years, many questions still remain unresolved, especially on liquid distribution and its effect on local mass transfer in a packed column, which has not been adequately investigated.

The aim of the present study is to investigate liquid distribution and its effect on local mass transfer coefficient at various axial, radial and angular locations throughout a packed column. More specifically, the objectives of the present study are to investigate the liquid distribution, the development of wall flow, and the distribution of local mass transfer coefficients for different initial liquid distributions, liquid and gas flow rates in a pilot-scale packed column of 25.4-mm Pall rings.

2. Literature Survey

2.1. Liquid Distribution in Packed Columns

In a packed column, the flow pattern can be under different regimes, such as: trickling flow, pulsing flow, full liquid flow and fluidized flow. One flow pattern may change to another by changing the flow conditions in the column.

In general, fluid distribution in packed columns is not uniform, especially for liquid phase. Liquid maldistribution, categorized as large-scale maldistribution or small-scale maldistribution, is usually used to evaluate the liquid distribution in a packed column. Large-scale liquid maldistribution characterized by liquid wall flow and non-uniform initial liquid distribution are the main reason for the loss of mass transfer efficiency found in practice, especially for large-diameter packed columns[1]. However, small-scale liquid maldistribution was considered as an inherent property of the packing and its adverse effect on mass transfer efficiency might be compensated by radial mixing. Although much work [1-5] was carried out on small-scale liquid maldistribution, good rational interpretation of the underlying mechanism has not been reported.

A traditional method [1,2,6-11], which uses a specially designed collecting vessel installed below the packing bed to collect liquid falling down, has been utilized to study liquid distribution. This method has been widely used due to its simplicity and direct measurement although it can only be used in liquid downflow configuration.

Other methods have also been used for this purpose, such as: tracing methods [12-18], conductance probes [19,20], and tomographic measurement

techniques [21-24]. Although some of them have special features such as instantaneous measurement (with conductance technique), accurate measurement (with tomography technique), the complicated measurement systems limit their application. In the present study, the liquid collecting method was used to investigate liquid distribution in a packed column of Pall rings.

The factors, which may affect the quality of liquid distribution in a packed column, can be categorized as follows:

- quality of the initial fluid distribution in the packed column (e.g. distributor design, distributor installation, distributor corrosion, plugging and damage),
- characteristics of the packed column (e.g. packing height),
- operational conditions (e.g. liquid & gas loads and operational pressure),
- characteristics of packing elements (e.g. type, size and material), and
- liquid physical properties (e.g. surface tension and viscosity), etc.

The quality of liquid distribution can be defined in many ways. Usually, liquid maldistribution factor, M_f, is used to assess the quality of liquid distribution. Eq. 2-1 is one of the M_f forms defined in the literature [25] and was applied in the present study.

$$M_f = \frac{1}{n}\sqrt{\sum_{i=1}^{n}\left(1-\frac{Q_i}{Q_{av}}\right)^2} \qquad \text{Eq. 2-1}$$

where n is the total number of collecting cells in the liquid collecting device, Q_i is the volumetric flow rate to the i^{th} collecting cell, and Q_{av} is the mean value of volumetric flow rate for all collecting cells.

In principle, M_f is equal to zero for the perfectly uniform liquid distribution (i.e. $Q_i = Q_{av}$) over the column cross section and increases when liquid maldistribution increases.

2.1.1. Initial Fluid Distribution

One of the major problems for scale-up is the quality of initial fluid distribution, especially for large-diameter packed columns. In some researches [10,26] the initial fluid distribution was assumed to be uniform and its effect was ignored. Obviously, this assumption is not valid. The assumption of a uniform initial fluid distributor will lead to inaccuracy in the conclusion drawn from the experimental data.

As early as 1935, Baker *et al.* [27] studied liquid distribution in a 0.3-m-ID column packed with spheres and saddles in the absence of gas flow. They observed that liquid was severely maldistributed and the initial liquid distribution was a key factor affecting the liquid distribution in whole height of the packed bed.

Veer *et al.* [28] studied the influence of the initial liquid distribution on the efficiency of a column packed with ceramic Raschig rings using an air/water countercurrent system. The authors reported that the liquid maldistribution decreased with increases in the number of distribution points per square meter until a constant value reached (i.e. 75 points per square meter). This finding agrees with that of Billet [29]. In addition, Hoek *et al.* [1] pointed out that an equilibrium flow pattern would be established after traversing a certain bed depth whichever liquid distributor was used.

Using a 0.5-m diameter column filled with 25-mm plastic Pall rings, Kouri and Sohlo [7] investigated the development of liquid flow patterns for two different

initial liquid distributions. It was found that a stable liquid distribution was reached faster for a better initial liquid distribution. That is, along the bed, the radial dispersion with a relative uniform initial liquid distribution was faster than that with a less-uniform initial liquid distribution. Similar studies on the development of liquid flow patterns along the bed depth were also reported by Sun *et al.* [30], Song *et al.* [31] and Yin *et al.* [12,14].

It should be noted that the loss of the overall mass transfer efficiency for the non-uniform initial liquid distribution is more than that for the uniform one, although the liquid distribution investigated at a sufficient bed depth would be very similar regardless of the initial liquid distribution. Therefore, for a packed column, the quality of initial liquid distribution can be considered as the most important factor accounted for the loss of mass transfer efficiency in practice.

As a device to provide initial liquid distribution, liquid distributors merit great importance on the performance of the packed columns because they serve to overcome the liquid maldistribution at the top of the packed bed, which may greatly impair the efficiency of large-diameter columns.

A good liquid distributor should possess the following attributes:

- uniform initial liquid distribution,
- resistance to plugging or fouling,
- low gas pressure drop,
- minimal distributor height to allow more room for the packing height, and
- good cross-mixing capability.

Klemas and Bonilla [32] attempted to quantitatively model the initial liquid maldistribution behavior in a packed column for distributor design and selection. However, the proposed assumption, which stated that a packing

element at the top of the bed was considered to be fully wetted if it received at least one drop point, is unreliable. Similar assumption was also used by of Semkov [33] for a mathematical model. Moreover, this hypothesis almost cannot be implemented in practice, especially for an industrial-size column.

Billet [29] demonstrated the fundamental design aspects of liquid distributors (e.g. liquid load and number of liquid outlets). The author also recommended the application of redistributors for high columns on an economic factor. No recommended length for the spacing of the redistributors was given. However, it was pointed out that the application of the redistributors and the number of them was based on the balance between the cost of installing the redistributors and the cost on increases in the packing and column heights. Nevertheless, in fact, in industrial mass-transfer columns liquid redistributors are widely used to remix liquid above a certain packing height before it is introduced to the next bed section [34]. The purpose of using liquid redistributors is to minimize the possible deterioration on the mass-transfer efficiency along the bed height caused by liquid wall flow and non-uniform initial liquid distribution. A redistributor was recommended for every 10 theoretical plates [35] and no more than 20 theoretical stages for modern packings [36]. For the small-diameter columns, no redistributor is needed when the ratio of the packing height over the column diameter (x/D) does not exceed a value of 5 – 10 [37,38].

For gas distribution in a packed column, many experimental works [7,39-41] for both random and structured packings have shown that the radial spreading of gas phase is much faster than that of liquid phase. The gas radial velocity profiles are quite even when the gas and liquid distribution are applied uniformly (at the gas and liquid inlet) to the column. For small-diameter columns, the gas maldistribution is usually ignored at low fluid flow rates. However, Kouri and Sohlo [7] found that a 0.5-m packing height was needed to

get uniform gas distribution for a poor initial gas distribution in a 0.5-m-ID dry bed.

Moreover, under two-phase countercurrent flow conditions, a poor initial liquid distribution may induce local flooding in the top section of the bed, and thus, causes gas maldistribution, especially at relative high gas flow rates. In turn, gas maldistribution will again deteriorate liquid distribution. This indicates that maldistribution in one phase may cause maldistribution in the other phase, especially at higher liquid and gas flow rates for a large-size column. Therefore, in practice, a proper designed gas distributor is essential to alleviate the liquid and gas maldistribution for industrial-size packed columns. Additionally, Kouri and Sohlo [7] found that under the same operational conditions, the gas maldistribution for 50-mm Pall rings was more pronounced than that for 25-mm Pall rings with a poor initial gas distribution. This indicates that the effect of radial dispersion increases with increases in the ratio of column diameter to packing diameter.

2.1.2. Liquid Radial Distribution

In general, increasing liquid radial dispersion tends to reduce liquid radial maldistribution, and thus, improves the mass transfer efficiency.

Many experimental studies [1,7,8,12,14,42,43] have shown that liquid radial distribution is far from uniform in a random packed column. This is likely caused by the non-uniform distribution of the void fraction and/or the poor initial liquid distribution generated by a poorly designed liquid distributor. However, regardless whether the initial liquid distribution is uniform or not, liquid tends to move towards the column wall forming fully developed wall flow and reaching equilibrium flow pattern after traversing a certain bed depth. On the other hand, for structured packings, due to regular flow channels and

self-distribution characteristics of the packing, the radial dispersion is faster than that of random packings. This can be seen from the experimental results obtained by van Bate *et al.* [18] and Hoek *et al.* [1].

Yin *et al.* [12,14] investigated the effect of fluid flow rates in a 0.6-m diameter column packed with 25.4-mm metal Pall rings. It was found that liquid wall flow reduced slightly with increases in liquid flow rates and liquid wall flow was fully developed earlier at higher liquid flow rates. On the other hand, liquid radial distribution was not affected significantly in bulk region. They also observed that liquid radial dispersion was more pronounced at the top of the column. At the position of 1.8 m below the top of the column, liquid radial mixing became steady.

With the measurements in a 0.2-m-ID column packed with 10-mm and 30-mm Raschig rings in the absence of a gas stream, Bemer and Zuiderweg [42] pointed out that at low liquid flow rates there was a tendency towards higher values of the maldistribution factor. But the maldistribution factor became a constant value beyond a certain flow rate.

Wang *et al.* [2] studied the small-scale and large-scale liquid maldistribution in a 0.28-m-ID trickle bed packed with 3-mm glass bead. It was found that a minimum liquid flow rate (a threshold) existed for fully wetting of the packing. This is in accordance with the finding of Xiong *et al.* [44] and Bemer and Zuiderweg [42]. In addition, the influence of liquid flow rate on small-scale distribution was more significant than that on large-scale distribution because the segregation of liquid flow at the wall region was less sensitive with changes in the liquid flow rate, which agrees with the observation of Herskowitz and Smith [45] and Borda and Gabitto [46].

In some research, liquid radial distribution was observed without the presence of gas phase [42] or the influence of gas flow was ignored considering that the interaction of gas and liquid was negligibly small at low fluid flow rates. However, the gas influence is still an important factor on the interaction of liquid and gas phases at high fluid flow rates, especially for industrial-size columns.

Based on the study of liquid distribution in a two-phase countercurrent column packed with small (5-6 mm) solid or hollow Polystyrene particles, Badr El-Din *et al.* [43] stated that an increase in a gas flow rate tended to flatten the liquid velocity profile due to a progressive increase in the liquid wall flow. In addition, it was also observed that liquid plugging occurred in the vicinity of the wall and liquid bounced back into the packings' body at a certain gas flow rate.

Yin *et al.* [12,14] observed that below the loading point, the effect of a gas flow rate on liquid radial dispersion was insignificant since the interaction between the gas phase and liquid phase was weak. However, liquid radial mixing increased significantly at the gas flow rate above the loading point, especially at the wall region. At a higher gas flow rate, the drag force of gas upon liquid became stronger, and hence, the resistance to the liquid flow in bulk region was higher than that in the wall region. That makes the liquid flow rate increase significantly at the wall region. Similar results were obtained by Kouri and Sohlo [7] and Badr El-Din *et al.* [43].

For the effect of liquid properties on liquid radial distribution, Yin *et al.* [12] reported that liquid viscosity reduced liquid radial spreading. However, liquid surface tension had little or no effect on liquid radial distribution. It is in accordance with the observation of Bemer and Zuiderweg [42]. However, Onda *et al.* [47] observed otherwise in their study.

As to the effect of packing type and size, Bemer and Zuiderweg [42] stated that packing size had a dominant effect on the maldistribution factor, and the radial spreading factor was dependent only on packing size. In addition, van Bate *et al.* [18] reported that the radial dispersion coefficient in a structured packing (KATAPAK-S) was about one order of magnitude higher than that in random packings.

2.1.3. Liquid Axial Distribution

Axial distribution, or longitudinal mixing, is an important non-ideal flow phenomenon in packed columns. It represents a deviation from plug flow and adversely influences the axial concentration profile in a flowing stream, causing a decrease in mass transfer driving forces and in consequence a drop in separation efficiency.

In general, this departure from plug flow mainly results from viscous effects, molecular diffusion as in laminar flow, and eddy diffusion for turbulent flow. Although packings can to some extent reduce axial dispersion, severe axial dispersion in a flowing stream may occur in packed beds under certain operational conditions (e.g. high flow rates and high pressure) [16].

It has been over five decades since the time at which Kramers and Alberda [48] first began to study the effects of axial dispersion in packed columns. Many of earlier studies on the subject are reviewed elsewhere [15,16].

Bodenstein number (Bo), the axial dispersion number, is one of the dimensionless numbers widely used to measure the axial dispersion. The definition of Bodenstein number is given in the appendix A3. As the value of Bo increases, axial dispersion decreases and vice versa.

Macias-Salinas and Fair [15,16,49] studied the axial mixing phenomena in columns packed with various random and structured packings for single-phase flow [15,50] and two-phase flow [16,49]. The authors pointed out that liquid axial mixing was much greater than gas axial dispersion since the liquid flow behavior appeared to be most affected by hydraulic factors such as wall effect, non-uniform distribution of the liquid, and bed capacitance (liquid retention in static holdup). Based on the experimental results, they reported that axial mixing in the liquid phase decreased with increases in liquid flow rates, while it was insensitive to gas flow rates up to the flooding point. This was in contrast to the findings on structured packing studies by van Bate *et al.* [18] and Mak *et al.* [50]. This phenomenon happened on the structured packings is likely due to the special structure of the structured packings, especially when the inclination angle of the structured packing elements is less than 60°.

For the effect of liquid properties on the axial distribution, Ebach and White [51] found that there was no significant effect of liquid viscosity on the axial dispersion coefficient. Usually, the effect of the liquid physical properties such as viscosity and surface tension on the liquid axial dispersion was ignored in the literature.

In addition, from several studies using various random packings, Kunugita *et al.*[52], Miller and King [53] and Ebach and White [51] observed that there was no significant effect of packing size and type on the axial dispersion coefficient. However, Liles and Geankoplis [54] and Tan and Liou [55] reported that the axial dispersion increased with the packing diameter.

2.2. Mass Transfer in Packed Columns

Improving the mass transfer efficiency is critical for upgrading the operational performance of a packed column. However, accurate prediction of the mass transfer rate is rather difficult because the fluid dynamic behavior near the inter-phases is so complicate and depends on many factors and their interactions. Usually, predictions are obtained from semi-empirical or empirical correlations based on the experimental results.

Three most frequently used techniques for mass transfer measurements are:

i) dissolution test technique by dissolving soluble packing [13,56-60],

ii) limiting current technique by an electrochemical redox reaction [61-71],

iii) gas absorption technique [72-78].

In mass-transfer measurements many factors affect the transfer rate. Also the interaction of the factors makes the situation more complicated. These factors include liquid and gas flow patterns, the characteristics of the packed column, the characteristics of the packing elements, initial liquid and gas distribution, liquid redistribution and operational conditions. Usually the effects of these parameters on mass transfer are lumped into empirical equations represented by the dimensionless numbers because they are implicitly included in the experimental data.

The typical form of correlations used to represent the mass transfer coefficient is expressed as:

$$\frac{Sh}{Sc^{0.33}} = a \cdot \mathrm{Re}^{b} \qquad \text{Eq. 2-2}$$

where a and b are the empirical coefficients.

The values of a and b are determined experimentally and the effects of many factors mentioned above are implicitly imbedded in these coefficients.

2.2.1. Overall Mass Transfer in Packed Columns

Generally, considering the complicity of the mass transfer process in a packed column, an overall value for mass transfer known as the overall mass transfer coefficient is used to simplify the analysis and design. This overall mass transfer coefficient is usually determined by measuring the concentration difference of a certain component between inlet and outlet. This overall value allows the mass transfer evaluation for different kinds of packings. Knowledge of the overall mass transfer coefficient is also important to put the profiles of local mass transfer coefficients into context. Comparison between the overall value and the individual values obtained locally can elucidate better understanding of the spatial variation of mass transfer under different operational conditions. Design equations could thus be adjusted or more generalized correlations could be developed.

The early work on mass transfer in a packed bed using the electrochemical technique can be traced back to the article of Akehata and Sato [79] in 1958. Since then, the electrochemical technique has become one of the major methods used in studies of mass transfer in a packed column. A literature review of mass transfer correlations in a packed bed with the electrochemical method can be found elsewhere [61]. However, most work was carried out on the traditional packings, such as: flat plates, spheres, cylinders and Raschig rings. In modern chemical industry, more efficient random packings such as Pall rings and structured packings are more popular, and yet detailed investigation of mass transfer on these packings have not been done and reported.

2.2.2. Local Mass Transfer in Packed Columns

An overall mass transfer coefficient only represents a composite of local phenomena. Local phenomena are of practical importance because solid-liquid mass transfer varies at different bed locations. Unfortunately, local mass transfer behavior hasn't been reported systematically in the literature. In recent years, the subject on local phenomenon in packed beds has received increased attention due to the efforts to better understand the internal flow mechanisms and to reduce the discrepancies between the laboratory data and full-scale performance.

From an investigation of the local mass transfer at cylindrical tubes immersed in a rectangular bubble bed using the electrochemical method, Del Giorgio *et al.* [70] found that mass transfer distribution around the cylindrical tubes was non-uniform and dependent on the system geometry and the tube arrangement. However, the physical properties of liquid and the superficial gas velocity affected the mass transfer profiles insignificantly. The non-uniformity of mass transfer increased as the geometrical complexity of the system increased.

Tsochatzidis and Karabelas [71] studied the local mass transfer and the radial distribution of mass transfer coefficients in a downward gas-liquid concurrent flow. Ferri-/ferrocyanide with sodium hydroxide were used as the electrolytic system. Four nickel spherical electrodes were placed along the bed cross section to examine the radial dependence of the local mass transfer coefficients. It was observed that the mass transfer rate increased with increases in liquid flow rates. This result is in accordance with the findings of Levec and Lakota [80], Satterfield *et al.* [81] and Rao and Drinkenburg [82]. They also reported that the local mass transfer coefficients near the column wall were lower than those at the rest radial positions. It was attributed to the high

porosity and the reduced local gas velocity in the wall region. However, the differences in mass transfer with the bed location decreased when the liquid flow rate was increased. Unfortunately, the reliability of the experimental data might be suffered by the side reactions caused by air, which was used as gas phase.

In some researches [7,83], mass transfer was studied using the analogy between heat transfer and mass transfer. By measuring the local temperatures with thermistors, Marcandelli *et al.* [84] investigated local heat transfer in a trickle-bed reactor. They found that the radial distribution of heat transfer coefficients was non-uniform and the average heat transfer coefficient increased with liquid flow rate. In trickle flow regime, heat transfer was not influenced by the gas flow rate. However, high discrepancies were found between the measured values and the calculated values using Chilton-Colburn heat and mass transfer analogy.

In order to quantify the effects of local structure and hydrodynamics on mass transfer, Guo and Thompson [13] studied mass transfer in a column of spheres using the dissolution method with full upward liquid flow. It was found that due to the local structural difference local Peclet numbers could vary over an order of magnitude, which in turn caused a spatial variation of mass transfer rates in bed. The exponent (n) in the Sherwood vs. Peclet number correlation ($Sh = mPe^n$) might vary between 0.3 and 0.7 with the location in the packed bed.

Recently, using the electrochemical technique, Gostick *et al.* [61-63] directly measured the spatial variation of the local mass transfer coefficient in a 0.3-m-ID column of 25.4-mm stainless steel Pall rings. It was found that the quality of initial liquid distribution has a considerable effect on the radial distribution of local mass transfer coefficients, especially at the top of the column. The overall mass transfer coefficient with a multipoint liquid distributor

was 14% higher than that with a single-point liquid distributor. At different liquid flow rates, the axial profiles of the mass transfer coefficients were similar. Due to the different flow conditions between the bulk region and wall region, the axial mass transfer profile in the outer section showed different trends compared to that in the inner or center sections. Unfortunately, in this study liquid distribution was not investigated, and hence, the relation of liquid distribution and local mass transfer coefficient can not be addressed. In order to unveil the relationship between local flow behavior and local mass transfer behavior, the spatial variations of liquid distribution and mass transfer coefficient under various conditions should be measured in the same packed bed.

2.3. Electrochemical Technique in Mass Transfer Studies

Electrochemical technique is one of the most widely used methods in measuring solid-fluid mass transfer coefficients. As early as 1947, it was reported to be used in measuring the effects of convective diffusion in electrode processes [85]. Since then, it has increasingly gained popularity and became an established technique for determining mass transfer coefficients and investigating hydrodynamics phenomena. A review on the early works was given by Tobias *et al.* [86].

2.3.1. Fundamental Principle of Electrochemical Technique

In electrochemical solution, ions transport from the bulk fluid to the surface of an electrode and react under enough electric potential at the electrode surface. The rate of reaction is a function of applied voltage as well as other parameters such as temperature.

Based on Faraday's law, the electrochemical reaction rate is directly proportional to the current through the cell and can be expressed as:

$$r_a = \frac{i_L}{zAF} \qquad \text{Eq. 2-3}$$

The notation of the variables in Eq. 2-3 can be found in appendix A1. From the shape of a typical current/potential curve, as shown in Fig. 2-1, it can be seen that the curve is comprised of three regions. At the plateau region, the current remains constant with increases in the voltage. This technique is thus also called the limiting current technique (LCT). In this region, the reaction rate is so quick that the ion concentration at the packing-solution interface reduces to near zero. This indicates that the reaction rate is controlled only by the mass transfer rate. However, besides ionic diffusion, ionic migration may exist due to

the electric field. If ionic migration transport is eliminated, the reaction can be considered as diffusion controlled only.

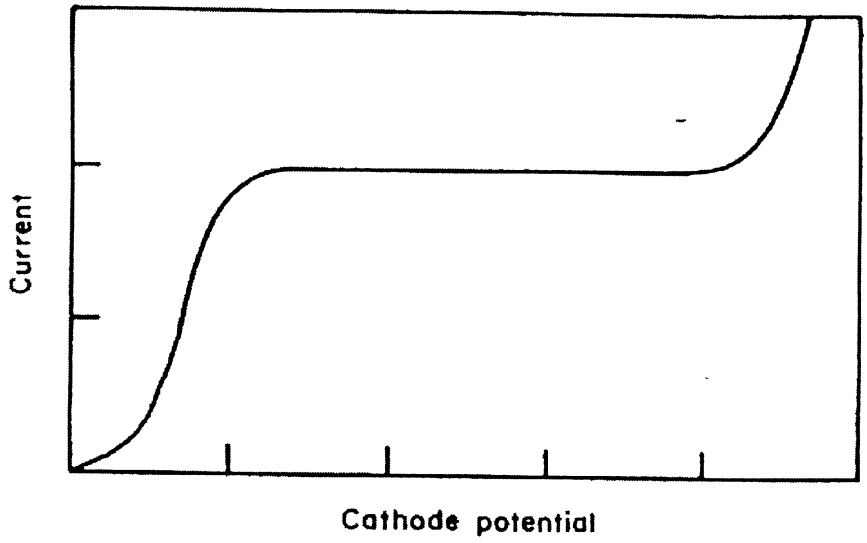

Fig. 2-1. Typical current-potential curve for a diffusion controlled reaction [87].

In this situation, based on the film theory, the mass transfer rate can be expressed in terms of the mass transfer coefficient as:

$$r_a = N = k_L C_\infty \qquad \text{Eq. 2-4}$$

From Eq. 2-3 and Eq. 2-4, the relationship between the mass transfer coefficient and the current can be determined by Eq. 2-5.

$$k_L = \frac{i_L}{zAFC_\infty} \qquad \text{Eq. 2-5}$$

The reason of the increases in the current at the end of the plateau is given elsewhere [61,88,89].

2.3.2. Characteristics of Electrochemical Technique

Compared with the other methods (such as solid dissolution method and absorption method) in investigating solid-liquid mass transfer, the electrochemical method has several advantages [61,63,89] including measuring

the mass transfer coefficient directly, instantaneously, accurately and simultaneously in all directions, unfaltering surface shape and texture of packing and utilizing for all flow patterns. Many important features such as unsteady and fluctuating mass transfer processes can only be investigated by instantaneous measurements.

Although this approach is relatively simple with above favorable characteristics, in practice, various problems arise. They need to be solved if measurements are to be accurate and cover the widest possible range of flow conditions. For instance, if the flow rates of the system exceed a critical value, the reaction rates at the electrode surface would not be fast enough. In addition, the solution may also be susceptible to the light, dissolved gases and organic materials [90]. However, with proper precautionary procedures, the effects of these factors can be minimized to maximum extent.

2.3.3. Effects of Liquid Flow Rate, Temperature and Ionic Migration on Limiting Current Technique

In electrochemical system, the value of the limiting current is mainly affected by flow conditions, temperature and ionic migration. The relationship between flow rate and cell current has been reported by many researchers [61,88,89,91]. In general, by increasing liquid flow rate, the limiting current increases due to the enhancement of diffusion rate. However, the range of limiting-current plateau will shrink to a point when the flow rate reaches a certain value known as the critical flow rate. Beyond this flow rate, the plateau disappears since the chemical reaction rate can not accommodate an increased rate of arrival of ions at the reaction surface by diffusion. This explains the onset delay of the limiting current plateau at higher liquid flow rates. Under this situation, the reaction is controlled by a combination of diffusion and kinetic limitations, instead of diffusion.

Since the physical properties of reaction system (e.g. current density and diffusivity) all depend on solution temperature, the effect of temperature on limiting current need to be considered. Berger and Ziai [88] stated that the current density increased approximately linearly with increases in temperature, as shown in Fig. 2-2. The variation of temperature should be kept in ±0.2 °C to reduce the test error in the limiting current less than 1%. In addition, the critical flow rate could be increased with temperature [88].

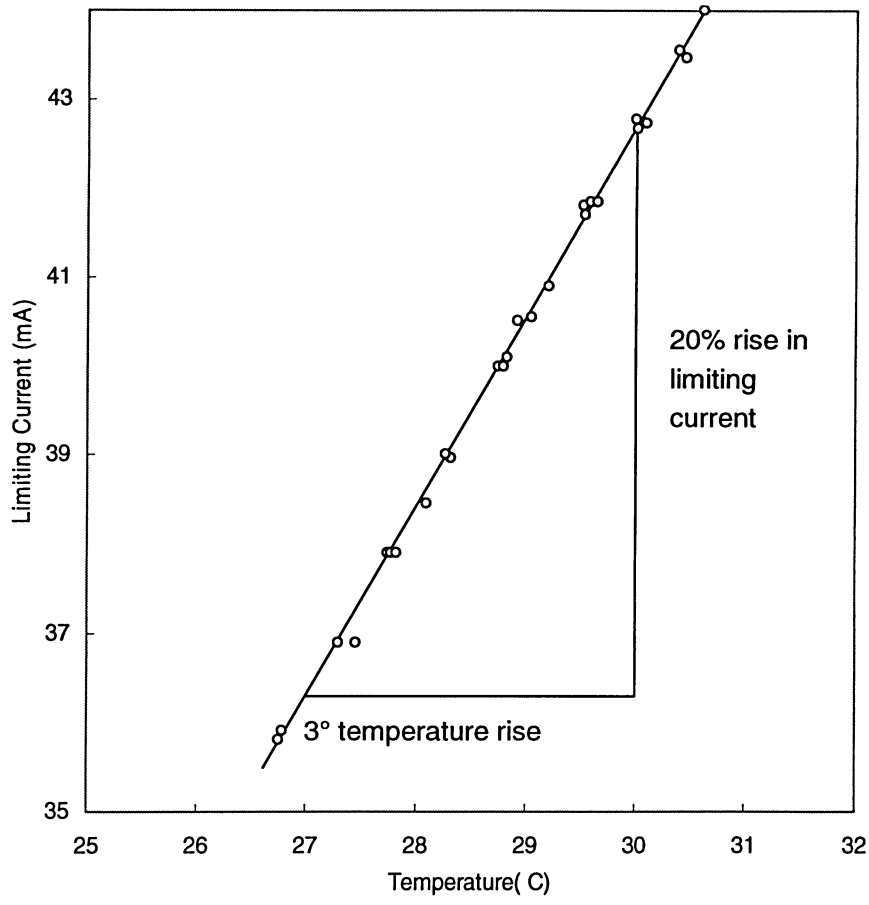

Fig. 2-2. Influence of temperature on limiting current [88].

Another factor affecting the overall mass transfer is ionic migration, which is caused by charged ions moving under the effect of the electric field. It is a major adverse transport that needs to be eliminated. In practice, a highly conductive inert supporting electrolyte is usually added to the solution for this purpose. Additionally, adding a supporting electrolyte to keep a high

conductivity can also reduce the resistance of the solution, and hence, can reduce the applied voltage. The concentration effect of indifferent electrolyte on ionic migration is shown in Fig. 2-3. The selection of concentration of supporting electrolyte will be discussed in Section 2.3.4.

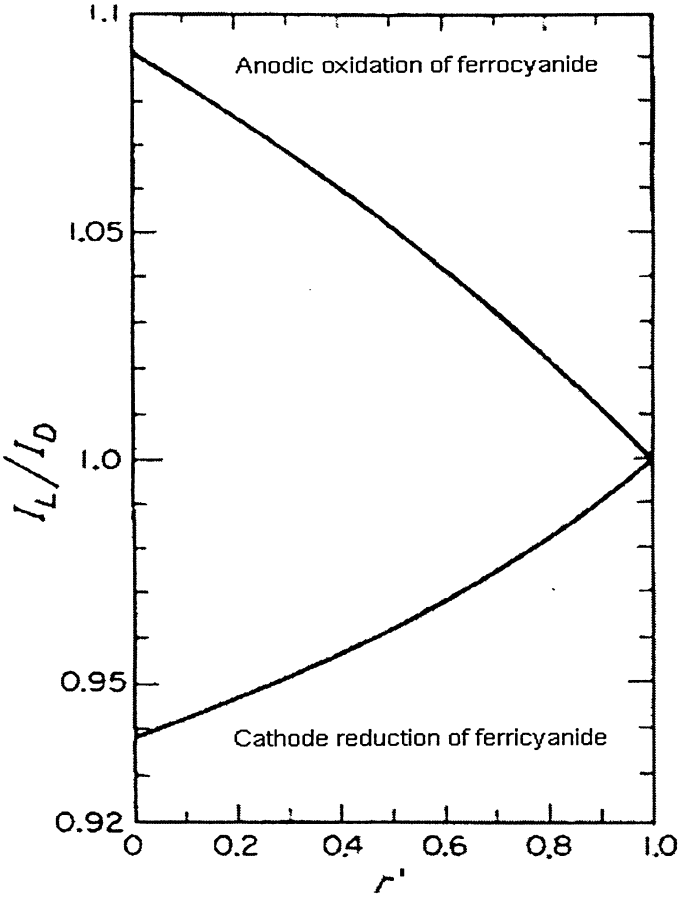

Fig. 2-3. The concentration effect of indifferent electrolyte on ionic migration [92]. r' = ratio of supporting electrolyte to total electrolyte [C_{OH^-}/C_{K^+}], I_D = measured diffusion current (A) and I_L = current due to diffusion only (A).

2.3.4. Selection of Experimental Conditions

The electrochemical reactions selected in mass transfer studies can be classified into two groups: deposition-dissolution reactions and aqueous-phase reactions [61]. As a typical aqueous-phase reaction, ferri-/ferrocyanide couple is

widely used because it not only offers an unaltered electrode surface and a constant bulk concentration but also has a relatively higher reaction rate constant than other redox systems [91]. The electrochemical reactions occur at the electrode surface as follows:

$$[Fe^{3+}(CN^{-})_6]^{3-} + e^{-} \underset{\text{Oxidation}}{\overset{\text{Reduction}}{\rightleftharpoons}} [Fe^{2+}(CN^{-})_6]^{4-} \qquad \text{Eq. 2-6}$$

Ferricyanide ion Ferrocyanide ion

In the literature [61,89,93,94], nickel and platinum were usually selected as electrodes for ferri-/ferrocyanide with sodium hydroxide reacting system due to their stable, chemical inert and anticorrosive abilities under the operational conditions used in experiments. However, they are not practical and economical in practice. Based on the test results [61,95], it was found that nickel-coated cathode/stainless steel anode could be used instead of pure nickel or platinum electrodes without apparent change in limiting current plateau.

In addition, the concentration of each reactant is critical for local mass transfer measurement. As mentioned above, the concentration of ferricyanide directly affects the value of mass transfer coefficient as shown in Eq. 2-5. A proper concentration of ferrocyanide must be used to maintain the constant concentration of ferricyanide in the solution by the oxidation of ferrocyanide to ferricyanide. Moreover, a large excess amount of sodium hydroxide is applied to reduce the effect of ionic migration.

In the literature, the equimolar ferri-/ferrocyanide solution was widely chosen in mass transfer studies. In addition, Levich [85] gave the approximate solution for selection of the supporting electrolyte in the form of

$$I_{mig} = \frac{1}{2}\frac{C_i^B}{C_{NaOH}^B} I_i \qquad \text{Eq. 2-7}$$

where I_{mig} is the current due to ionic migration (A); I_i is the measured current (A); C_i^B is the bulk concentration of species i (mol m^{-3}); and C_{NaOH}^B is the bulk concentration of supporting electrolyte (mol m^{-3}). In the present study, species i indicates the ferricyanide ion ($[Fe(CN)_6]^{3-}$). It can be seen that increasing the ratio of the concentration of NaOH to the concentration of ferricyanide can reduce the percentage of the current due to ionic migration (I_{mig}) in the measured current (I_i).

2.3.5. Adverse Reactions and Precautionary Measures

Maintaining the electrochemical solution stable and chemical inert is critical in mass transfer study. Ferri-/ferrocyanide are decomposed in the presence of light and air. Accordingly, exclusion of light and air is indispensable to ensure the experimental data reliable.

Possible reactions for ferrocyanide and ferrocyanide decomposition in light were proposed as below [88,89,96-99].

For ferricyanide,

$$[Fe(CN)_6]^{3-} + H_2O \xrightarrow{\text{Light}} [Fe(CN)_5H_2O]^{2-} + CN^- \qquad \text{Eq. 2-8}$$

$$[Fe(CN)_5H_2O]^{2-} + 2H_2O \xrightarrow{\text{Light}} Fe(OH)_{3(S)} + 5CN^- + 3H^+ \qquad \text{Eq. 2-9}$$

$$4Fe^{3+} + 3[Fe(CN)_6]^{4-} \longrightarrow Fe_4[Fe(CN)_6]_{3(S)} \text{(Prussian blue)} \qquad \text{Eq. 2-10}$$

For ferrocyanide:

$$[Fe(CN)_6]^{4-} \underset{\text{Dark}}{\overset{\text{Light}}{\rightleftharpoons}} [Fe(CN)_5]^{3-} + CN^- \qquad \text{Eq. 2-11}$$

$$CN^- + H_2O \rightleftharpoons HCN + OH^- \qquad \text{Eq. 2-12}$$

$$[Fe(CN)_5]^{3-} + H_2O \longrightarrow [Fe(CN)_5H_2O]^{3-} \qquad \text{Eq. 2-13}$$

$$4[Fe(CN)_6]^{4-} + 2H_2O + O_2 \longrightarrow 4[Fe(CN)_6]^{3-} + 4OH^- \qquad \text{Eq. 2-14}$$

Detailed discussions can be obtained elsewhere [88,89,96-99]. As the byproducts of side reactions, hydrogen cyanide (HCN) contaminates the solution and poisons the electrode surface. Therefore, the solution should not be exposed to light at any point in the apparatus, and hence, any transparent part of equipment must be covered with an opaque material (e.g. aluminum foil).

In addition, air-exposure deterioration of ferri-/ferrocyanide electrolyte is well recognized, although the mechanism is complex and uncertain. As reported in the literature [88], oxygen and hydrogen sulphide were likely the substance that could poison the electrode or contaminate the solution. Poisoned electrode usually resulted in the chemical polarization increasing and/or part of the electrode surface being blocked off. Aggerwaal and Talbot [100] suggested that the possible side reaction involving oxygen at the cathode was

$$O_2 + 2H_2O + 4e^- \longrightarrow 4OH^- \qquad \text{Eq. 2-15}$$

However, Berger and Ziai [88] stated that the reaction like Eq. 2-15 was unlikely occurred by the analysis of the discharge potential of this reaction.

Sutey and Knudsen [101] investigated the effect of dissolved oxygen in the ferri-/ferrocyanide redox couple for mass transfer measurement. They reported that if the electrolyte solution was purged fully with nitrogen, future exposure to air for a period of time didn't greatly affect the mass transfer and the error was acceptable.

Accordingly, at the beginning of the experiment, the solution in the electrolyte tank must be purged with nitrogen gas for several minutes in order to replace the dissolved oxygen and hydrogen sulphide in the solution.

Due to the above adverse effects on the electrodes, electrode pretreatment is essential for accurate measurements. Different ways have been suggested to resolve this issue. Some treatments are limited by the electrode geometry (e.g. physical surface sanding); others are so complicated in practice (e.g. cathodic activation). A detailed discussion on electrode pretreatments can be found elsewhere [88,102].

In the present study, it was found that after several runs, a white film was formed on the surface of the electrode. The same phenomenon is reported in the literature [61,88,95] and the nature of the film is uncertain. In order to avoid the reduction of active area caused by the side reactions, special acid treatments were applied by Dawson [95] and Gostick [61]. Gostick [61] stated that around 2-min soak in 5% acetic acid could fully return the electrode activity. Dawson [95] suggested dipping the polluted electrode in dilute (0.5N) sulphuric acid for 10 - 15 seconds. In the present study, 5% acetic acid was applied to remove the white film.

3. Experimental Work

This section describes the apparatus and experimental procedures used in the present study to investigate the liquid distribution and local mass transfer coefficient with and without the presence of gas through a packed bed of Pall rings.

3.1. Experimental Setup

The experimental apparatus consisted of three main parts: (1) the column and its accessories, (2) the measuring systems including liquid collection system for liquid distribution measurement (LDM), and electric circuitry system for mass transfer coefficient measurement (MTM), and (3) the gas and liquid flow system.

3.1.1. Packed Column and Its Accessories

A pilot-scale packed column having an inside diameter of 0.30 m and a height of about 3.3 m was used in the present study. The column was constructed of transparent PVC to allow visual observation of wall flow and liquid flow behavior inside the column. The column was divided into four flanged sections: (a) a top section used for liquid-distributor connection and liquid-feed; (b) a 2.1-m-high packed section; (c) a short section with support and (d) a bottom part for liquid collection and/or gas-feed as shown in Fig. 3-1. The unit used in this and the following figures is millimeter.

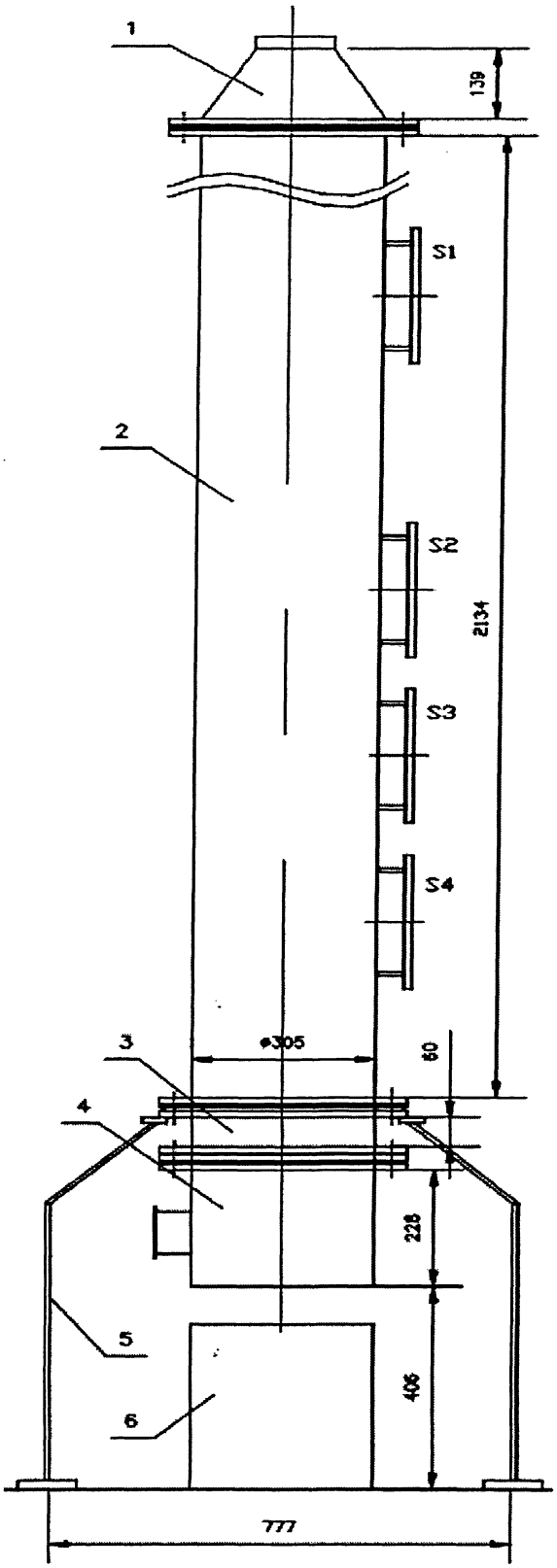

Fig. 3-1. Detailed schematic diagram of the column and its relevant dimensions. 1–Top section, 2–Packed section, 3–Short section, 4–Liquid collector, 5–Support, 6–A set of liquid receiving cells.

For liquid distribution measurement, selection of wall-region width is critical for investigating the wall flow because different wall-region widths will give different amounts of liquid wall flow. Different wall-region widths have been used. Follows are some of the typical values reported in the literature: (1) equal area concentric rings [27], (2) one packing particle diameter from the wall [9,26,103], and (3) very small distance (< 5 mm) from the wall [12,104-108] etc.

The dimensions of wall region and the related column diameter are tabulated in Table 3-1. For large wall region, not only real wall flow but also liquid from the bulk region could be collected and classified as liquid wall flow. On the other hand, with small width, wall flow may be only partially collected by the wall region, especially at higher liquid flow rate and at the presence of gas flow countercurrently. It is clear that the wall-flow thickness varies with liquid and gas flow rates. So in fact, it's impossible to find a fixed wall region suitable for all operational conditions in packed beds.

Table 3-1. The dimensions of wall region and the related column diameter.

Reference	D (m)*	δ_w (mm)@	Area ratio #
Present study	0.30	12	15.13%
Kouri and Sohlo [7]	0.5	15	11.64%
Baker *et al.* [27]	0.3	20	25%
Gunn [26]	0.3	25	30.56%
Yin *et al.* [12]	0.6	4.7	3.12%
Templeman and Porter [104-106]	0.30	3.2	4%
Dutkai and Ruckenstein [107,108]	0.30	3.2	4%

* is the diameter of the packed column;
@ is the width of the wall region;
# is the percentage of wall region area over total column cross-sectional area.

In the present study, considering the variation of the wall flow region, 12 mm was used as the width of wall region. This corresponds to 15.13% of the total column cross-sectional area. The wall flow was drained through a 22-mm-ID

tube in the bed wall. For mass transfer measurement, seven holes opened at the side of the wall were used as the cathode-lead entrances.

The column was operated at atmospheric pressure and ambient temperature. Air/water system was used for liquid distribution measurements. For local mass transfer coefficient measurements, air was replaced by nitrogen, and electrolyte was the liquid phase. Both gas and liquid phases flowed countercurrently in the packed bed.

To investigate the effect of initial liquid distribution on liquid distribution and mass transfer, three types of liquid distributors were designed and used in the present study as shown in Table 3-2. SPLD, CLD and LLD stand for single-point liquid distributor, cross-type liquid distributor and ladder-type liquid distributor, respectively. In addition, in order to ensure even liquid distribution in each arm of the multipoint liquid distributors, there was no nozzle in the center of the multipoint liquid distributors (LLD and CLD).

Table 3-2. The information of three liquid distributors.

Type	No. of nozzles	Nozzle Diameter (mm)	Nozzle Density (per m^2)
SPLD	1	23.8	14
CLD	16	4.8	219
LLD	34	4.0	466

Fig. 3-2, Fig. 3-3, and Fig. 3-4 depict the design of the distributors (SPLD, CLD and LLD, respectively). These distributors were able to rotate about the column axis. Liquid was fed into the column through a 38-mm-ID tube, which was connected to one of the liquid distributors at each run. Upon entering the column, liquid was spread out to the packing through the nozzle(s) of the liquid distributor, which was set 30 – 40 mm above the packed bed. Cold-model tests

were conducted to check the performance of LLD and CLD. Compared with the average flow rate, the variations of the flow rates through the individual nozzles were approximately 2% and 4% for LLD and CLD, respectively, in the range of liquid loads in the present study.

The packings used in the present study were Pall rings provided by Koch-Glitsch. The geometric characteristics of the Pall rings are tabulated in Table 3-3. They were dumped into the dry column randomly to a given height. The weight of the packing in column was supported by a PVC grid. Besides supporting the packings, the packing support must also have a high percentage of free area for unrestricted flow of downcoming liquid and upward gas.

Table 3-3. Geometric characteristics of Pall rings.

Packing type	Random packing	
Packing name	Pall ring	
Properties	Nominal size	25.4 mm
	Void fraction	0.95
	Approx. surface area	219 m^2 per m^3
	Wall thickness	24 gage mm
	Outside diameter and length	25.4 mm
	Approx. No. elements	49600 per m^3
	Approx. weight	480 kg per m^3
	Material	stainless steel, nickel-coated and polymer-coated

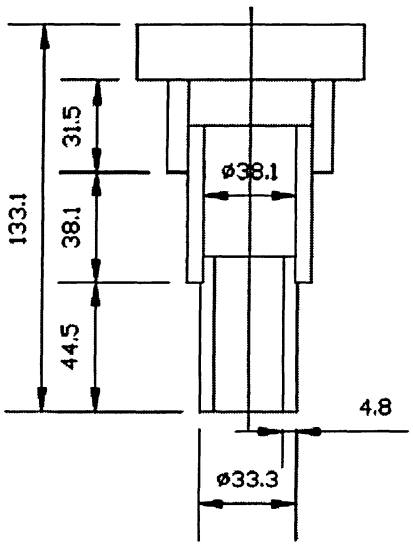

Fig. 3-2. Single-delivery point liquid distributor (SPLD) layout.

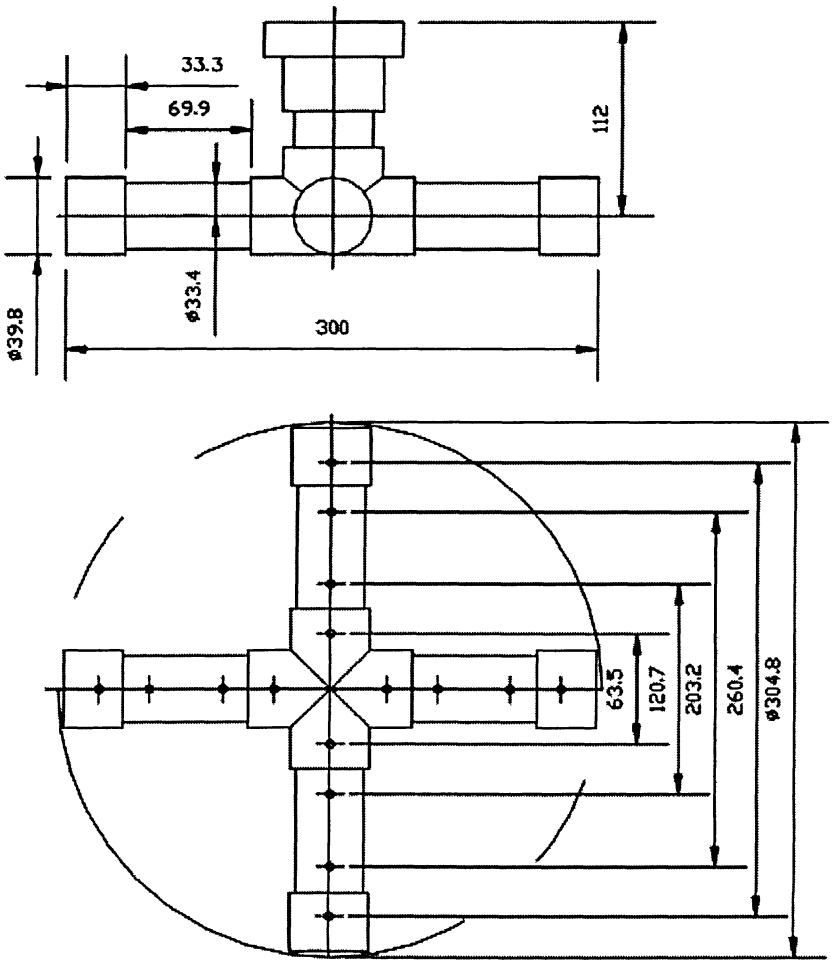

Fig. 3-3. Cross-type liquid distributor (CLD) layout.

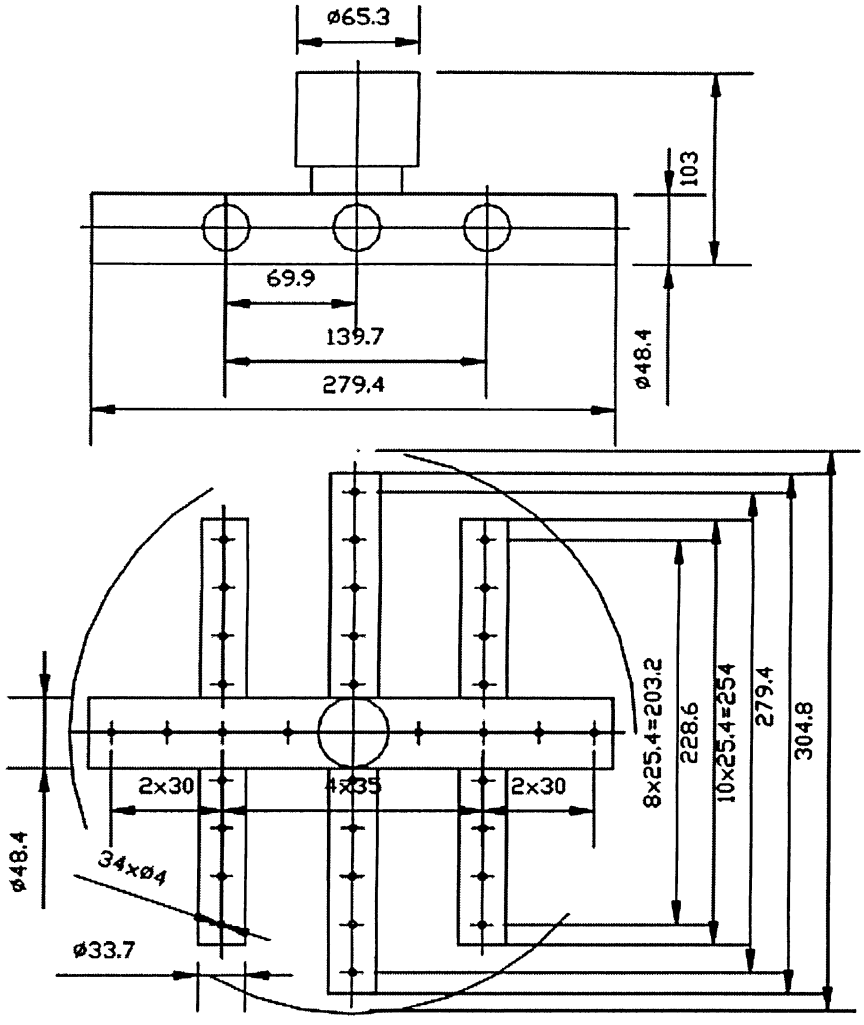

Fig. 3-4. Ladder-type liquid distributor (LLD) layout.

3.1.2. Measuring Systems

The liquid volume was measured at the bottom of the column. This system consisted of three parts: (a) a liquid collector, (b) a set of liquid receiving cells and (c) a steel track for the set slid in and out.

A specially designed liquid collector (also served as gas inflow distributing device) was made up of 39 tubes (25.4-mm diameter each) and 58 holes (14.1-mm diameter each) on the plate, as shown in Fig. 3-5a and Fig. 3-5b.

Water was collected by these 39 tubes laid out concentrically according to its radial position.

Water flowing into the liquid collector was conducted out by water drain tubes and air was blown upward through the holes on the plate. Water from drain tubes was collected in the cells of the liquid receiving device, which was made up of 39 tubes (31.8-mm diameter and 330-mm depth each).

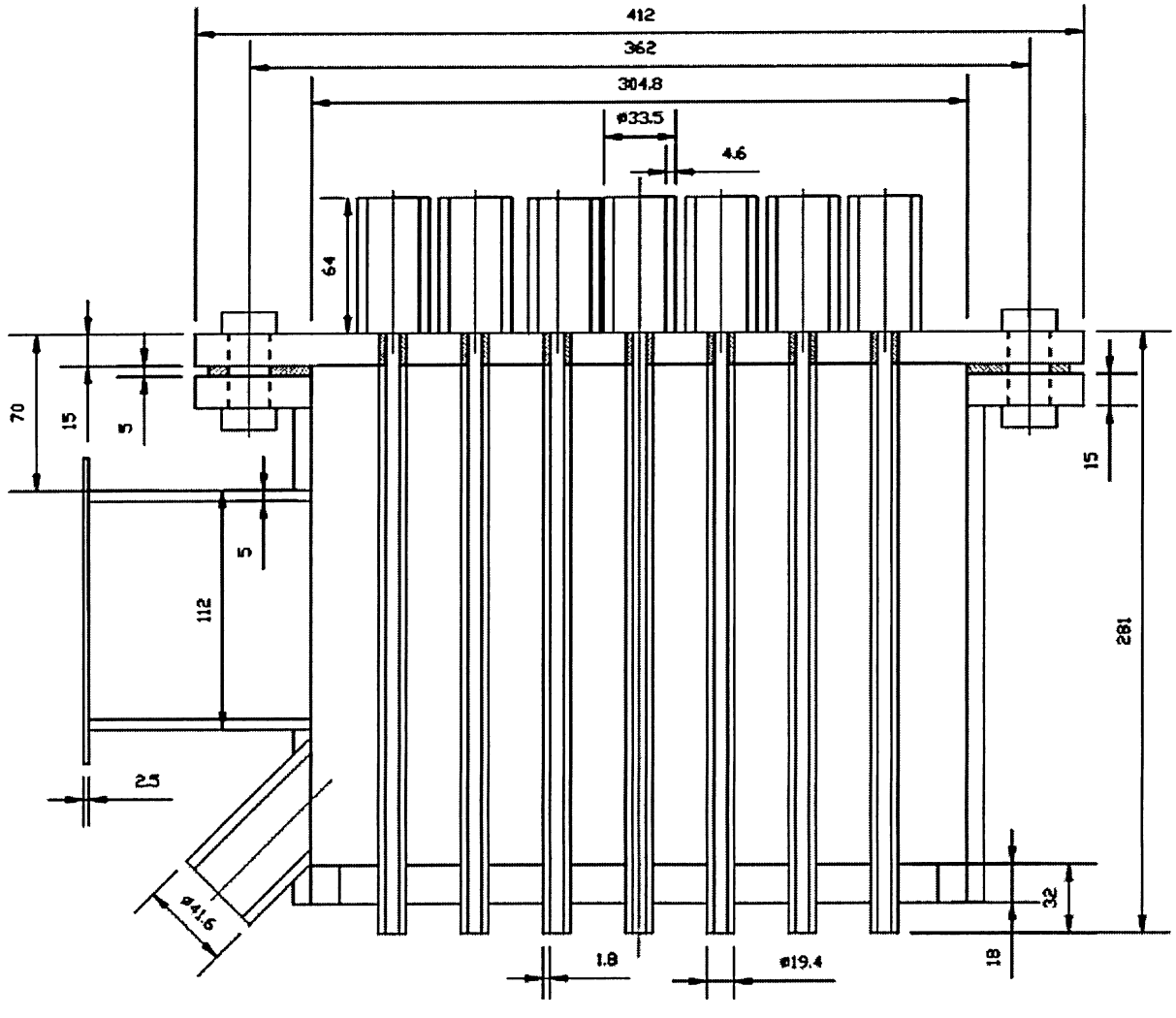

Fig. 3-5a. Schematic diagram of the side view of liquid collector:

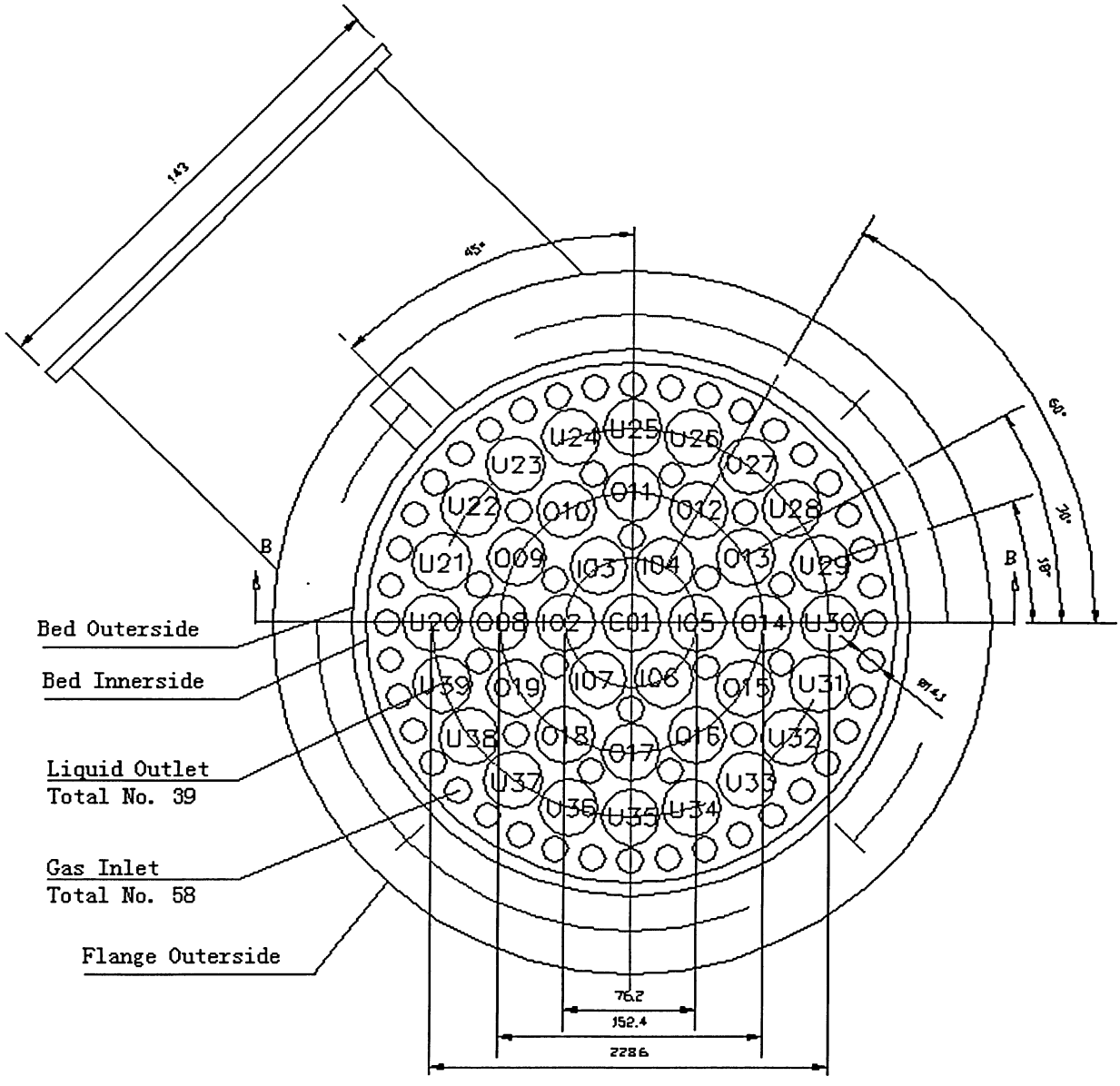

Fig. 3-5b. Schematic diagram of the top view of liquid collector.

Fig. 3-5a and Fig. 3-5b illustrate the layout of the cells with the code number for each cell. The letters, C, I, O and U, stand for four different radial positions from center to outer, respectively. They are all numbered in clockwise order. Each cell of the liquid receiving device was placed just below the lower end of each tube of liquid collector. Accordingly, water falling down from each tube was collected by a corresponding cell. The liquid volume in each cell was determined from the liquid height in the cell.

Another main objective of this study is to measure the local values of mass transfer coefficient on the scale of a single packing element. In order to carry out this objective the voltage drops across fixed resistors under the condition of limiting current need to be determined by the electrochemical method. Then the corresponding local value of mass transfer coefficient for each testing element can be gained by this voltage drop.

For ferri-/ferrocyanide redox, the nickel-coated Pall rings were chosen as cathodes, which were placed in the column. By arranging the location of each cathode in the bed, the values of the mass transfer coefficient at various locations were obtained. In this way, variations in any spatial positions can be investigated. Fig. 3-6 illustrates the layout of the cathodes in the packed bed and the naming convention for each cathode. The letters, CC, IC and OC, stand for the center, inner and outer radial positions, respectively.

Each cathode was surrounded by electrochemically inactive polymer-coated Palling rings to insulate it from other cathodes and anodes that were stainless steel Pall rings. In order to have a sufficient surface area of anode, all stainless steel Pall rings in one layer were in contact to each other and all anodes in different layers were wired together. For investigating the development of wall flow along the bed, the 'OC' cathodes were placed against the inner wall of the column by their ends, as shown in Fig. 3-6. The 'IC' cathodes were located half way between the center and the wall. It was found that the measured voltage drop varied a lot in center region. In order to minimize the variation in data, two cathodes were wired together as a single 'CC' cathode.

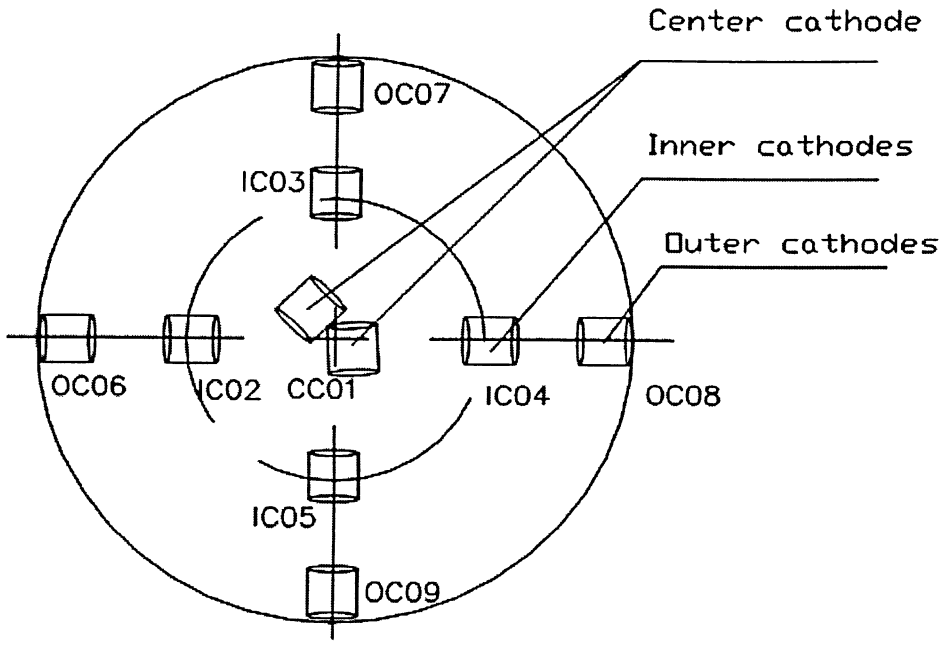

Fig. 3-6. Arrangement of nine cathodes at one given layer.

Along the packed column, the cathode arrays as described above are set at several bed axial positions to investigate the axial profiles of the mass transfer coefficient. Considering the height limit of the column, two configurations (lower position configuration and upper position configuration) were used in the present study as shown in Fig. 3-7. With this configuration, eleven different bed axial positions can be observed by seven cathode layers. In the present study, nine different bed axial positions (x/D = 0.5, 1.0, 2.0, 2.5, 3.0, 3.5, 4.0, 5.0 and 5.5) were measured by five cathode layers. First, the lower position configuration was applied with five cathode arrays arranged. Then the packing height was raised to the upper position by dumping more packing without disturbing the cathode arrays. It was found that the same-axial-position profiles obtained from different configurations nearly matched to each other. Fig. 3-8 shows the cathode-anode arrangement in the column.

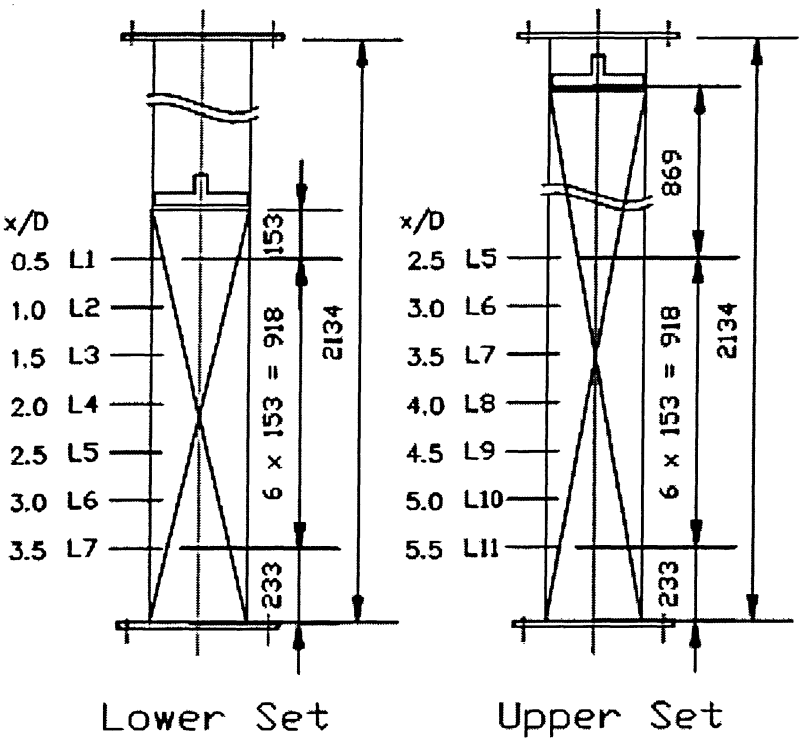

Fig. 3-7. Axial arrangement of cathode arrays in two configurations.

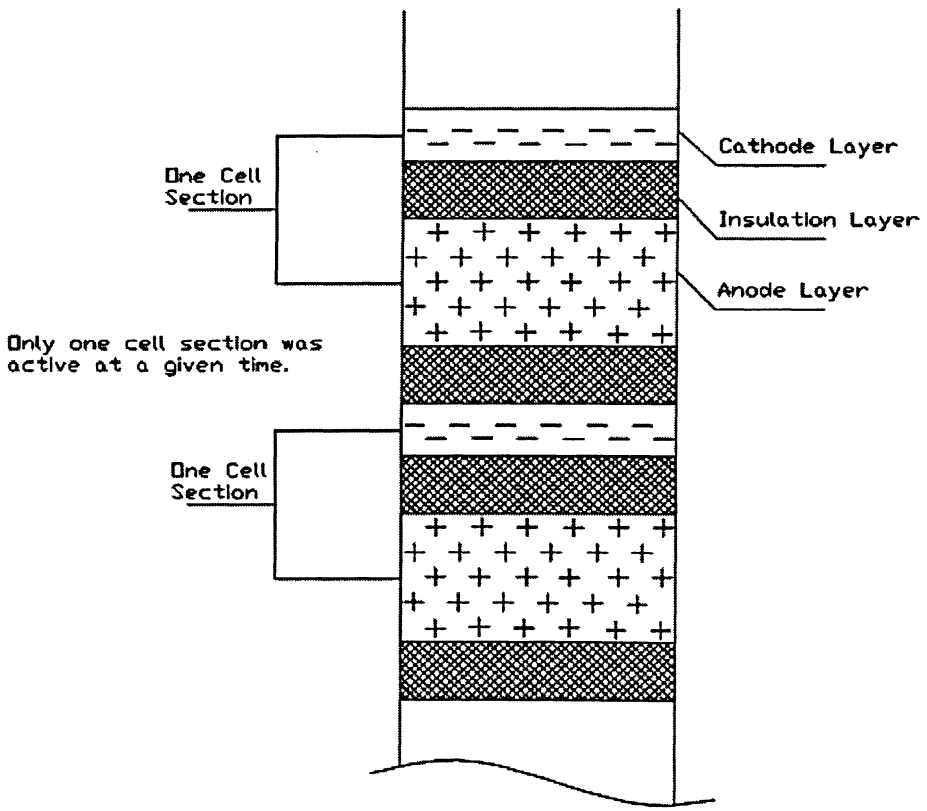

Fig. 3-8. Cathode-anode arrangement in the column.

Either configuration (lower or upper position) had five cathode arrays present. That means 45 cathodes existed for each configuration. Hence, 45 electric circuitries were needed for measuring the voltage drops across the fixed resistors.

In the present study, Daytronic Model 10S-ACFG data acquisition system (DAS) was used to collect the data of the applied voltage on each cathode, the voltage drop across each fixed resistor and the liquid temperatures in the electrolyte tank and the column bottom.

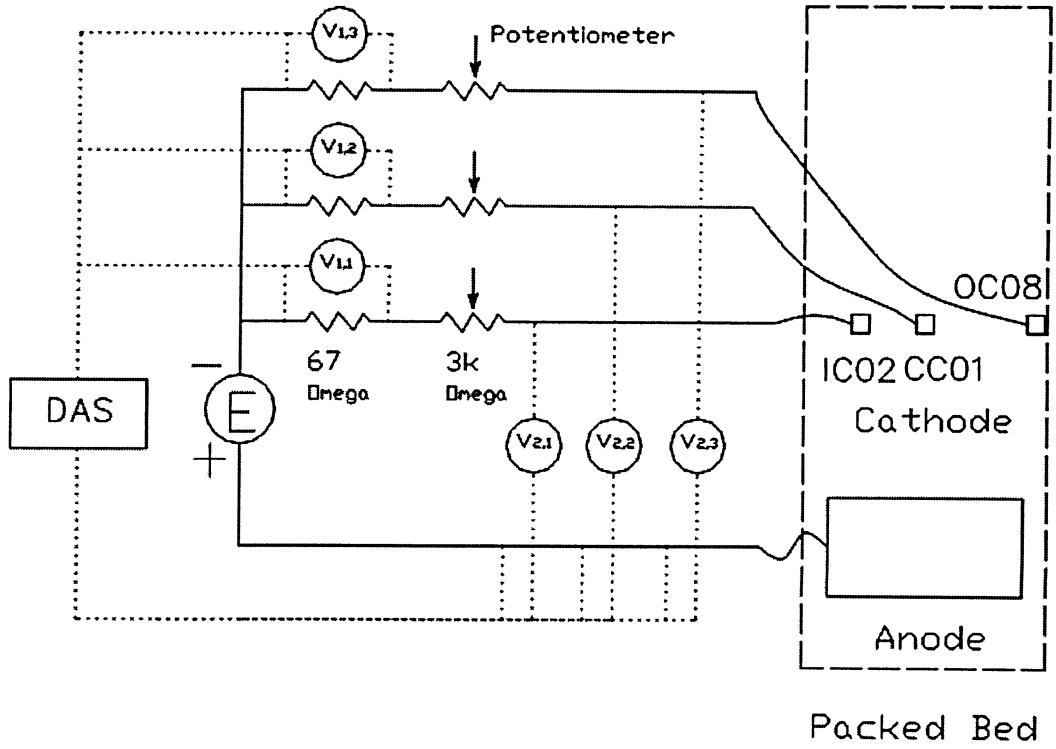

Fig. 3-9. Prototype of electric circuitry for three different radial cathodes at a given layer.

Fig. 3-9 shows the electric circuitry for three different radial cathodes at a given layer. The other six cathodes were wired similarly. The power supply was kept at a constant voltage level. It can be seen from Fig. 3-9 that the voltage drops (e.g. $V_{1,1}$) across fixed resistors (67 ohms each) were collected by DAS. Due to different hydrodynamic conditions around the cathodes, it was required to

adjust the applied voltage on each cathode by a potentiometer to achieve a limiting current plateau and keep the measurement in the range of limiting current plateau. Therefore, for each circuit, one pair of channels was used to measure the voltage drop across a fixed resistor and another pair of channels needs to detect the applied voltage on cathode. Consequentially, only 11 possible units were available for voltage drop measurements at a time with the total number of 22-pair channels available on the DAS. Accordingly, for each layer with nine cathodes, only one layer can be activated to measure at a given time. But alternative layers can be activated easily by just switching the cathode leads of the circuitry.

3.2. Experimental Procedure

The experimental configurations are quite different for liquid distribution measurement and mass transfer coefficient measurement. The following two sections will give the configurations for both.

3.2.1. Configuration for Liquid Distribution Measurement

Air/water system was used in liquid distribution measurement. Fig. 3-10 depicts the process flow diagram for liquid distribution measurement.

First, the packings were dumped into the empty column randomly to a given height (e.g. x/D = 1.64). One of the liquid distributors was installed at about 30 – 40 mm above the packed bed. Water in the tank was pumped into the column through the liquid distributor at a high flowrate (i.e. 17.3 kg $m^{-2} s^{-1}$) to pre-wet the packing for 10 minutes. The flowrate was then set to a predetermined value (e.g. 2.6 kg $m^{-2} s^{-1}$) by adjusting V4. The flow rate of liquid stream entering the column was measured by a flow meter (FP7001 Paddlewheel Sensor, Omega). This meter has an accuracy of ±2%. At the bottom, water collected in the container was returned to the water tank by a recycle pump. The column was allowed to run continuously for about 20 minutes to reach steady state before the quantitative measurement of liquid distribution. For liquid single-phase mode, a set of liquid receiving cells was slid in and out to collect the liquid falling down the column for a certain period. The radial profile of liquid distribution at this layer could be gained by measuring the height of liquid collected in each cell. For a countercurrent air/water flow, an air blower (450 cfm PAPST Dual Inlet AC Blower) was used to introduce air to the bottom of the column. It was connected to the liquid

collector by a flange from the side. After entering the column, air passed through 58 holes (14.1-mm diameter each) on the plate in the liquid collector and was redistributed by a packing-support grid to produce uniform air flow through the packing. The air was discharged to the atmosphere through a vent line (38-mm diameter) located at the top of the column. The gas flow rates were measured by an anemometer (HHF710, Omega). The liquid falling down the column was collected and measured after a steady state reached in the same way as for the single-phase experiments.

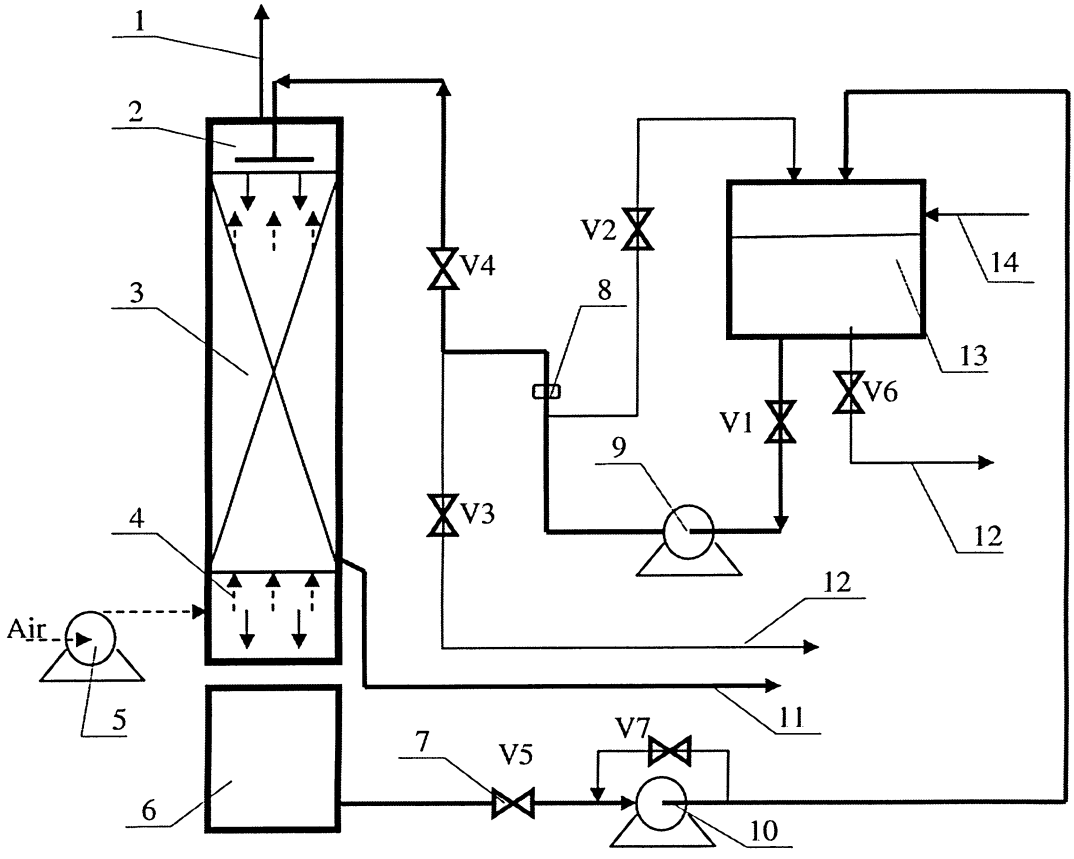

Fig. 3-10. Process flow diagram for liquid distribution measurement. 1–Air outlet, 2–Liquid distributor, 3–Packed column, 4–Liquid collector, 5–air blower, 6–Collecting-cell set or container, 7–Valve, 8–Liquid flowmeter, 9–Feed pump, 10–Recycle pump, 11–Liquid wall flow, 12–Drain, 13–Water tank, 14–Tap water in.

In the present study, the data were obtained for any combination of three liquid distributors, four packing heights (x/D = 1.64, 3.28, 4.92 and 6.56), five liquid flow rates (2.6, 3.9, 5.2, 6.5 and 7.8 kg $m^{-2} s^{-1}$) and two gas flow rates (0 and 0.9 kg $m^{-2} s^{-1}$). Due to fixed volumes of the collecting cells, the water-collecting time decreased with increases in liquid flow rate. As a result, the error would increase. Considering the error, the maximum liquid flow rate used in this measurement was 7.8 kg $m^{-2} s^{-1}$.

3.2.2. Configuration for Local Mass Transfer Measurement

The system used in the local mass transfer coefficient measurement was nitrogen/electrolyte. Fig. 3-11 illustrates the process flow diagram for this measurement.

First step was packing the column and setting the liquid distributor to the proper position as described in Section 3.1 with the arrangement of cathodes and anodes insulated by polymer-coated Pall rings. Then, the column, the electrolyte tank and anywhere exposed to the light was covered with aluminum foil to avoid the side reactions. The ferri-/ferrocyanide redox electrolyte was prepared in the electrolyte tank and the concentration of ferricyanide was determined using the iodometric method. The electrolyte and column were purged with nitrogen gas to replace the oxygen before starting experiments. The whole apparatus was filled with nitrogen to avoid side reactions. The electrolyte in the electrolyte tank was pumped into the column through the liquid distributor. After the packing pre-wetted, the flow rate was set to a predetermined value (e.g. 2.6 kg $m^{-2} s^{-1}$) by adjusting V4. The column was allowed to operate until the stable hydrodynamic situation was reached (~ 20 minutes). In order to eliminate the effect of temperature variation, the liquid temperature in the electrolyte tank was maintained at a constant value by adjusting the flow rate of tap water through a cooling coil.

After circuit checking, all potentiometers in the circuit were adjusted to their highest resistance to ensure the minimum potential drop on cathodes once the power supply was turned on. The first set of cathode leads was connected to the data acquisition system with the power supply turned off. The power supply was then turned on and the resistance of each potentiometer was reduced gradually to get the potential across the whole circuit in the range of the limiting current.

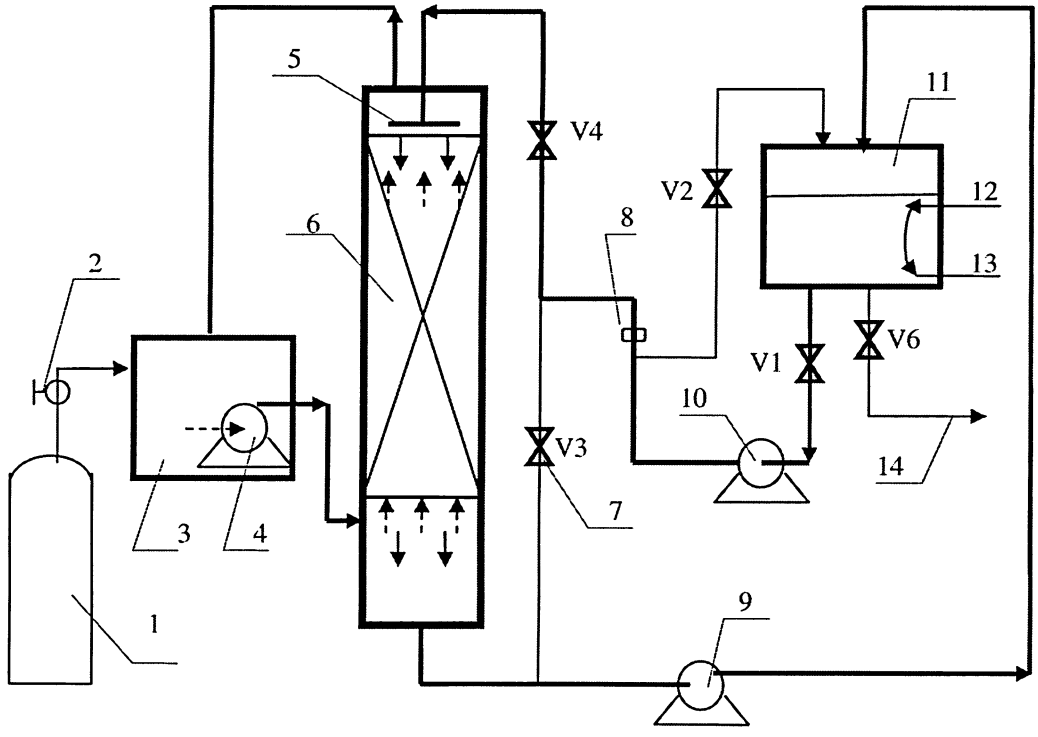

Fig. 3-11. Process flow diagram for mass transfer measurement. 1–N_2 cylinder, 2– Regulator, 3–Gas tank, 4–N_2 blower, 5–Liquid distributor, 6–Packed column, 7–Valve, 8–Liquid flowmeter, 9–Recycle pump, 10–Feed pump, 11–Electrolyte tank, 12–Tap water in, 13–Tap water out, 14–Drain.

In the present study, the limiting current plateau occurred at the voltage drop between cathode and anode from 500 mV to 1000 mV. Once all the cathodes were operating at the limiting current conditions, the DAS system sampled the

voltage drops across fixed resistors (one for each cathode) once every second.

In order to eliminate the effect of electrical noise and fluctuations on the readings, sampling times between 80 to 100 seconds were used to ensure that representative data were obtained. For measurements in a countercurrent gas-liquid flow, the blower was turned on for 15 – 20 minutes before starting measurements. The same steps as for experiments with a single liquid phase were repeated. In the present study, 3.6 mol m^{-3} potassium ferricyanide and 4.0 mol m^{-3} potassium ferrocyanide was applied. In order to reduce the effect of ionic migration to less than 1%, 500 mol m^{-3} NaOH was applied, which led the effect of ionic migration to 0.36 %. The temperature was maintained in 20°C. The data of local mass transfer coefficients were obtained for any combination of three liquid distributors, nine axial positions (x/D = 0.5, 1.0, 2.0, 2.5, 3.0, 3.5, 4.0, 5.0 and 5.5), seven liquid flow rates (2.6, 3.9, 5.2, 6.5, 7.8, 9.4 and 13 kg $m^{-2} s^{-1}$) and two gas flow rates (0 and 0.9 kg $m^{-2} s^{-1}$). The range of liquid flow rates chosen in the present study was to compare with the results obtained from other literature studies.

3.3. Analytical Method

3.3.1. Determination of Electrolyte Concentration

The iodometric method was used in the determination of ferricyanide concentration. The procedure of this method is shown in Fig. 3-12. As shown in Fig. 3-12, in a fumehood, 25 ml aliquot of the electrolyte was added to a 250 ml conical flask. The color of the solution was yellow. Next, 20 ml of 20 wt% potassium iodide (KI) and approximately 5 ml of concentrated sulfuric acid (>95 wt%) were added into the solution. Reversible reaction as shown in Eq. 3-1 occurred under the acidic condition and the color turned from yellow to dark red.

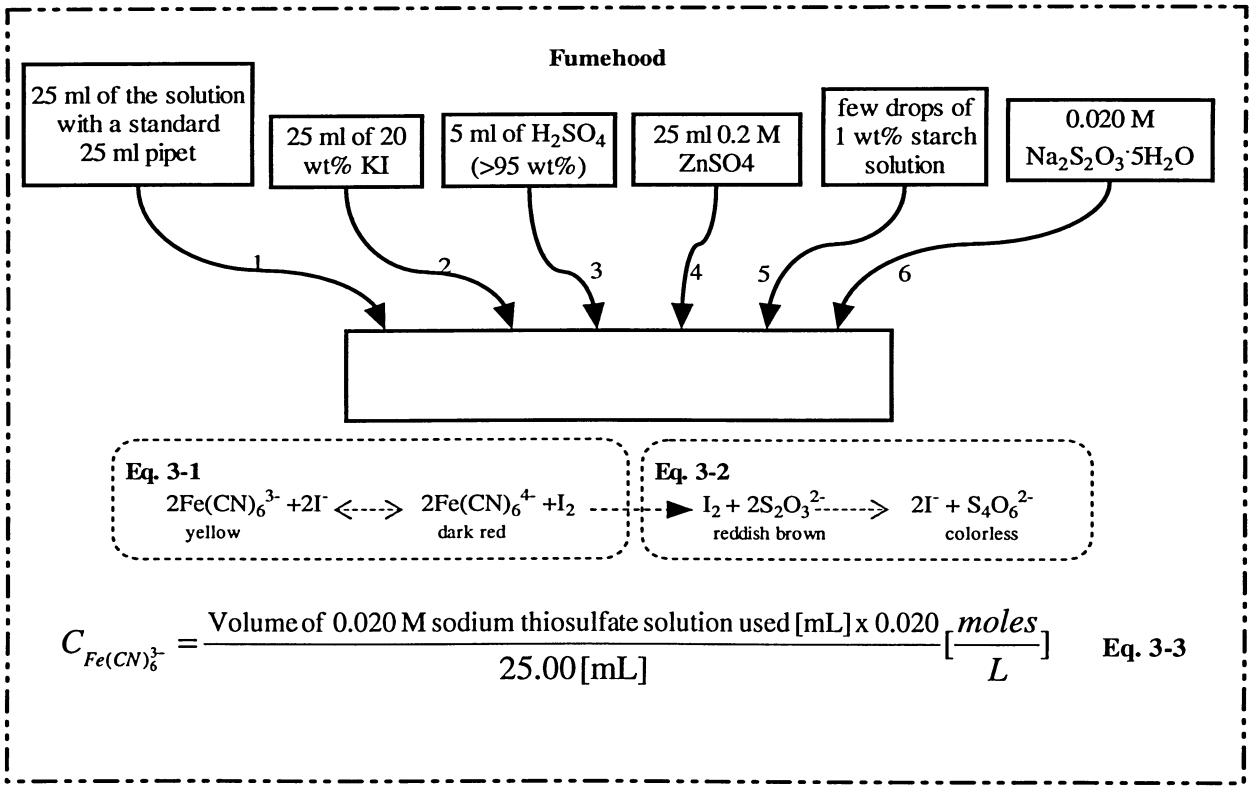

Fig. 3-12. Procedure of ferricyanide determination.

After that, a few drops of 1 wt% starch indicator was added into the solution. Due to the formation of starch-iodine complexes, the solution turned from dark red to reddish brown. Finally, the solution was titrated with 0.020 M sodium thiosulphate solution ($Na_2S_2O_3 \cdot 5H_2O$) until the colorless endpoint was reached, as shown in Eq. 3-2. According to chemical stoichiometry, the concentration of ferricyanide could be determined by Eq. 3-3.

Although the presence of a higher acid concentration and an excess amount of KI tended to shift the reaction to the right, an addition of 25 ml 0.2 M zinc sulphate ($ZnSO_4$) was recommended in order to eliminate any uncertainty in the determination of the concentration of ferricyanide [109]. The reaction formed a non-soluble substance (zinc ferrocyanide) as shown in Eq. 3-4.

$$2Zn^{2+} + [Fe(CN)_6]^{4-} \longrightarrow Zn_2Fe(CN)_{6(S)} \qquad \text{Eq. 3-4}$$

3.3.2. Other Physical Properties (Viscosity and Diffusivity)

Physical properties of the electrolyte solution such as ferri-/ferrocyanide redox couple have been widely studied by many workers [93,94,110,111]. They are a function of temperature and composition of electrolytes.

Although diffusivity and viscosity all fit exponential law with respect to temperature, the thermal effects were opposite to each other. The diffusion coefficients increased with increases in temperature, while the viscosity decreased with increases in temperature. Additionally, the diffusion coefficient increased as the total ionic strength decreased [110].

Based on the experimental results of Bazan and Arvia [110], the diffusion coefficient showed a slight dependence on the concentration of the diffusing species, tending to a very slow decrease when concentration was increased.

Gostick [61] did a regression on the experimental data and correlated the factors of temperature and concentrations for calculating the viscosity and diffusivity of ferri-/ferrocyanide/NaOH system. The equations and the regression constants for predicting the viscosity and diffusivity are given in Eq. 3-5, Eq. 3-6 and Table 3-4. These equations were verified with the experimental data of Bazan and Arvia [110]. The errors in diffusivity and kinetic viscosity prediction were less than 2% and 2.5%, respectively. Based on the physical properties obtained by these two equations, the value of Schmidt number was calculated around 1500.

$$v = A_0 + A_1 C_{NaOH} + A_2 (C_{NaOH})^2 + A_3 C_{Ferri} + A_4 (C_{Ferri})^2 + A_5 C_{Ferro} + A_6 (C_{Ferro})^2 + A_7 T + A_8 T^2 + A_9 C_{NaOH} C_{Ferri} + A_{10} C_{NaOH} C_{Ferro} + A_{11} C_{NaOH} T + A_{12} C_{Ferri} C_{Ferro} + A_{13} C_{Ferri} T + A_{14} C_{Ferro} T \quad [m^2 s^{-1}] \qquad \text{Eq. 3-5}$$

$$D_v = B_0 + B_1 C_{NaOH} + B_2 (C_{NaOH})^2 + B_3 C_{Ferri} + B_4 (C_{Ferri})^2 + B_5 C_{Ferro} + B_6 (C_{Ferro})^2 + B_7 T + B_8 T^2 + B_9 C_{NaOH} C_{Ferri} + B_{10} C_{NaOH} C_{Ferro} + B_{11} C_{NaOH} T + B_{12} C_{Ferri} C_{Ferro} + B_{13} C_{Ferri} T + B_{14} C_{Ferro} T \quad [m^2 s^{-1}] \qquad \text{Eq. 3-6}$$

Table 3-4. Equation constants for calculating the kinetic viscosity and diffusivity [61].

Constants in Eq. 3-5					Constants in Eq. 3-6			
A_0	-3.792E-05	A_8	-4.878E-10		B_0	3.662E-08	B_8	4.545E-13
A_1	-7.775E-10	A_9	-7.414E-12		B_1	6.663E-13	B_9	-3.658E-16
A_2	4.892E-14	A_{10}	6.391E-12		B_2	2.436E-17	B_{10}	-2.348E-16
A_3	2.877E-06	A_{11}	2.815E-12		B_3	-1.371E-09	B_{11}	-2.828E-15
A_4	-7.593E-12	A_{12}	1.777E-10		B_4	3.419E-16	B_{12}	-1.719E-14
A_5	-2.745E-06	A_{13}	-9.658E-09		B_5	1.332E-09	B_{13}	4.608E-12
A_6	-1.463E-10	A_{14}	9.215E-09		B_6	1.606E-14	B_{14}	-4.474E-12
A_7	2.759E-07				B_7	-2.556E-10		

4. Results and Discussion

The data obtained for both liquid distribution measurement (LDM) and local mass transfer coefficient measurement (MTM) are tabulated in Appendix D and E.

4.1. Reproducibility of Experimental Data

Reproducibility of experimental results is an important aspect for assessing the validity of the experimental data for different operational and repacking conditions. Therefore, the reproducibility of the experimental result was evaluated.

Reproducibility tests were carried out for various liquid and gas flow rates at different packed bed heights for three liquid distributors. Fig. 4-1 presents the results of duplicate runs for liquid distribution measurement with the ladder-type liquid distributor (LLD) at the packing height of 1.0 m (x/D = 3.28). In this paper, the particle-fluid Reynolds number was calculated by using the liquid superficial velocity and the equivalent diameter, which equals to the diameter of a sphere having the same surface area as the packing. In Fig. 4-1 the relative velocity of liquid (V/V_{av}) is plotted against the dimensionless radial position (r/R). V is the average volumetric flow rate of liquid to the collecting cells that have the same radial distance to the center of the bed cross section. V_{av} is the average volumetric flow rate of liquid to all collecting cells. It was found that the liquid volume obtained for C01 varied widely due to only one cell in the center region, as shown in Fig. 3-5b. In order to better represent the liquid distribution in the center region, an average value was used for both r/R = 0 and 0.25. This average value was obtained from the average of liquid flow

PROPERTY OF
RYERSON UNIVERSITY LIBRARY

rates to seven cells (C01 and I02 - I07). If liquid is uniformly distributed across the bed, the liquid relative velocity should have the value of 1.0, as the dashed line shown in Fig. 4-1. The deviation of the liquid velocity profile from the dashed line provides a measure of the degree of liquid maldistribution.

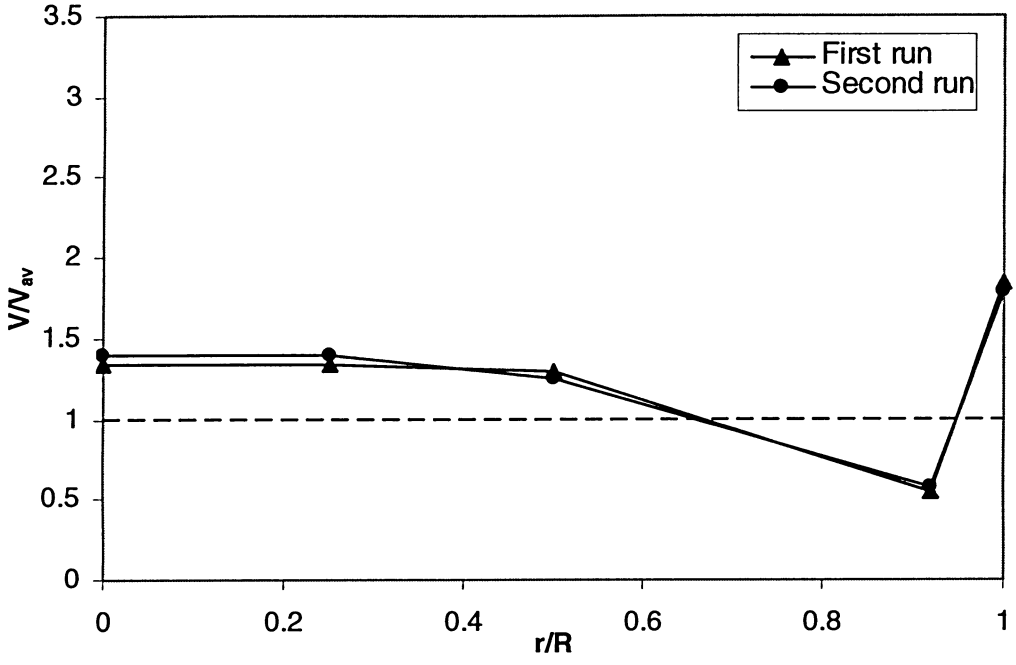

Fig. 4-1. Radial profiles for liquid distribution reproducibility test, LLD, x/D = 3.28, Re = 194 and G = 0.9 kg m^{-2} s^{-1}.

For mass transfer coefficient measurements, similar reproducibility tests were conducted. In Fig. 4-2, $(Sh/Sc^{0.33})_r$ of the ordinate is the average value of the dimensionless groups for all the sampling cathodes at the same radial position at a certain x/D.

For LLD, the largest percent differences between the two runs were 4.4% and 3% for LDM and MTM, respectively. This can be considered acceptable for these pilot-scale experiments. Similar results of the reproducibility tests were obtained with the single-point liquid distributor (SPLD) (5.6% and 3.6% for LDM and MTM, respectively) and the cross-type liquid distributor (CLD) (4.9% and 3.2% for LDM and MTM, respectively).

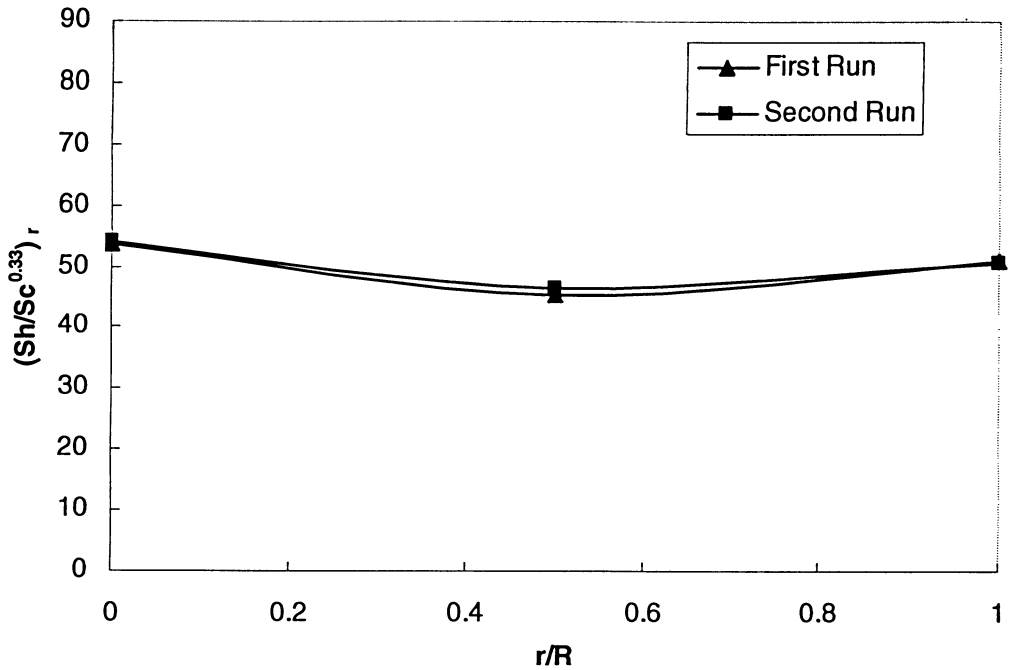

Fig. 4-2. Radial profiles for mass transfer reproducibility test, LLD, x/D = 3.5, Re = 194 and G = 0.

In order to investigate the effect of repacking on liquid distribution, the packing was redumped three times to 1-m height. The variations of liquid velocity profiles due to repacking are shown in Fig. 4-3. For LLD, the largest percent deviation from the mean value of the liquid relative velocity for the three tests was 5.3%. Similar tests were conducted on mass transfer coefficient measurements. It is worth noting that in order to keep the positions of sampling cathodes only the packings over the sampling layer were repacked. The result for LLD is illustrated in Fig. 4-4. The largest percent difference of $Sh/Sc^{0.33}$ value from the mean value of the three tests was 3.1%. The variations of LDM and MTM with repacking were also obtained with SPLD (7% and 3.8% for LDM and MTM, respectively) and CLD (5.6% and 3.2% for LDM and MTM, respectively).

The reproducibility tests for different runs and repacking show a low deviation in the data obtained for replicate runs. This indicates that the present

experimental setup can be used reliably to measure liquid and mass transfer distribution.

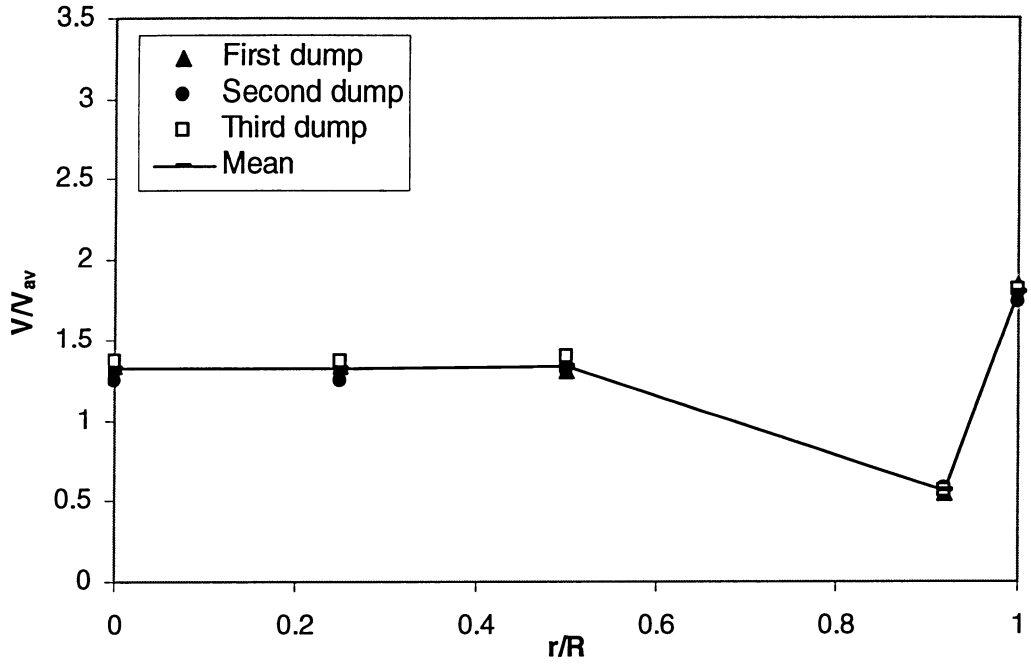

Fig. 4-3. Effect of repacking on LDM, LLD, x/D = 3.28, Re = 194 and G = 0.9 kg $m^{-2} s^{-1}$.

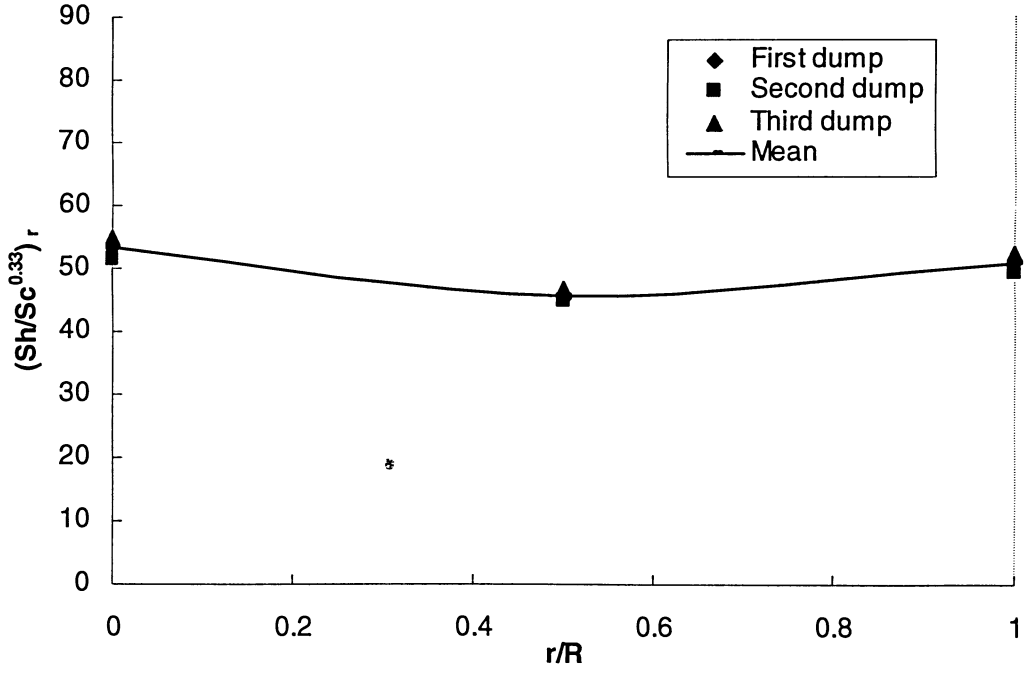

Fig. 4-4. Effect of repacking on MTM, LLD, x/D = 3.5, Re = 194 and G = 0.

4.2. Effects of Design and Operational Parameters on LDM and MTM

The performance of the packed column is affected by many factors. In the present study, in order to demonstrate the relationship between liquid distribution and local mass transfer behavior clearly, the effects of several factors such as initial liquid distribution, liquid and gas flow rate were studied.

4.2.1. Effects of Liquid Distributor Design on LDM and MTM

Although the initial liquid distribution will develop to an equilibrium flow pattern sooner or later in the column no matter which liquid distributor is employed [7], it will affect the mass transfer process, especially in the upper section of the packed bed. In the present study, three different liquid distributor designs were used to investigate the effect of initial liquid distribution on the quality of liquid distribution over the whole bed.

Fig. 4-5 shows a comparison of the radial profiles of liquid relative flow rate obtained with three liquid distributors at four bed heights. From Fig. 4-5, it can be seen that the liquid velocity profiles for these three liquid distributors vary significantly with the radial position, especially for that obtained by SPLD. For LLD and CLD, the liquid velocity profiles exhibit less fluctuation in the bulk region of the packed bed than that for SPLD.

Moreover, the difference between the liquid velocity profiles obtained with these liquid distributors becomes smaller as the packing height increases. The non-uniform liquid distribution over the top of the packing generated by SPLD is smoothed out gradually along the bed height. This indicates that the packing has the ability to spread the liquid flow radially.

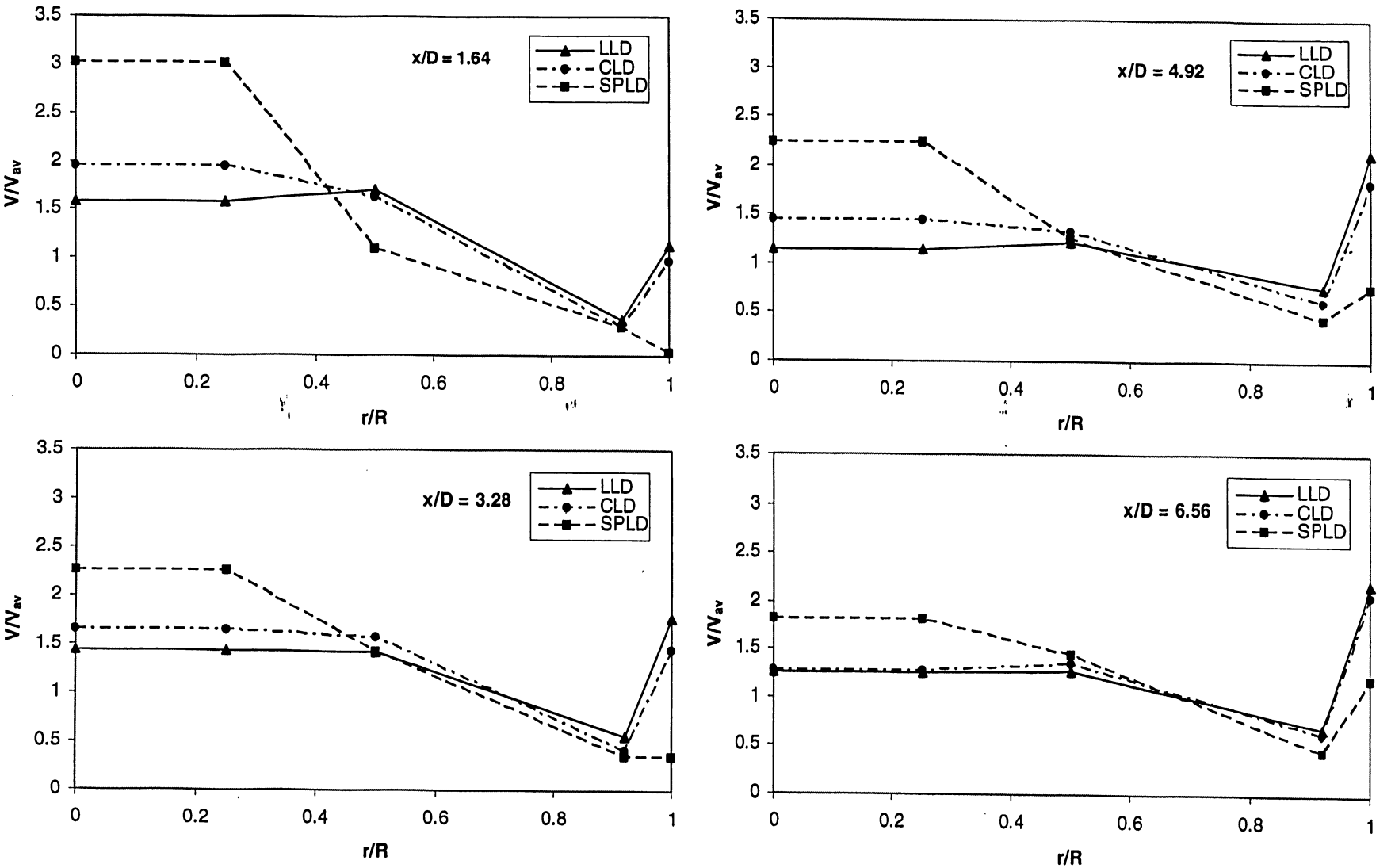

Fig. 4-5. Effect of initial liquid distribution on liquid distribution for different liquid distributor designs, Re = 194 and G = 0.

As shown in Fig. 4-5, at x/D = 1.64, the liquid flow in the bulk region is higher than that in wall region. At this height, there was almost no wall flow observed for SPLD. With increases in the packing height, wall flow increased while the flow rate in bulk region decreased. For LLD, as can be seen in Fig. 4-6, the liquid velocity profiles for x/D = 4.92 and 6.56 are very close. The largest percent difference between the two profiles is 10.2%. However, the liquid velocity profile for x/D = 4.92 is slightly closer to the dash line than that for x/D = 6.56. This indicates that liquid distribution for LLD might become deteriorated in the region of x/D = 6.56. This phenomenon has been observed by several researchers. In order to improve the overall liquid distribution, it was proposed by Eckert [37] and Striggle [38] that for small-diameter columns (< 0.5 m), a redistributor should be considered to install at x/D within the range of 5 to 10.

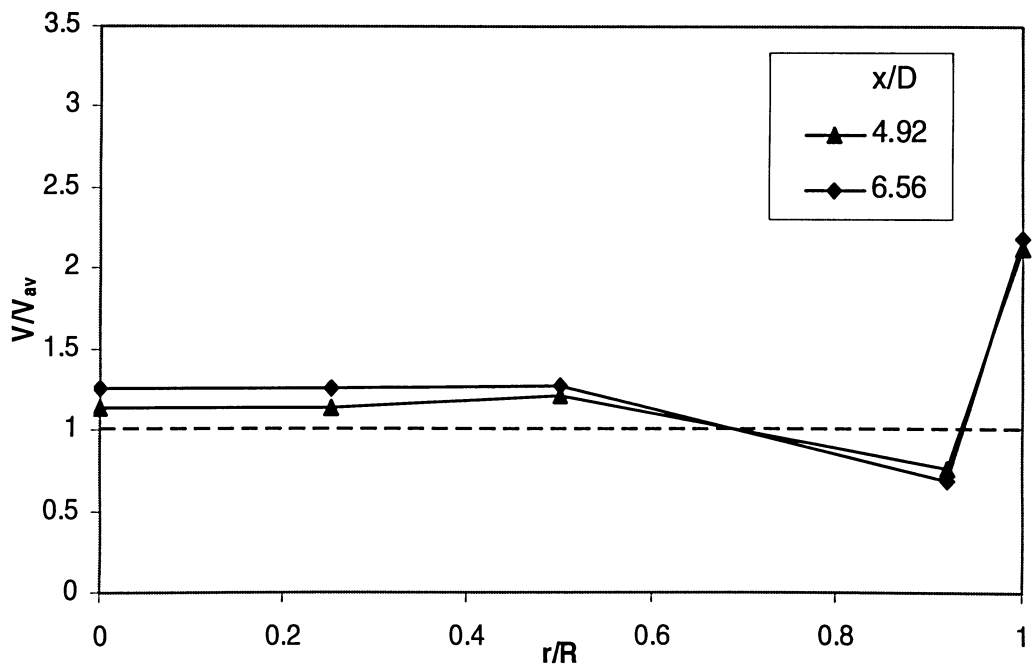

Fig. 4-6. Comparison of liquid velocity profiles for LLD at two axial positions, Re = 194 and G = 0.

Based on this analysis, it can be concluded that for LLD, the liquid distribution fully developed around x/D = 4.92. This stable liquid flow pattern is also referred to as liquid natural flow [1,7,12].

For CLD, the equilibrium liquid flow pattern was established at x/D = 6.56 as can be seen in Fig. 4-5. However, for SPLD, the liquid flow pattern did not reach equilibrium even at x/D = 6.56. This indicates that the more uniform the initial liquid distribution, the less the packing height needed to reach the fully developed flow pattern.

Although liquid distribution in packed beds can reflect how it performs, the performance of columns is assessed in the final analysis of the mass transfer efficiency.

Fig. 4-7 illustrates the radial profiles of mass transfer coefficients for three liquid distributor designs at different axial positions.

For SPLD, the local mass transfer rate was highest in the center section but almost zero in the outer section at x/D = 1.0. This indicates that almost no liquid reached to the outer section at x/D = 0.5 and 1.0. This can be attributed to the fact that SPLD only has one central liquid delivery point, which concentrates all liquid flow to the central region of the packed bed.

On the other hand, the radial mass transfer profiles for LLD and CLD demonstrate much less radial dependence due to their better initial liquid distribution abilities as shown in Fig. 4-5. The profiles only vary significantly in the inner section (r/R = 0.5). At the top of the column the local mass transfer coefficient in the inner section was higher than those at the center and outer sections. This might have resulted from the design of multipoint liquid distributors and the angular position of the liquid distributor to the cathodes in

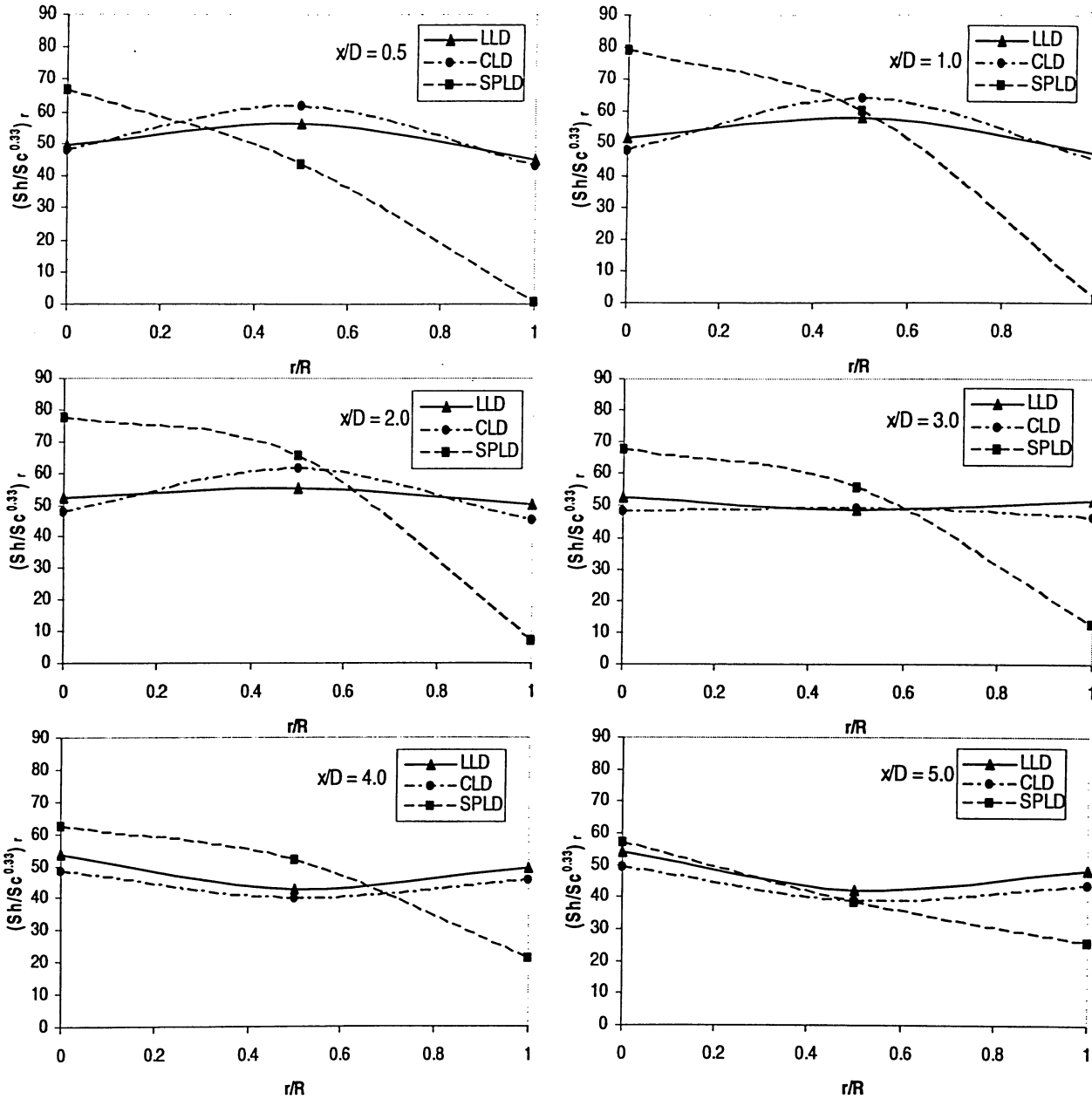

Fig. 4-7. Radial profiles of mass transfer coefficients at various axial positions for different liquid distributor designs, Re = 194 and G = 0.

column. The effect of angular position on LDM and MTM will be discussed in Section 4.2.5. With increases in the packing height, the coefficients declined in the inner section probably due to liquid spreading and the loss of liquid velocity.

In order to better observe the variation of local mass transfer coefficients in the column, the axial profiles for three liquid distributors at three different radial positions are plotted in Fig. 4-8, Fig. 4-9 and Fig. 4-10.

For the multipoint liquid distributors (i.e. LLD and CLD), the mass transfer coefficients of both center and outer cathodes had little dependence on axial positions. On the other hand, the local mass transfer coefficient at inner cathodes decreased significantly with the distance down the column due to the loss of liquid velocity after a slight rise attributed to a gain in cathode wetting at the top of the column. The coefficients, however, became relatively unchanged for fully developed flow pattern that was established at x/D in the range of 4 to 5. For SPLD, the coefficients of the inner cathodes peak around x/D = 2.0 and then declined with the distance down the column. Along the packed bed height, the mass transfer coefficient decreased in the center region but increased continuously in the outer section due to liquid spreading out and the development of wall flow. This is in agreement with the findings of liquid distribution measurements.

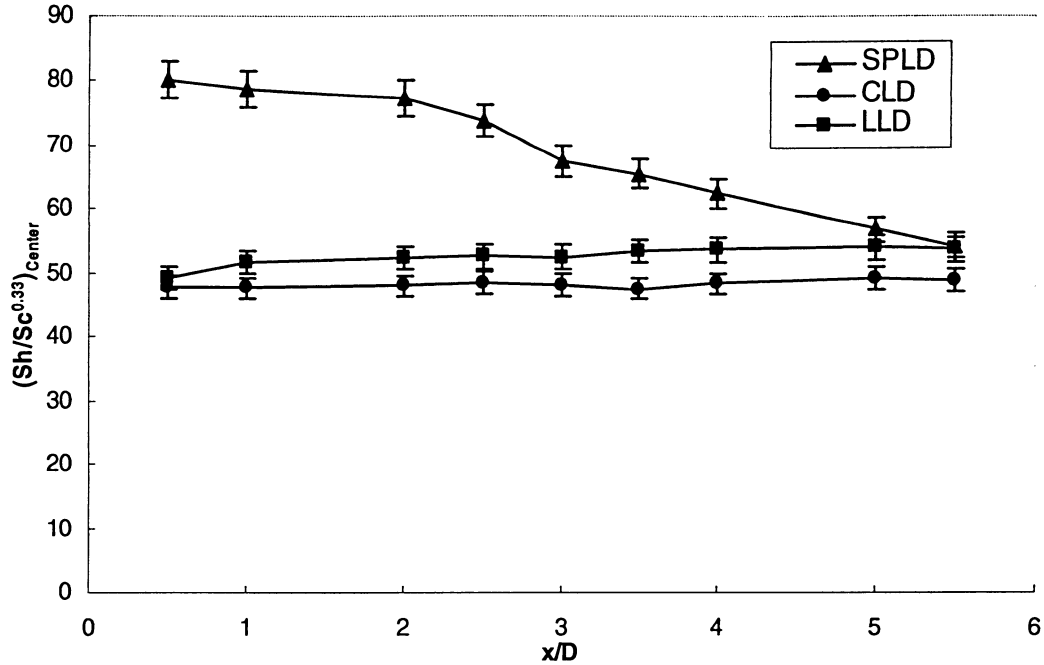

Fig. 4-8. Axial profiles of mass transfer coefficients of center cathodes (r/R = 0), Re = 194 and G = 0.

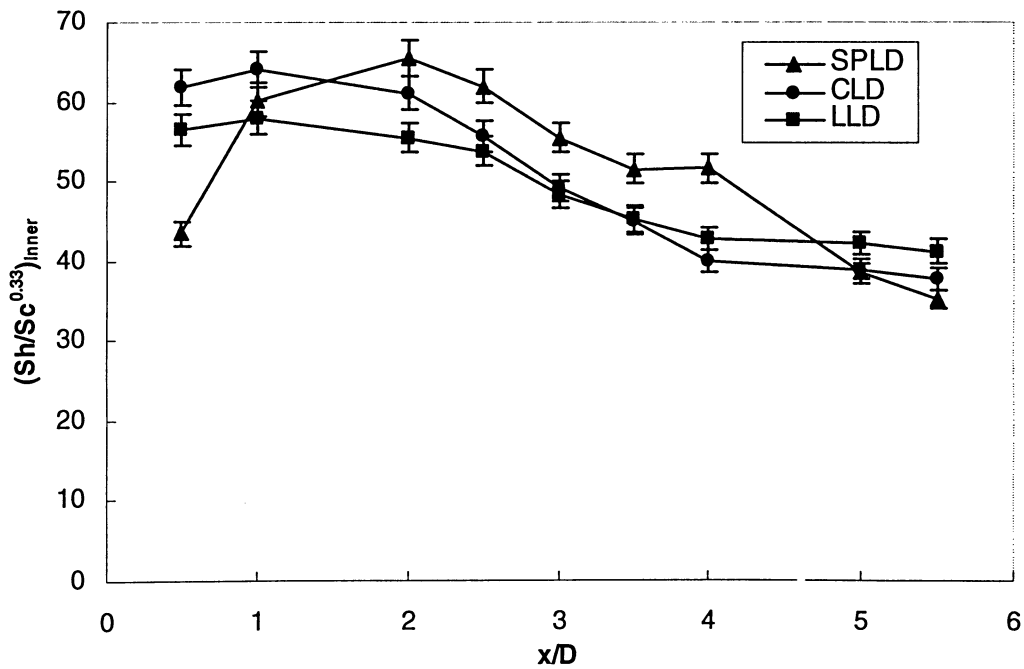

Fig. 4-9. Axial profiles of mass transfer coefficients of inner cathodes (r/R = 0.5), Re = 194 and G = 0.

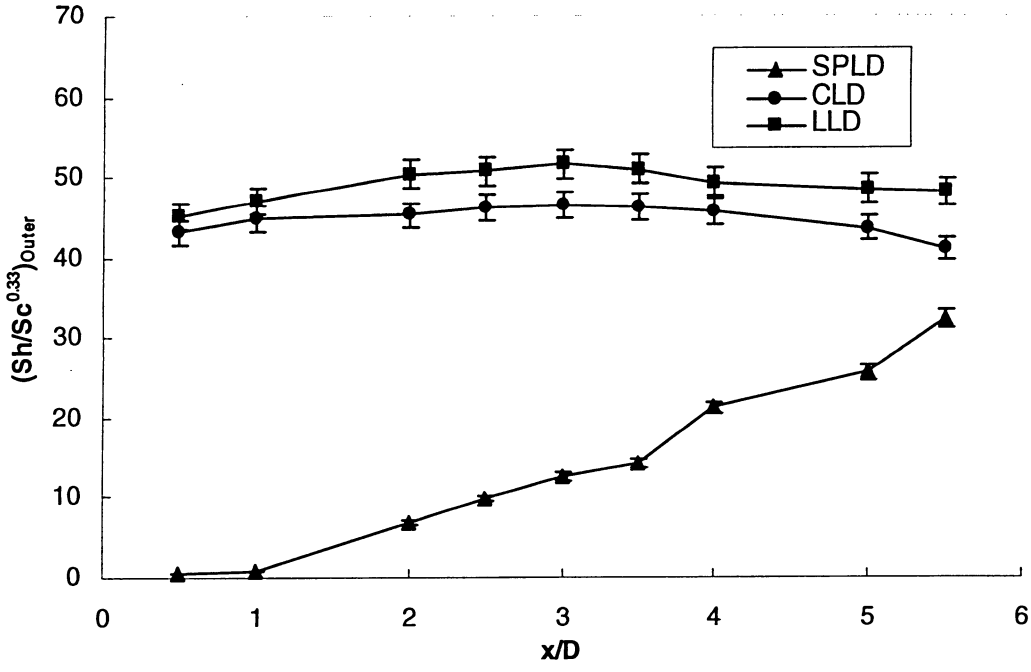

Fig. 4-10. Axial profiles of mass transfer coefficients of outer cathodes (r/R = 1.0), Re = 194 and G = 0.

4.2.2. Effect of Liquid Flow Rate on LDM and MTM

In liquid distribution measurement, the liquid flow rate was varied from 2.6 to 7.8 kg m^{-2} s^{-1} ($97 \leq Re \leq 291$). Fig. 4-11 illustrates the effect of liquid flow rate on liquid radial distribution at x/D = 6.56 with LLD. The liquid distribution profiles were smoothed out slightly with increases in liquid flow rate. This indicates that increasing liquid flow rate improves the uniformity of liquid distribution slightly.

This phenomenon can be explained as follows. When the packing in the column was well wetted, a rise in liquid flow rate increased the thickness of the liquid film on the packing surface, and the liquid holdup increased accordingly. This rise in the liquid film thickness with increases in the liquid flow rate might occur proportionally within the packing, thus liquid distribution was not affected significantly in the bulk region. However, the drag force of the packing

elements on liquid reduced slightly with increases in the thickness of liquid film on the packing surface, and hence, the relative liquid velocity decreased slightly in the bulk region.

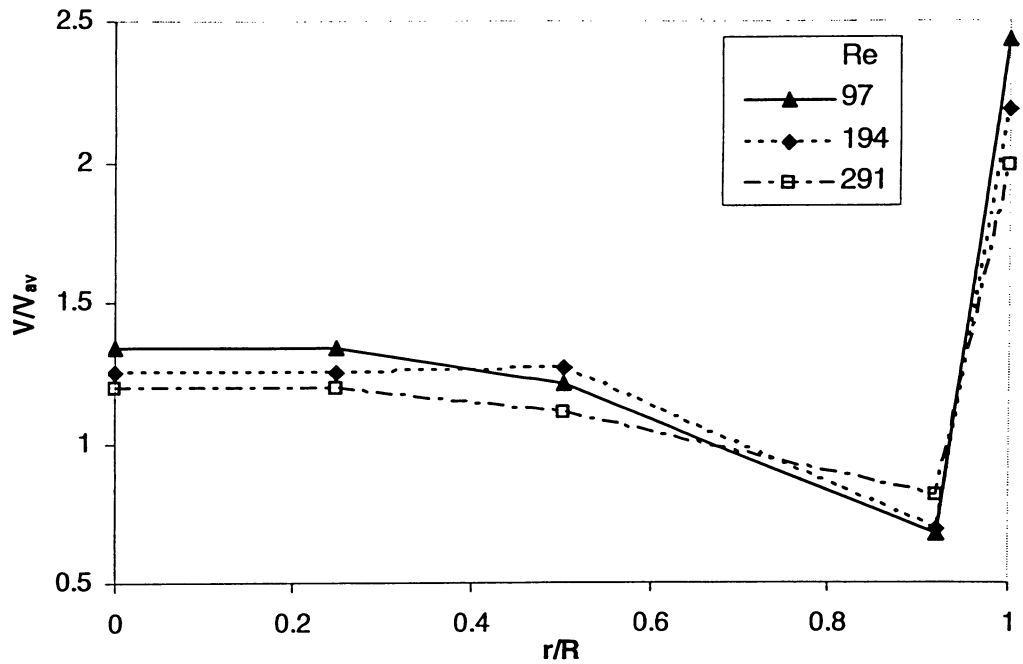

Fig. 4-11. Effect of liquid flow rate on liquid radial distribution, LLD, x/D = 6.56 and G = 0.

In addition, it was found that the liquid wall flow reduced slightly with increases in liquid flow rate. This can be attributed to the increases in liquid hold-ups within the packing resulted from the increases in the liquid loading. This observation is in agreement with the findings reported by Templeman and Porter [104,105], Yin *et al.* [12] and Kouri and Sohlo [7].

Fig. 4-12 illustrates the trends of the relative liquid velocity profiles for LLD at various Reynolds numbers. For the center section (r/R = 0.25), the values of V/V_{av} decreased slightly with increases in Reynolds number.

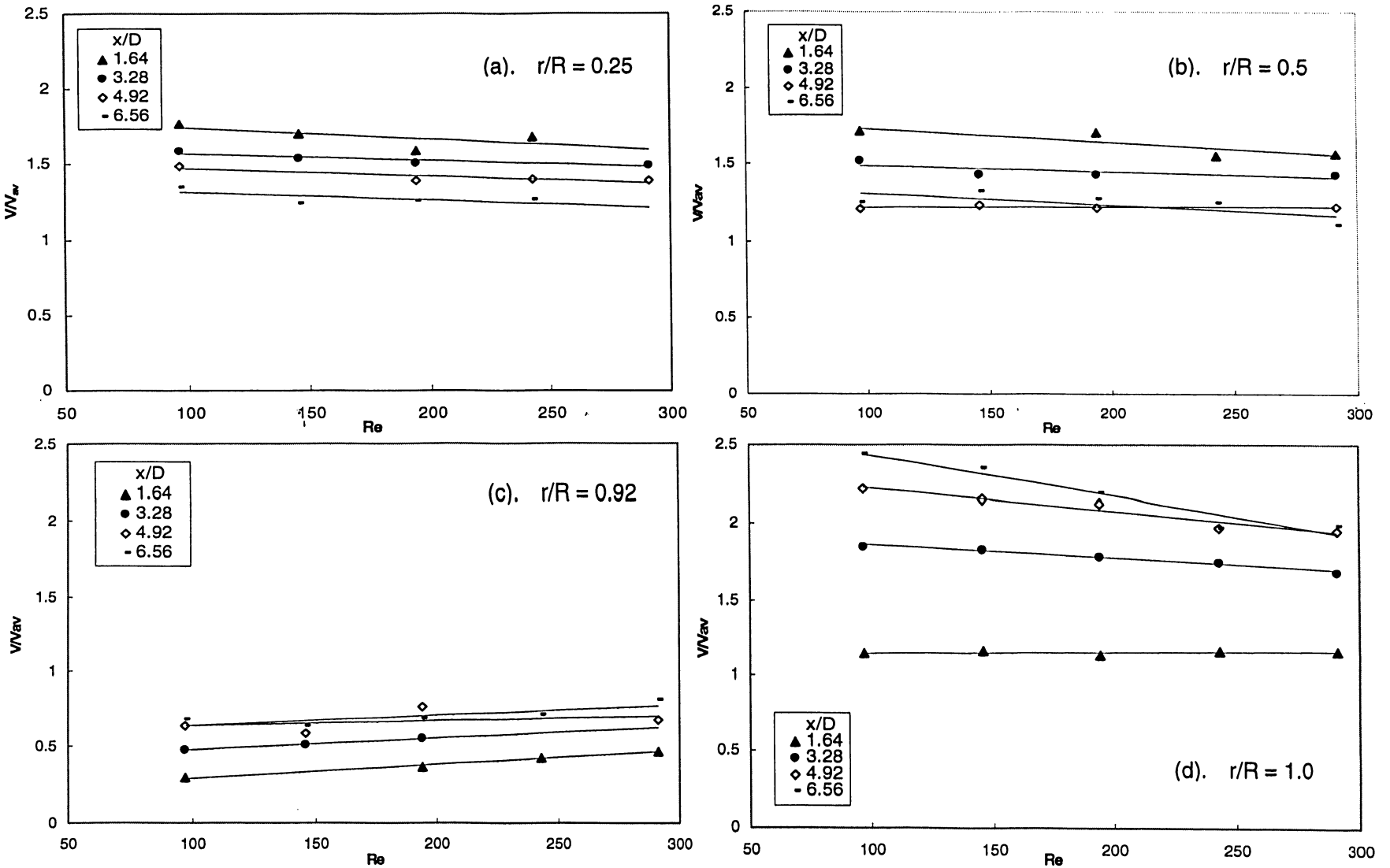

Fig. 4-12. Effect of liquid flow rate on relative liquid velocity along packing height at four radial positions, LLD.

It is more accurate to say that the values of V/V_{av} were closer to 1.0. This indicates that liquid spreading enhanced when liquid flow rate increased. Similar trends were also observed for the inner (r/R = 0.5) and outer sections (r/R = 0.92).

However, for the wall region (r/R = 1.0), the values of V/V_{av} were getting further away from 1.0 along the bed height due to the development of wall flow. Similar results for CLD and SPLD are shown in Appendix C.

Fig. 4-13 shows the effect of liquid flow rate on liquid wall flow development. The liquid wall flow reaches its fully developed state earlier at a higher liquid flow rate than at a lower one. This result is expected. Similar results were also obtained for CLD as demonstrated in Appendix C. However, for SPLD, the flow was still far away from the fully developed state even at x/D = 6.56 and Re = 291 as shown in Appendix C.

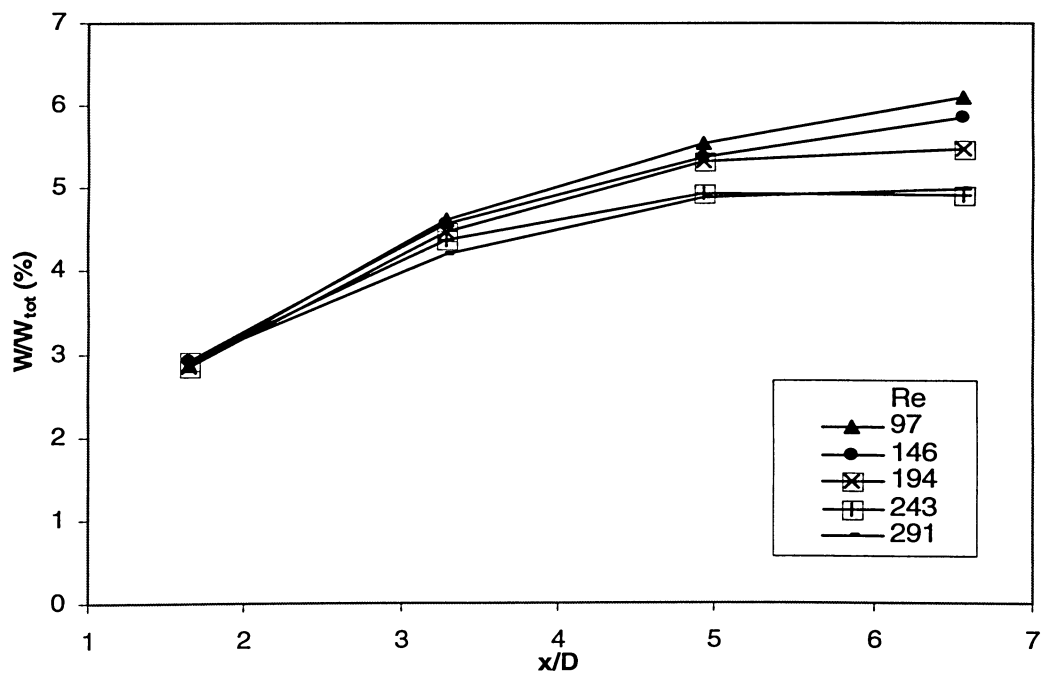

Fig. 4-13. Effect of liquid flow rate on wall flow development along packing height, LLD.

Similarly, the effect of liquid flow rate on local mass transfer behavior was also investigated. Fig. 4-14 shows the variation of mass transfer coefficients at various Reynolds numbers with LLD at x/D = 5.5 in absence of gas. It can be seen that the mass transfer rate increased slightly with increases in Re. This is not unexpected because the higher liquid flow rate results in the higher local Reynolds number, and hence, enhances the local mass transfer process at the surface of the electrodes. Similar trends were observed by Gostick *et al.* [61-63] and Gabitto and Lemcoff [112].

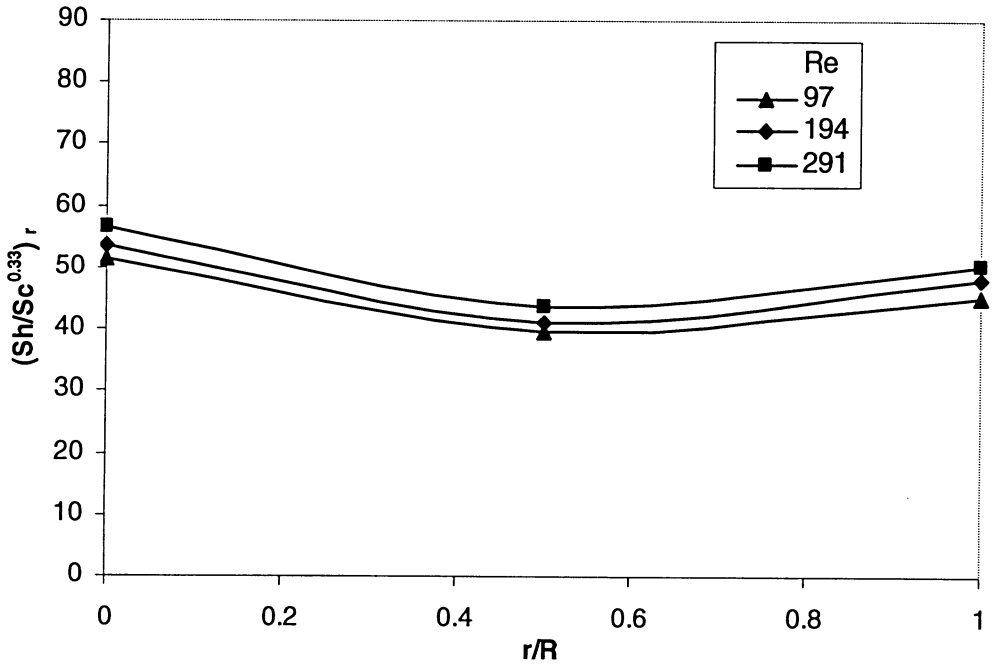

Fig. 4-14. Radial profiles of mass transfer coefficients at various Reynolds numbers, LLD, x/D = 5.5 and G = 0.

In addition, in order to address the effect of the liquid flow rate on the mass transfer coefficient more clearly, Fig. 4-15, Fig. 4-16 and Fig. 4-17 demonstrate the axial profiles of mass transfer coefficients at various Reynolds numbers for three liquid distributors used. It can be seen that for all three liquid distributors, the mass transfer coefficients increased with increases in liquid flow rate. For

CLD and LLD (Fig. 4-16 and Fig. 4-17), the profiles have similar shapes at different liquid flow rates.

On the other hand, for SPLD (Fig. 4-15), the profile at the low liquid flow rate (i.e. Re = 97) differs from others with higher liquid flow rates. For SPLD, liquid was delivered initially at the center of the column. The liquid radial distribution was thus mainly dependent on the self-distribution ability of the packing elements and liquid momentum to break up liquid to smaller streams. At low liquid flow rates, liquid concentrated intensive in the zone where it was sprayed directly. Less liquid streams were thus formed contributing to its lower liquid momentum. Moreover, the drag force of packing elements on liquid lessens the liquid radial distribution due to the thinner liquid film on the wetted packing surface. When liquid flow rate is reduced to a certain value (a critical point), the mass transfer behavior changes, especially at the top of the column.

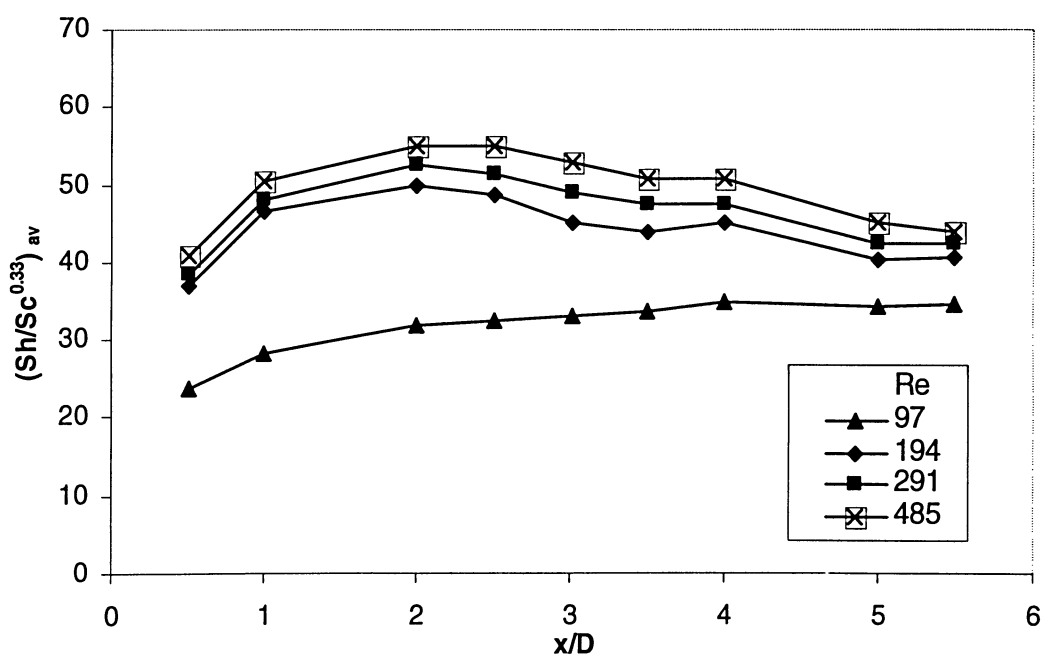

Fig. 4-15. Axial profiles of mass transfer coefficients at various Reynolds numbers, SPLD and G = 0.

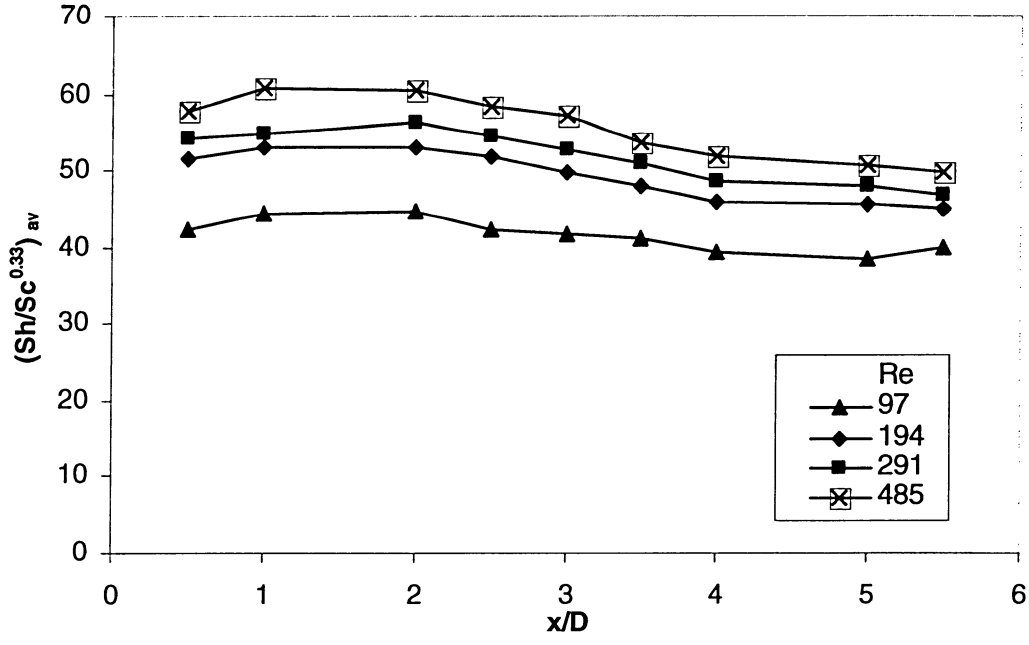

Fig. 4-16. Axial profiles of mass transfer coefficients at various Reynolds numbers, CLD and G = 0.

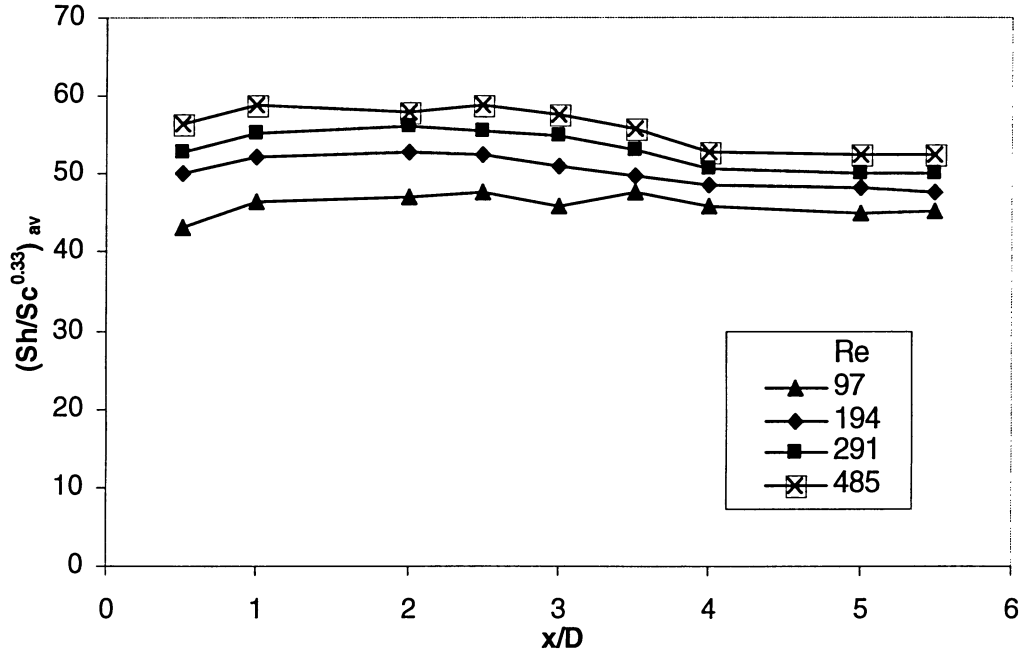

Fig. 4-17. Axial profiles of mass transfer coefficients at various Reynolds numbers, LLD and G = 0.

4.2.3. Effect of Gas Flow Rate on LDM and MTM

The hydrodynamic behavior for gas-liquid two-phase flow in a randomly packed column above the loading point is much different from that below the loading point. Generally, the operational condition of a packed column is maintained below the loading point. The loading point can be determined from a pressure drop profile in log-log scale plot of total pressure drop as a function of the gas flow rate at which the slope starts rising over a value of 2 [12]. The loading point can also be predicted by using the pressure drop correlations such as equations from Robbins [113] and Leva [114]. The gas flow rate used in the present study (i.e. 0.9 kg $m^{-2} s^{-1}$) is much lower than the loading point (i.e. 2.2 kg $m^{-2} s^{-1}$), which is predicted by Robbins' equation for air/water system.

In the present study, liquid distribution was observed under a countercurrent gas-liquid flow. The effects of the gas flow rate on liquid distribution and liquid wall flow development are shown in Fig. 4-18 and Fig. 4-19, respectively. These results were all obtained with LLD. More attention has been given to the interaction between gas and liquid phases and the effect of the gas flow rate on liquid wall flow. Fig. 4-18 shows a comparison of liquid radial distribution profiles measured for two gas flow rates at x/D = 6.56 and Re = 194. It can be seen that the liquid velocity profiles remain similar for both cases. Analogous results were obtained by Kouri and Sohlo [7] and Yin *et al.* [12].

This conclusion is reconfirmed by Fig. 4-19 indicating similar wall flow with and without gas flow. Overall, it can be concluded that the interaction between gas and liquid phases is so weak that liquid distribution and wall flow development is only weakly dependent on the gas flow rate below the loading point.

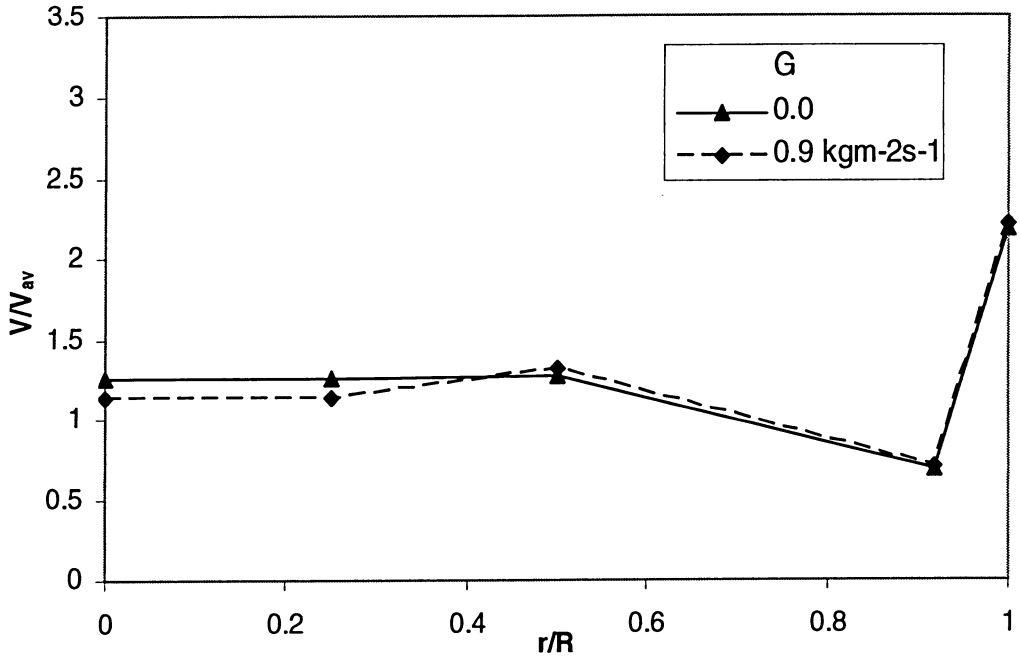

Fig. 4-18. Effect of gas flow rate on liquid radial distribution, LLD, x/D = 6.56 and Re = 194.

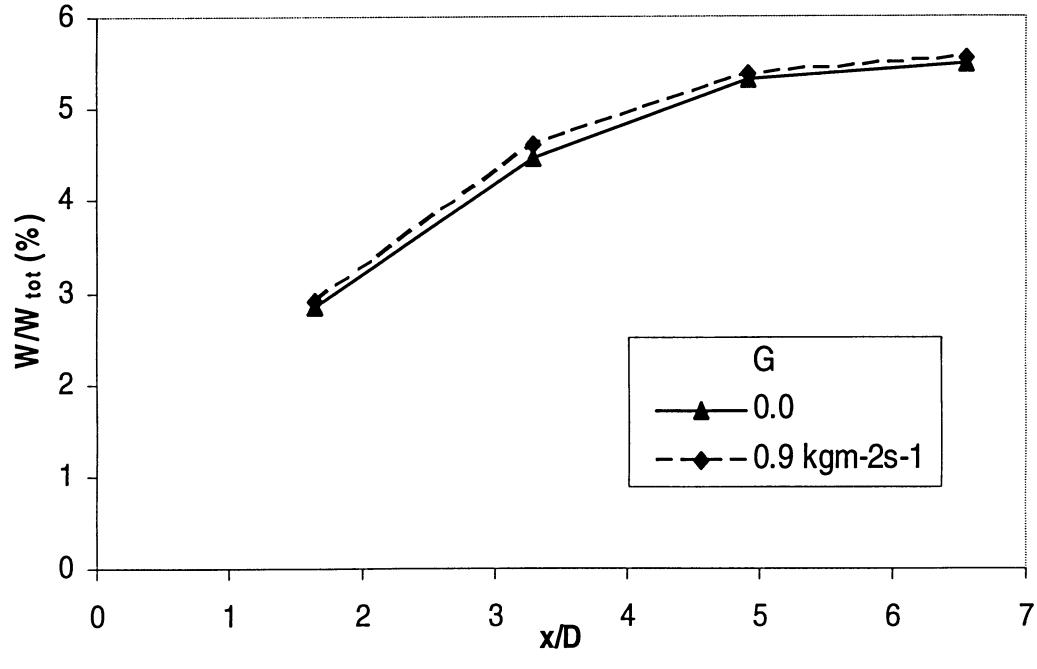

Fig. 4-19. Effect of gas flow rate on liquid wall flow development, LLD and Re = 194.

Similar trends were also observed for SPLD and CLD. The profiles for CLD and SPLD are given in Appendix C.

Fig. 4-20 shows the effect of the gas flow rate on the local mass transfer coefficient. It can be seen that the presence of the gas flow did not affect the local mass transfer coefficient significantly. This is in agreement with the observation of Delaunay *et al.* [115] and Bartelmus [116]. Using the electrochemical method, Delaunay *et al.* [115] stated that there was no influence of gas velocity on mass transfer. This phenomenon had also been observed by Bartelmus [116].

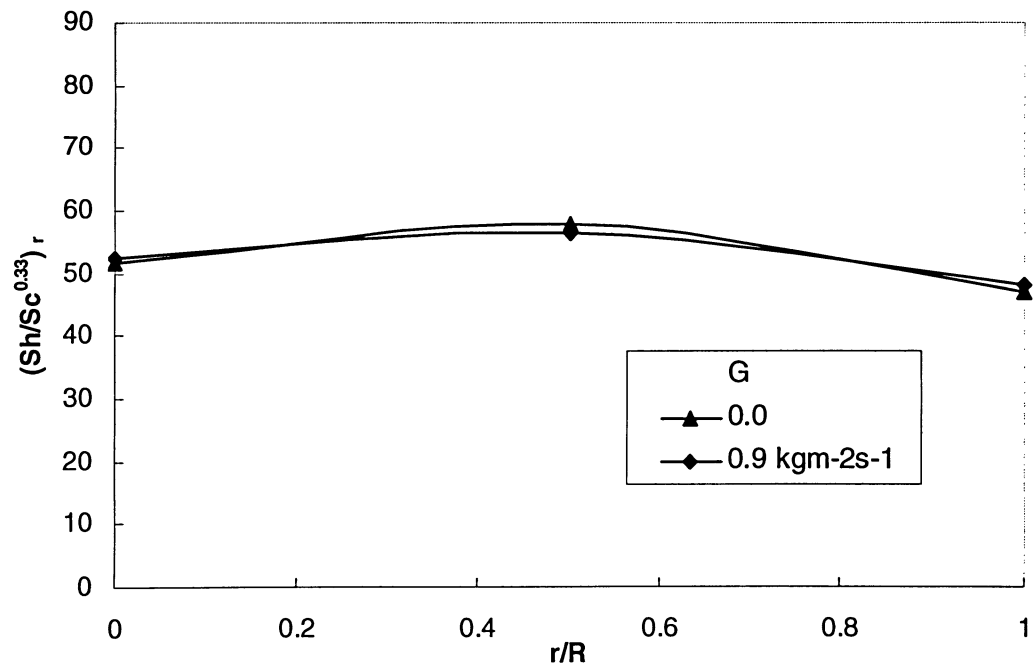

Fig. 4-20. Effect of gas flow rate on local mass transfer coefficients, LLD, x/D = 1.0 and Re = 194.

4.2.4. M_f and MT_{VAR}

Liquid maldistribution factor (M_f) is usually used to quantify the quality of liquid distribution through a packed bed. It is defined as an average standard

deviation of individual liquid flows collected in the liquid collecting cells as below:

$$M_f = \frac{1}{n}\sqrt{\sum_{i=1}^{n}\left(1-\frac{Q_i}{Q_{av}}\right)^2} \qquad \text{Eq. 2-1}$$

Fig. 4-21 illustrates the variation of M_f along the packed bed for three liquid distributors used in the present study. It can be seen from Fig. 4-21 that M_f decreases along the bed height and reaches a relatively constant value above a certain x/D. Accordingly, liquid maldistribution still exists even when a fully developed flow is established. It's the nature of liquid flow behaviour, which has long been observed in packed columns. Moreover, due to its higher uniformity on initial liquid distribution, M_f profile for LLD is lower and flatter than the other two. Therefore, in the present study, LLD has the best quality of liquid distribution through the packed bed.

In addition, the variations of M_f at various liquid flow rates for LLD, CLD and SPLD are shown in Fig. 4-22, Fig. 4-23 and Fig. 4-24, respectively. In Fig. 4-22, Fig. 4-23 and Fig. 4-24, the largest percent differences among the different packing heights for a certain Re are 23%, 35.1% and 79.3% for LLD, CLD and SPLD, respectively. The trend of M_f for various x/D and Re can be seen from Fig. C-9, Fig. C-10 and Fig. C-11 for LLD, CLD and SPLD, respectively in Appendix C. In general, for LLD and CLD, at a certain bed height, M_f is not affected significantly with the variation of the Reynolds number. However, for SPLD at x/D = 1.64, M_f is much higher at lower Reynolds numbers (e.g. 97). This indicates that the ability of the packing to spread out liquid was enhanced when the liquid flow rate was increased.

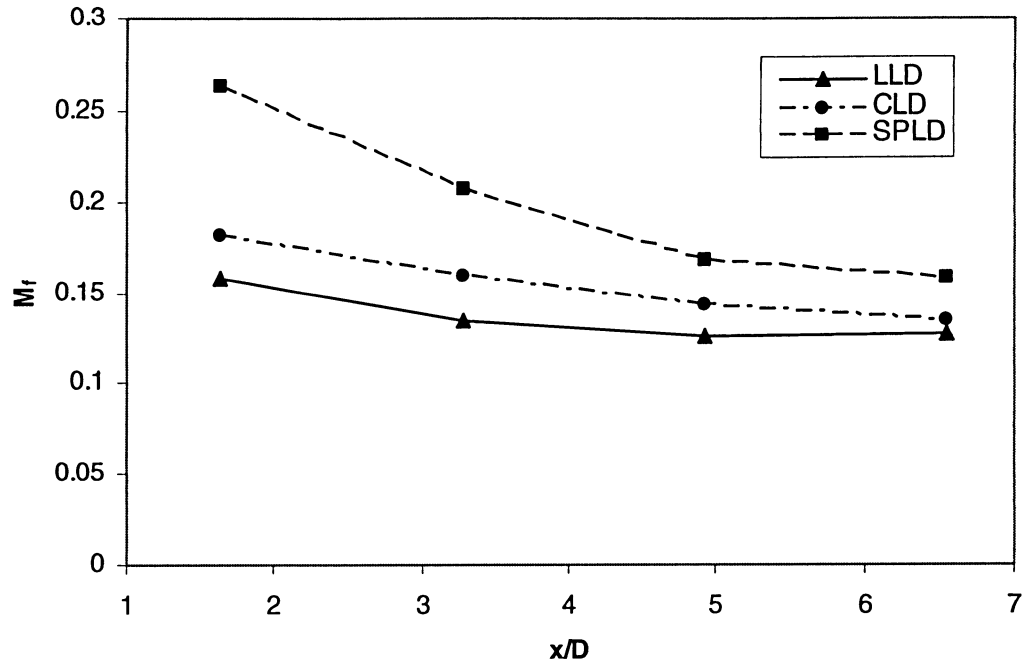

Fig. 4-21. M_f along packing heights for three liquid distributors, Re = 194 and G = 0.

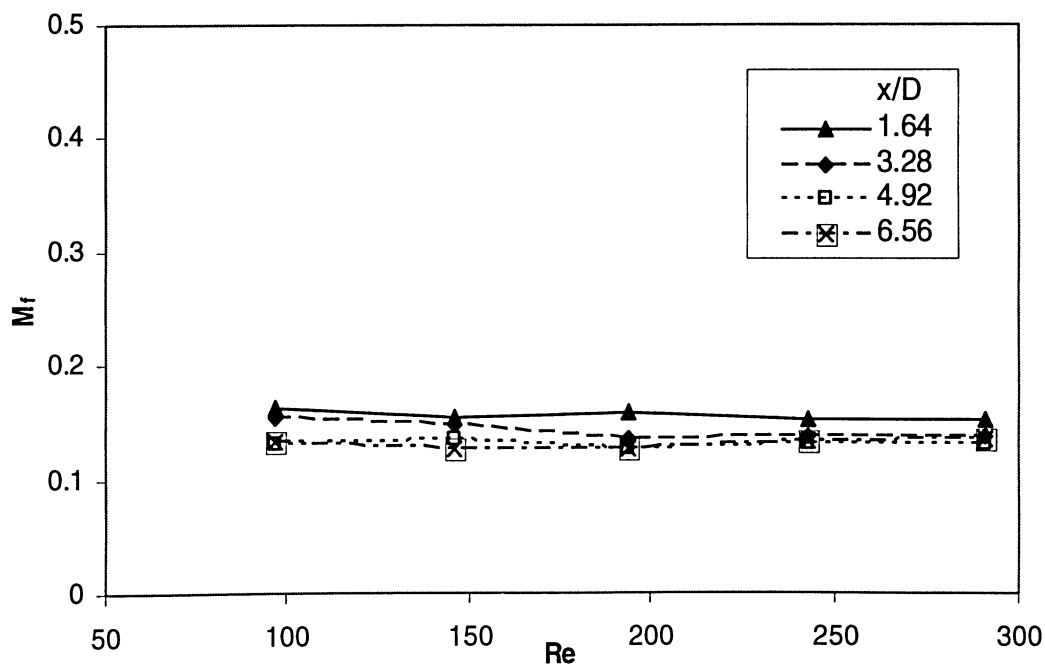

Fig. 4-22. Variation of M_f at various Reynolds numbers for different packing height, LLD and G = 0.

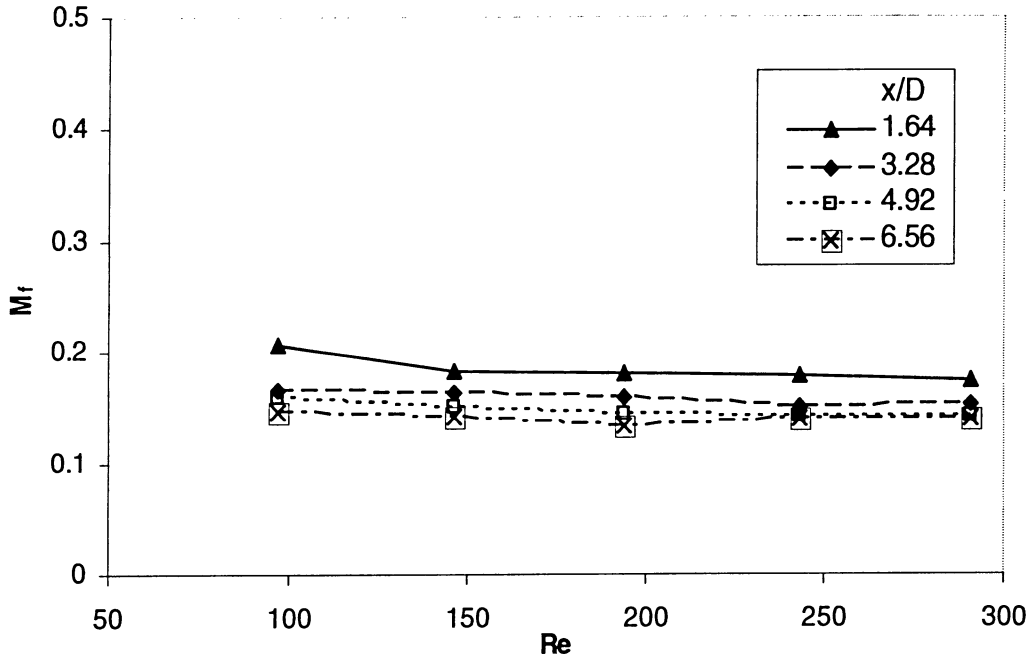

Fig. 4-23. Variation of M_f at various Reynolds numbers for different packing height, CLD and G = 0.

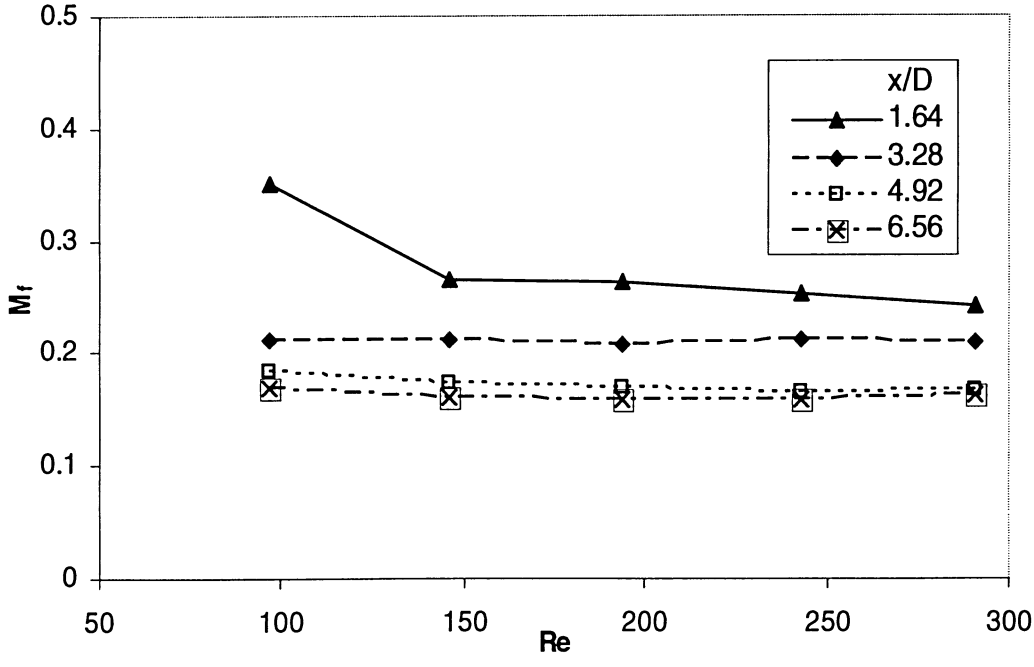

Fig. 4-24. Variation of M_f at various Reynolds numbers for different packing height, SPLD and G = 0.

Furthermore, below the loading point, due to the weak interaction between gas-liquid phases, the values of liquid maldistribution factors (M_l) are almost the same regardless of the presence of gas flow (0.9 kg m^{-2} s^{-1}) or not. For example, at Re = 194 and X/D = 3.28, the values of M_l with and without the gas flow (given inside brackets) are 0.13 (0.13), 0.15 (0.16) and 0.2 (0.21) for LLD, CLD and SPLD, respectively.

Similarly, in order to quantify the variation of the mass transfer coefficient in a packed bed, a mass transfer maldistribution factor (MT_{VAR}), which was defined by Gostick *et al.* [61-63], is given as:

$$MT_{VAR} = \frac{1}{n}\sum_{i=1}^{n}\left(\frac{\left|\left(Sh/Sc^{0.33}\right)_i - \left(Sh/Sc^{0.33}\right)_{av}\right|}{\left(Sh/Sc^{0.33}\right)_{av}}\right) \qquad \text{Eq. 4-1}$$

where n is the total number of sampling cathodes in the column, $(Sh/Sc^{0.33})_i$ is the value of the dimensionless groups at the i^{th} sampling cathode, and $(Sh/Sc^{0.33})_{av}$ is the mean value of the dimensionless groups for all sampling cathodes in the packed bed.

In the present study, MT_{VAR} was applied to calculate the mass transfer maldistribution. Fig. 4-25 shows the relative deviation of the mass transfer coefficient at various Reynolds numbers. For example, at Re = 388, MT_{VAR} for SPLD, CLD and LLD are approximately 0.46, 0.25 and 0.22, respectively.

MT_{VAR} - Re profiles for LLD and CLD fluctuate slightly around a relative constant value whereas for SPLD the profile declines with increases in liquid flow rate and levels out at Re about 291. This indicates that when liquid is better distributed at the top of the bed, the packings at all radial positions have been wetted to some extent. Although the increases in liquid flow rate enhances the mass transfer efficiency due to a higher liquid velocity at the packing surface, the improvement for each packing element is relatively even

due to the relatively uniform initial liquid distribution. Therefore, the variation remains at a certain level.

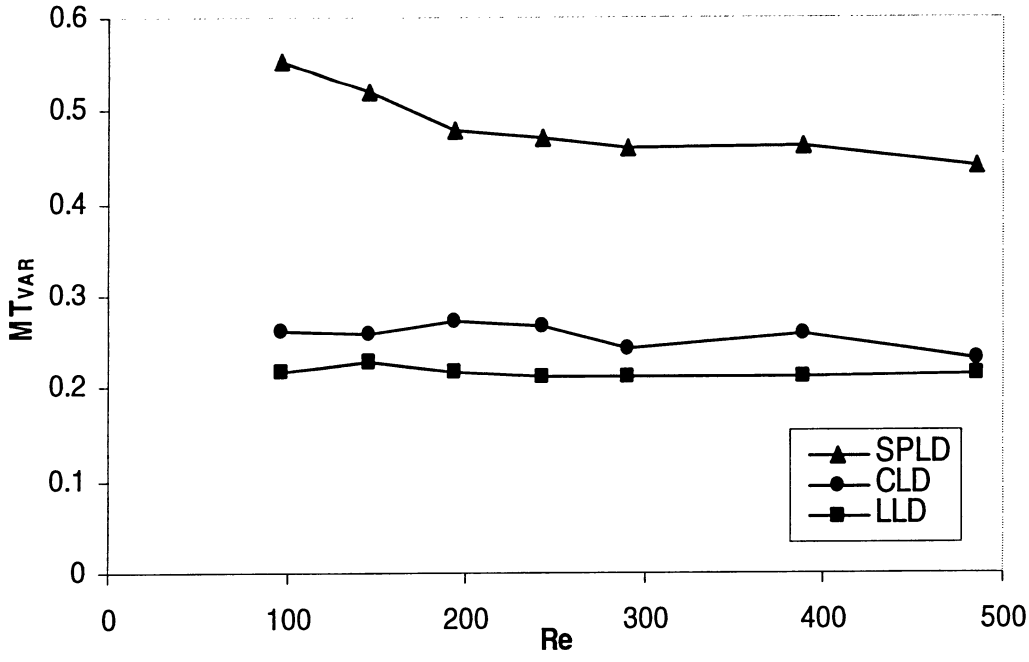

Fig. 4-25. Relative deviation of mass transfer coefficients at various Reynolds numbers, G = 0.

However, for poor initial liquid distribution (i.e. SPLD), liquid distribution at the top of the bed is only concentrated in some part of the cross section. The rest may be still dry, and hence, is not used for mass transfer. For SPLD, the liquid spreading significantly depends on the liquid flow rate and the packing itself along the packed bed, as shown in Fig. 4-24. Accordingly, it causes a higher variation of mass transfer coefficients, especially for the lower liquid flow rates.

In Fig. 4-26, the relation of maldistribution factors (M_f and MT_{VAR}) is illustrated. The values of M_f (MT_{VAR}) in Fig. 4-26 are the average values for all M_f (MT_{VAR}) values obtained at various r/R, x/D and Reynolds numbers without the presence of gas for a certain liquid distributor.

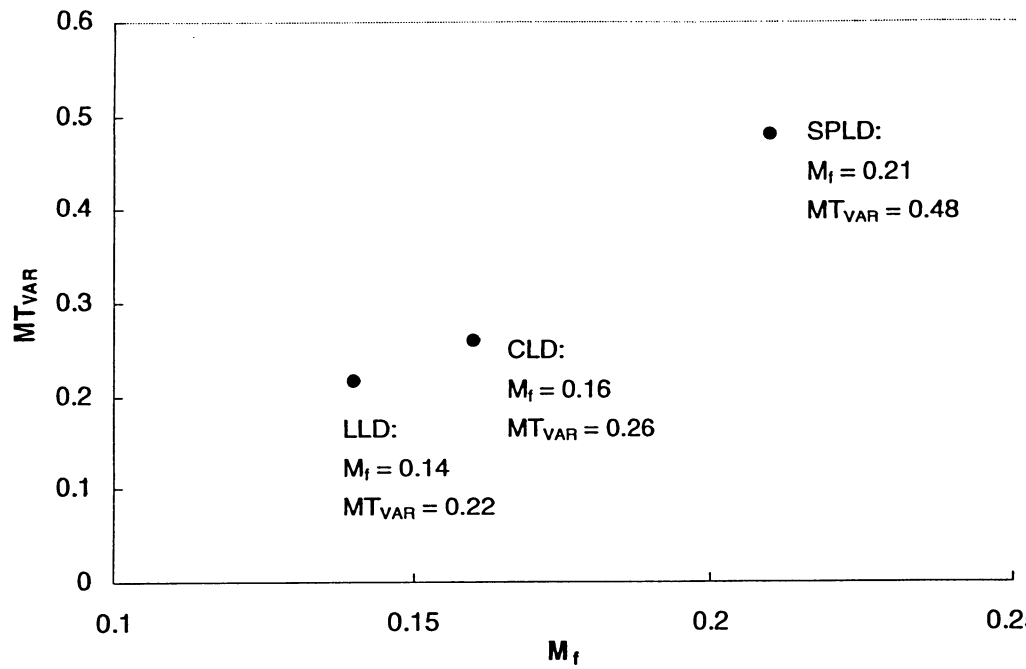

Fig. 4-26. Liquid maldistribution factor (M_f) vs. mass transfer maldistribution factor (MT_{VAR}).

As shown in Fig. 4-26, a correlation exists between the maldistribution factors M_f and MT_{VAR}. Higher M_f corresponds to higher MT_{VAR}. This correlation was observed by Kouri and Sohlo [7] and Groenhof [117,118]. Based on the study of the temperature distribution in a packed bed, Kouri and Sohlo [7] found that the values of temperature maldistribution factor (i.e. 0.021) were an order of magnitude less than the values of liquid maldistribution factor (i.e. 0.4). On the other hand, Groenhof [117,118] found that the concentration maldistribution factor and its corresponding liquid maldistribution factor were 0.17 and 0.39, respectively. Due to differences in the experimental methods, configuration, conditions and definition of maldistribution factors, it is hard to compare with the results obtained in the present study. Under similar experimental conditions and the same definition of MT_{VAR} as those used in the present study, Gostick *et al.* [61-63] found MT_{VAR} for MPLD, SPLD and full liquid flow condition were around 0.25, 0.7 and 0.07, respectively.

4.2.5. Effect of Angular Position on LDM and MTM

Based on the design, the liquid distributors can be rotated about the axis of the column. For SPLD, this central sprayed liquid distributor exhibits homogeneity for all directions. So the liquid distributed at the top of the column does not depend on the angular position of the liquid distributor with respect to an arbitrary reference axis on the horizontal plane. However, for multiple liquid distributors (e.g. LLD and CLD), the measurements of hydrodynamic and mass transfer behaviors on each individual packing element depend on both the design of the liquid distributor and the angular position of the liquid distributor in column. Two angular configurations (0° and 45°) of the multipoint liquid distributors (LLD and CLD) were tested to see the angular effect on LDM and MTM. All the data presented in the previous sections were obtained from the angular position of 0°.

Liquid distribution was investigated by using a liquid collector at the end of the column. It consisted of 39 liquid collecting tubes arranged symmetrically at four radial positions. From Fig. 4-27 and 4-28, it can be seen that the areas of the collecting tubes directly under the liquid distributors are almost same. Accordingly, the effect of the liquid-distributor angular positions is expected to be insignificant in liquid distribution measurement. This is indeed a case as shown in Fig. 4-29 and 4-30, which show the angular effect of liquid distributors on liquid distribution measurement for two multiple liquid distributors. Here x/D = 1.64 was chosen to demonstrate the angular effect because the difference of liquid radial distribution between packing elements will reduce with increases in packing height as discussed previously. The average variations are 11.4% and 12.4% for LLD and CLD, respectively.

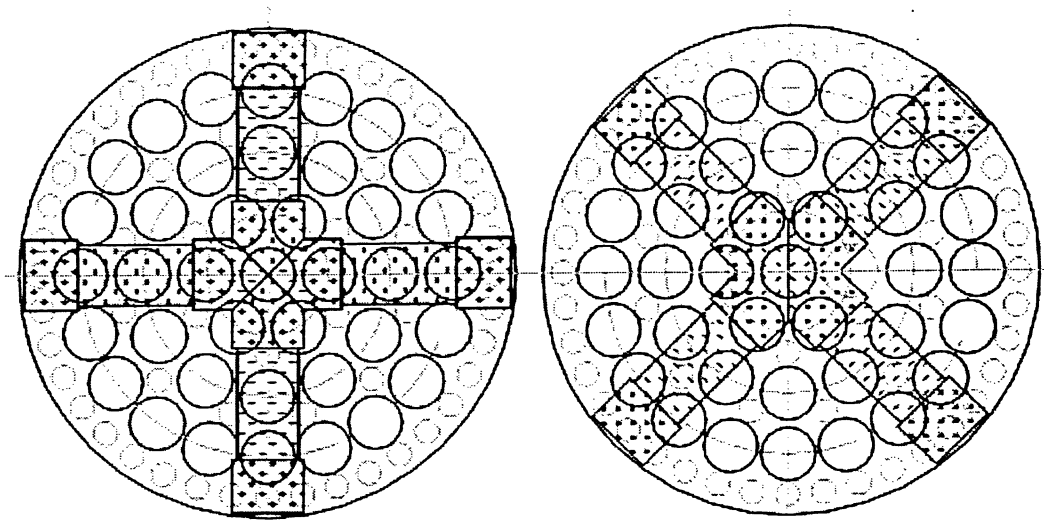

Fig. 4-27. Relative positions between CLD and liquid collector. (a) 0°, (b) 45°.

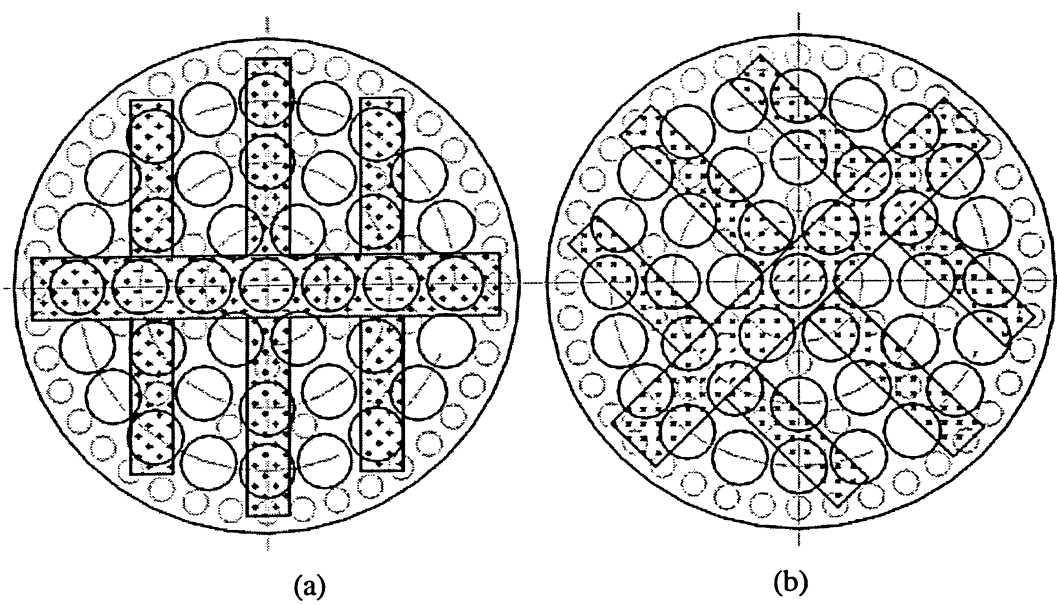

Fig. 4-28. Relative positions between LLD and liquid collector. (a) 0°, (b) 45°.

Considering the difference resulted from the reproducibility, these variations from the angular effect of liquid distributors are not significant. This result is good enough to match the analysis on the liquid-distributor physical configurations made above.

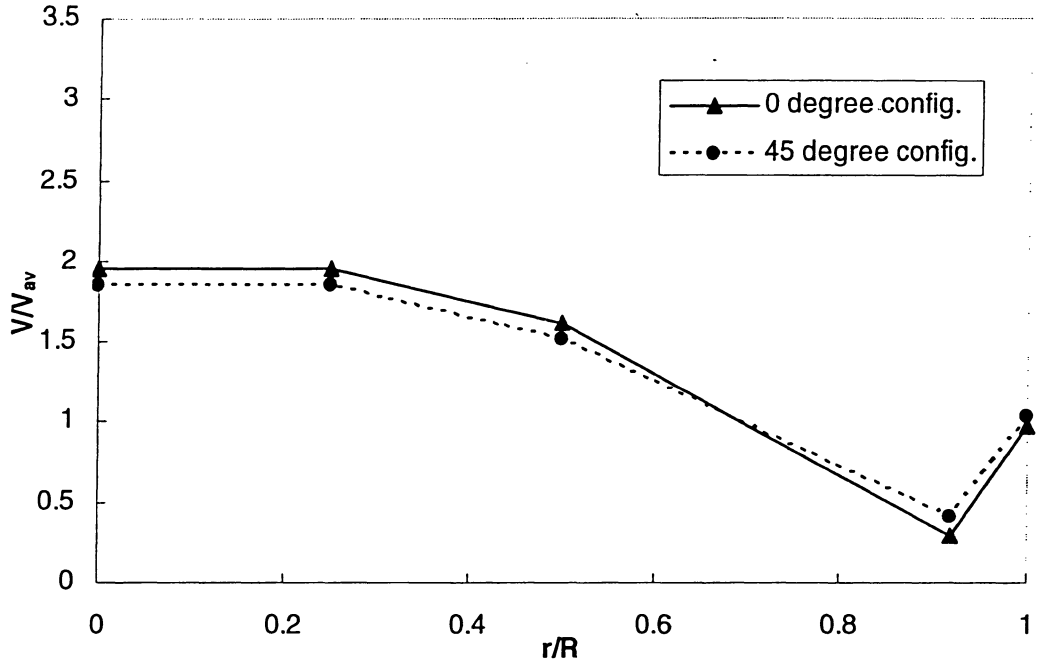

Fig. 4-29. Angular effect on liquid distribution measurement, CLD, x/D = 1.64, Re = 194 and G = 0.

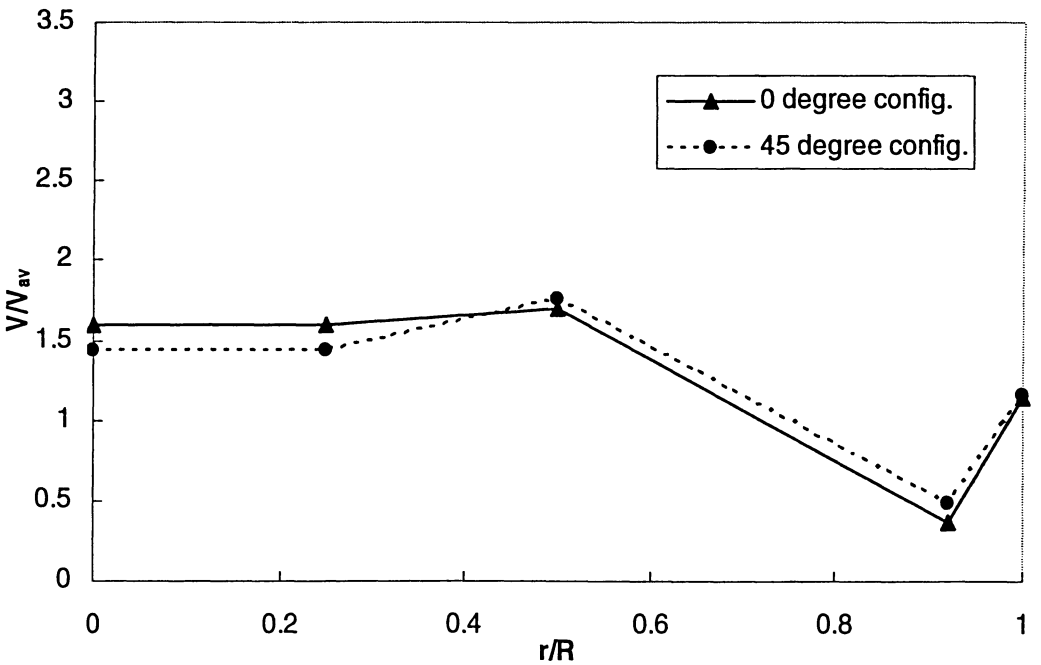

Fig. 4-30. Angular effect on liquid distribution measurement, LLD, x/D = 1.64, Re = 194 and G = 0.

Although the angular position of the liquid distributor had an insignificant effect, its effect on the local mass transfer coefficient was quite different. As presented in Section 3, in local mass transfer coefficient measurements, only nine cathodes were arranged at a certain cross section of the packed bed. Accordingly, the relative position between the cathode and the liquid delivery nozzles may influence the local mass transfer at the cathode significantly, especially at the top of the column. Fig. 4-31 and 4-32 illustrate the relative positions between the liquid distributors and the cathodes for CLD and LLD, respectively. It can be seen that for the 0° configuration, the liquid distributor arms cover all cathodes in a layer for both liquid distributors. There was no liquid delivery nozzle in the center area for the multipoint liquid distributors (LLD and CLD). Therefore, the cathode, CC01, wasn't sprayed directly for either configuration. For CLD, the liquid delivery nozzles were not right above the inner and outer cathodes at the 45° configuration. On the other hand, for LLD, the situation is much better than that for CLD. There is one arm located between any two cathodes. In addition, LLD has almost twice the number of nozzles (34) as those of the CLD (16) and a smaller distance between nozzles. All of these can make the variation between two angular configurations much smaller for LLD. However, all the discussion above is just an analysis based on the physical configuration. Finally, it needs to be verified by the quantitative measurement on local mass transfer coefficient.

Fig. 4-33 and 4-34 demonstrate the angular effect on the variation of the local mass transfer coefficient for CLD and LLD, respectively. For the 45° configuration, local mass transfer variation at the top of the column is higher for both liquid distributors. However, it decreases quickly to the values obtained for the 0° configuration. In addition, at the top of the column, MT_{VAR} for CLD is higher than that for LLD.

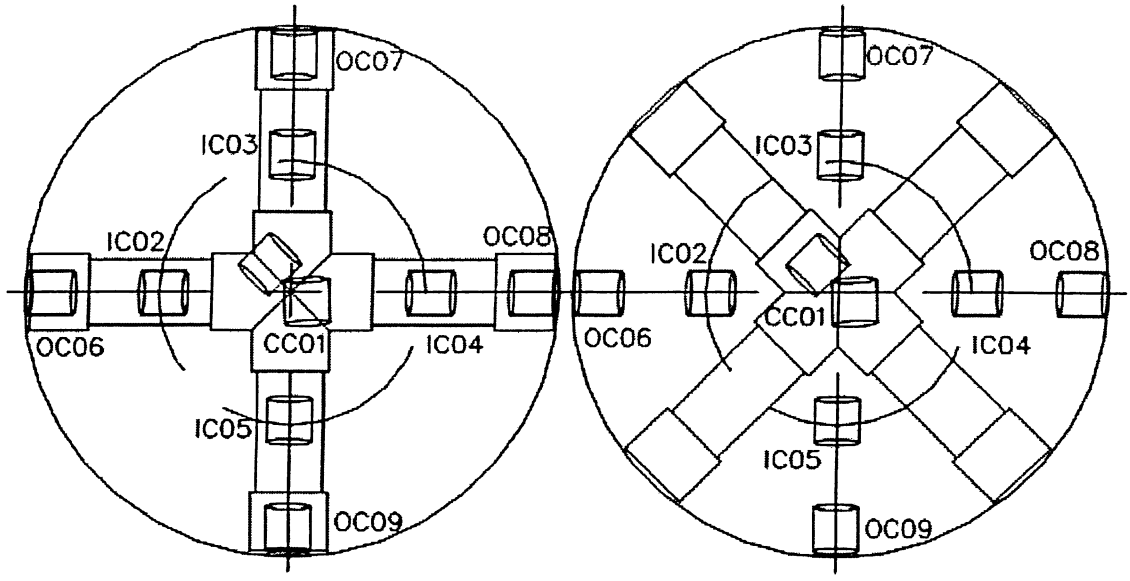

Fig. 4-31. Relative positions between CLD and cathodes. (a) 0°, (b) 45°.

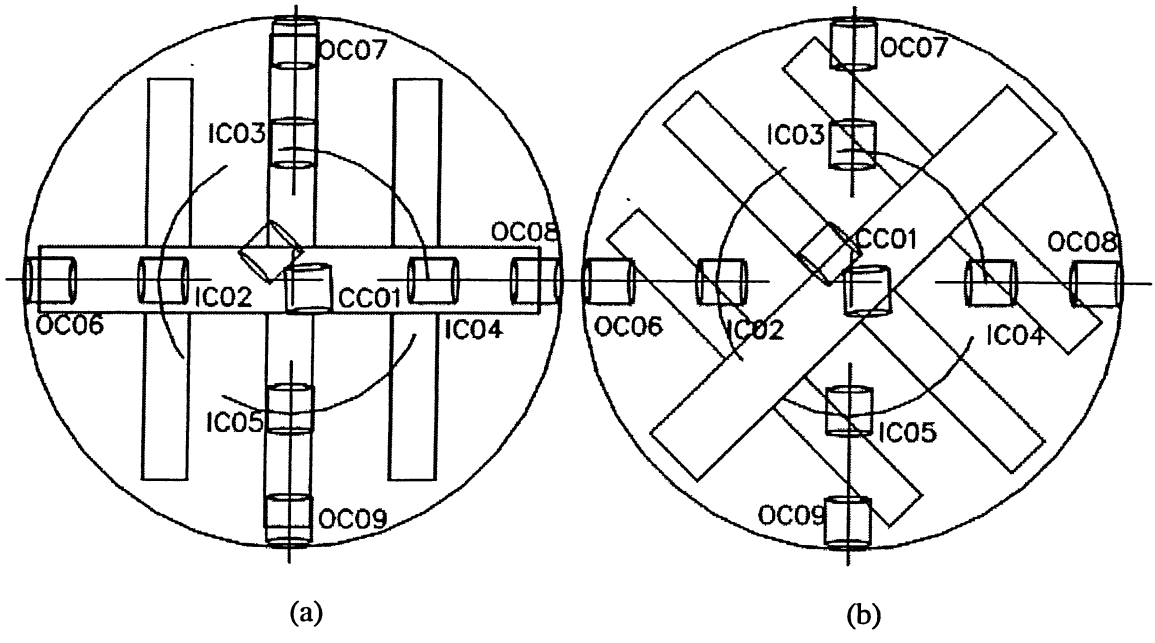

Fig. 4-32. Relative positions between LLD and cathodes. (a) 0°, (b) 45°.

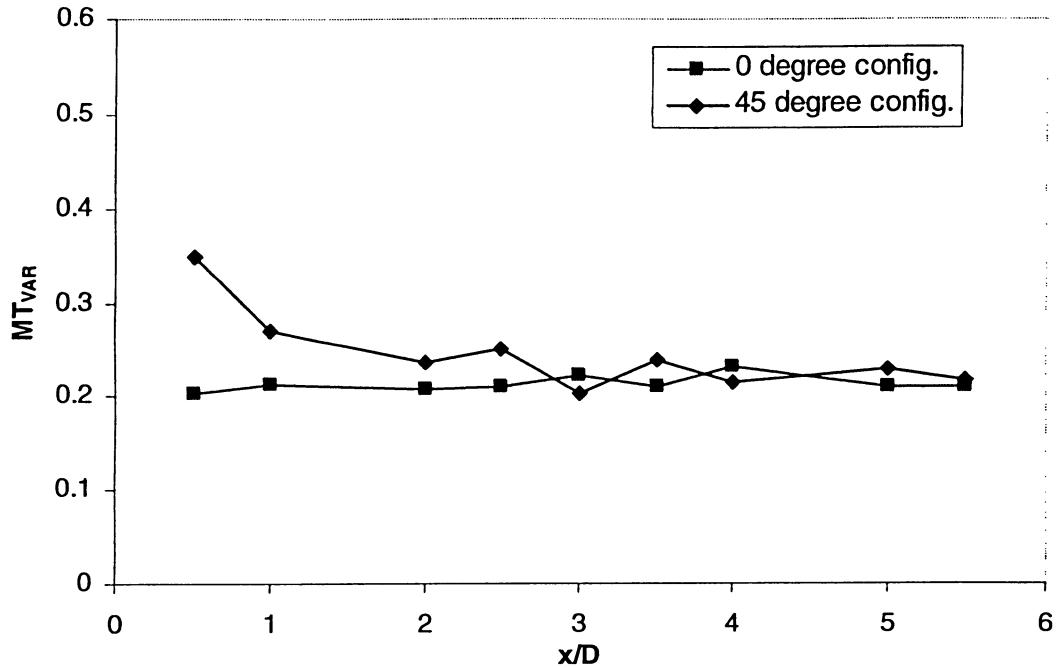

Fig. 4-33. Angular effect on local mass transfer coefficient measurement, LLD, Re = 388 and G = 0.

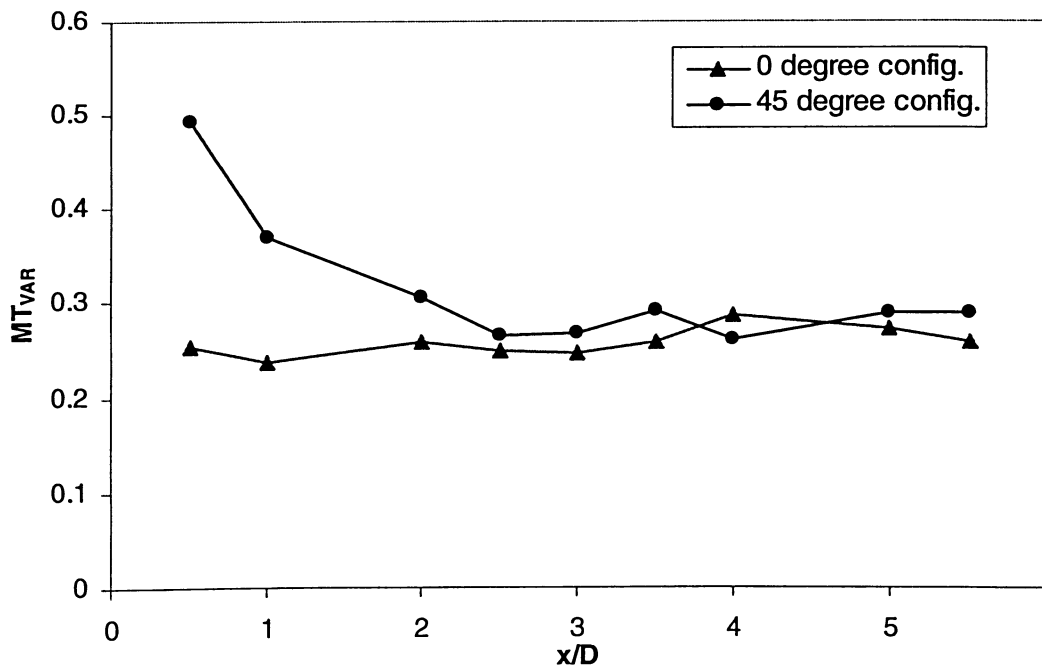

Fig. 4-34. Angular effect on local mass transfer coefficient measurement, CLD, Re = 388 and G = 0.

4.3. Empirical Correlation Development

Mathematical correlations and models on mass transfer in a packed bed have been developed by many researchers [13,65,66,119-124]. The Schmidt number to the power of 1/3 has been widely adopted due to its theoretical basis and the acceptable accuracy [125] although other powers of the Schmidt number were used in the literature (e.g. 0.25 [126], 0.42 [60], 0.5 [127]). Therefore, the typical form as Eq. 2-2 is used in the present study.

$$\frac{Sh}{Sc^{0.33}} = a \cdot \mathrm{Re}^{b} \qquad \text{Eq. 2-2}$$

Gostick [61] developed an empirical model for the local mass transfer coefficients obtained in a bed packed with Pall rings. It is expressed as:

$$\frac{Sh}{Sc^{0.33}} = a \cdot \mathrm{Re}^{0.44} \qquad \text{Eq. 4-2}$$

where a = $f\left(\frac{x}{D}\right) = 6.793\left(1-e^{\left(-1.778\frac{x}{D}\right)}\right)\cdot\left(0.1+0.9e^{\left(-0.475\frac{x}{D}\right)}\right)^{0.44}$.

It can be seen that only the axial factor (x/D) was considered for coefficient a in the model.

In the present study, in order to quantitatively demonstrate the relationship between the dimensionless group ($Sh/Sc^{0.33}$) and the Reynolds number, an empirical correlation is developed based on the data obtained.

Eq. 2-2 can be rewritten as

$$\ln\left(\frac{Sh}{Sc^{0.33}}\right) = \ln a + b \cdot \ln \mathrm{Re} \qquad \text{Eq. 4-3}$$

For each cathode at a given x/D and r/R, the coefficients (a and b) in Eq. 4-3 can be obtained from linear regression of $\ln\left(\frac{Sh}{Sc^{0.33}}\right)$ against $\ln \mathrm{Re}$.

In order to exhibit the spatial variation of the coefficients, coefficient a and b can be expressed in terms of x/D and r/R as in Eq. 4-4 and Eq. 4-5.

$$a = C_0 + C_1 \times \left(\frac{x}{D}\right) + C_2 \times \left(\frac{r}{R}\right) \qquad \text{Eq. 4-4}$$

and

$$b = C_0^{'} + C_1^{'} \times \left(\frac{x}{D}\right) + C_2^{'} \times \left(\frac{r}{R}\right) \qquad \text{Eq. 4-5}$$

C_0, C_1, C_2 are the correlation coefficients in Eq. 4-4. They can be regressed from the data of a and its corresponding x/D and r/R values. The correlation coefficients ($C_0^{'}$, $C_1^{'}$, $C_2^{'}$) in Eq. 4-5 can be evaluated similarly.

Eq. 4-6, Eq.4-7 and Eq. 4-8 are the resulting correlation equations of local mass transfer coefficient for SPLD, CLD and LLD, respectively.

For single-point delivery liquid distributor (SPLD):

$$\frac{Sh}{Sc^{0.33}} = a_{SPLD} \cdot \mathrm{Re}^{b_{SPLD}}$$

$$= \left[12.05 + 3.18 \cdot \left(\frac{x}{D}\right) - 13.01 \cdot \left(\frac{r}{R}\right)\right] \cdot \mathrm{Re}^{\left[0.39 - 0.06\left(\frac{x}{D}\right) + 0.12\left(\frac{r}{R}\right)\right]} \qquad \text{Eq. 4-6}$$

For cross-type liquid distributor (CLD):

$$\frac{Sh}{Sc^{0.33}} = a_{CLD} \cdot \mathrm{Re}^{b_{CLD}}$$

$$= \left[13.81 + 0.24 \cdot \left(\frac{x}{D}\right) + 6.96 \cdot \left(\frac{r}{R}\right)\right] \cdot \mathrm{Re}^{\left[0.26 - 0.01\left(\frac{x}{D}\right) - 0.09\left(\frac{r}{R}\right)\right]} \qquad \text{Eq. 4-7}$$

For ladder-type liquid distributor (LLD):

$$\frac{Sh}{Sc^{0.33}} = a_{LLD} \cdot \mathrm{Re}^{b_{LLD}}$$

$$= \left[23.24 + 1.67 \cdot \left(\frac{x}{D}\right) - 3.53 \cdot \left(\frac{r}{R}\right)\right] \cdot \mathrm{Re}^{\left[0.16 - 0.02\left(\frac{x}{D}\right) + 0.01\left(\frac{r}{R}\right)\right]} \qquad \text{Eq. 4-8}$$

The average R^2 for linear regression on the coefficients (a and b) are 0.89, 0.93 and 0.92 for SPLD, CLD and LLD, respectively.

In addition, in order to validate the proposed correlation, the values of $\ln\left(\frac{Sh}{Sc^{0.33}}\right)_{cor,i}$ calculated with Eq. 4-6, Eq. 4-7 and Eq. 4-8 (for SPL, CLD and LLD, respectively), are compared to the experimental data $\ln\left(\frac{Sh}{Sc^{0.33}}\right)_{exp,i}$ by means of RRMS [128] as shown in Eq. 4-10.

$$RRMS = \sqrt{\frac{\sum_{i=1}^{n}\left[\ln\left(\frac{Sh}{Sc^{0.33}}\right)_{exp,i} - \ln\left(\frac{Sh}{Sc^{0.33}}\right)_{cor,i}\right]^2}{\sum_{i=1}^{n}\left[\ln\left(\frac{Sh}{Sc^{0.33}}\right)_{exp,i}\right]^2}} \qquad \text{Eq. 4-10}$$

The results of RRMS obtained for the experimental data are equal to 7.2%, 7.8% and 6.4% for SPLD, CLD and LLD, respectively. Considering the testing errors given in Section 4.5, the empirical correlations show good agreement with experimental data obtained in the present study.

4.4. Overall Mass Transfer Coefficient

The local mass transfer behavior and its relationship with liquid distribution were presented previously. It provides an overview of the mass transfer behavior on the scale of individual packing elements in a randomly packed column. Usually, correlations of the overall mass transfer coefficient were reported in the literature. Generally, the overall mass transfer coefficient is determined by measuring the concentration difference of a certain component between the inlet and the outlet. There is no method or relationship that can be used to relate the local mass transfer coefficients obtained in different spatial positions to overall mass transfer coefficient. In order to compare the results of the present study with the ones obtained by other researchers, the overall mass transfer was obtained from the experimental data of the present study.

The coefficients (a and b) in the typical overall mass transfer equation (Eq. 2-2) were obtained by linear regression for each liquid distributor. All values of the dimensionless group ($Sh/Sc^{0.33}$) and its corresponding Reynolds numbers for each cathode were used in the linear regression. Eq. 4-11, Eq.4-12 and Eq. 4-13 were the overall mass transfer equations for SPLD, CLD and LLD, respectively.

For SPLD, $$\frac{Sh}{Sc^{0.33}} = 2.46\,\mathrm{Re}^{0.41} \qquad \text{Eq. 4 -11}$$

For CLD, $$\frac{Sh}{Sc^{0.33}} = 17.86\,\mathrm{Re}^{0.17} \qquad \text{Eq. 4 -12}$$

For LLD, $$\frac{Sh}{Sc^{0.33}} = 24.22\,\mathrm{Re}^{0.13} \qquad \text{Eq. 4 -13}$$

It can be seen from Eq. 4-11, Eq. 4-12 and Eq. 4-13 that the higher value of a corresponds to the lower value of b and vice versa.

Some interpretations are made here to explain this phenomenon. For instance, for the liquid distributors with better initial liquid distribution (e.g. LLD), liquid is delivered uniformly in the bed cross section. Accordingly, a rise on liquid flow rate affects the mass transfer behavior smaller, and hence, it results in a smaller value of b. For liquid distributors with poor initial liquid distributions (i.e. SPLD), liquid distribution at the top of the bed is only concentrated in some part of the cross section. The rest may be still dry, and hence, is not used for mass transfer. The liquid spreading significantly depends on the liquid flow rate besides the packing itself. Therefore, it results in a larger value of b. In addition, based on Eq. 4-3, a is equal to $Sh/Sc^{0.33}$ when lnRe equals to 0, as shown in Fig. 4-35. The value of a is higher for the better initial liquid distribution than that for poor initial liquid distribution. This indicates that the value of a represents the characteristics of liquid distributor.

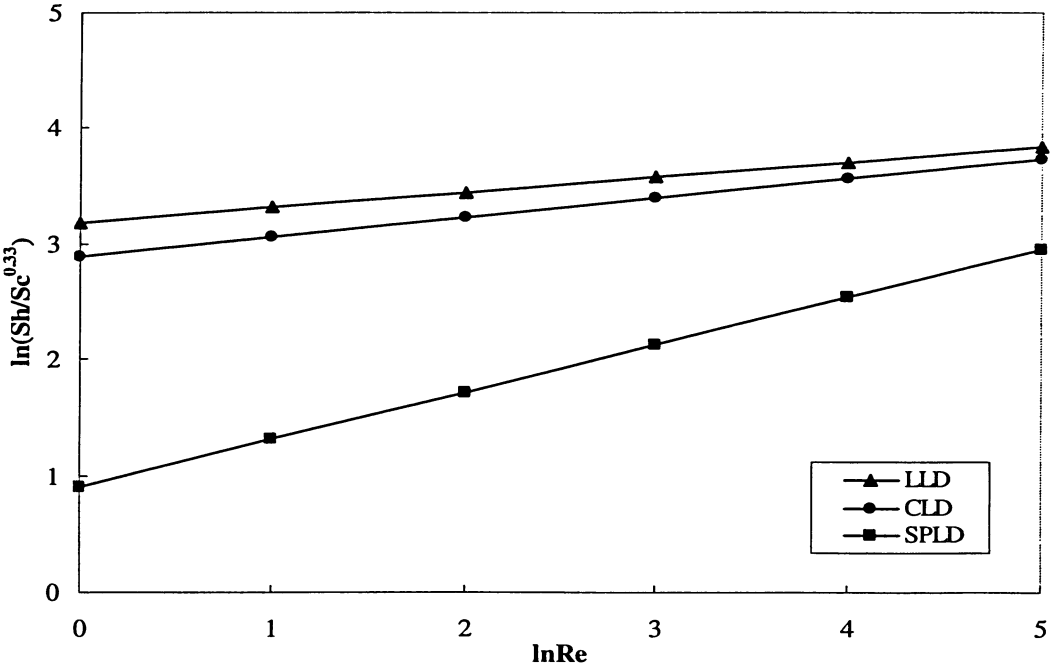

Fig. 4-35. $\ln\left(Sh/Sc^{0.33}\right)$ vs. $\ln \mathrm{Re}$.

Fig. 4-36 presents a comparison of the correlation equations obtained from the present study with several correlations reported in the literature. All the

correlations shown in Fig. 4-36 were obtained from electrochemical method in a packed bed with a trickle flow liquid in downward direction. It can be seen from Fig. 4-36 that the exponent (b) for SPLD agrees with the data reported in the literature. However, the exponents for CLD and LLD are lower. It may result from the different methods used in the studies to get the overall mass transfer correlation.

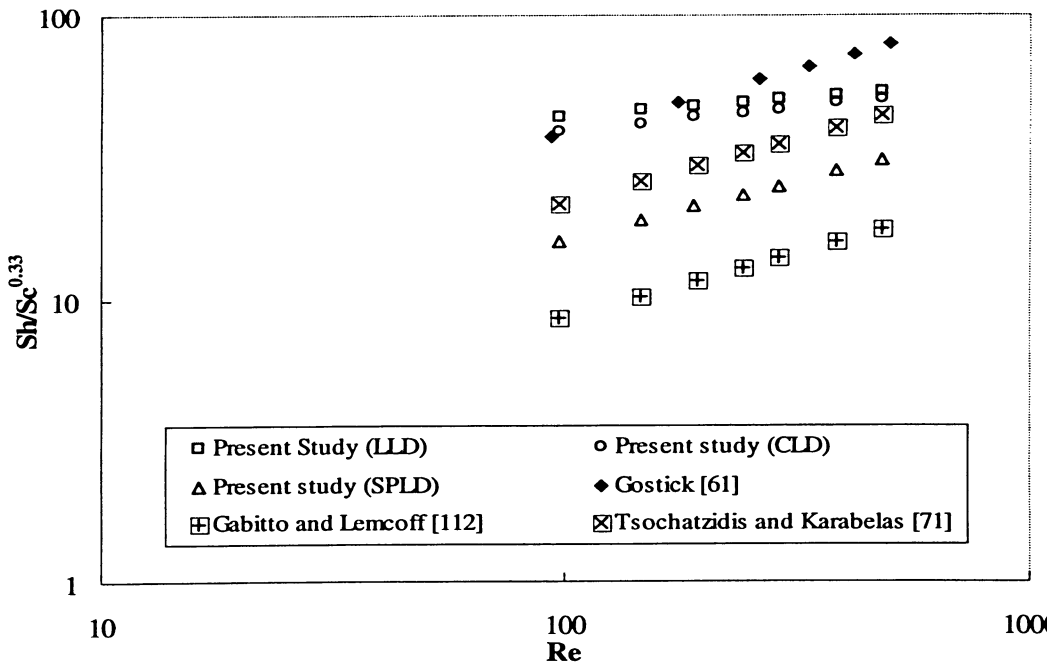

Fig. 4-36. Comparison on several overall mass transfer correlations.

4.5. Uncertainty Analysis

The instrumental errors and the sample calculations on uncertainty analysis can be seen from Appendix B.

4.5.1. Uncertainty in LDM

In liquid distribution measurement, the errors mainly consisted of instrumental and reading errors of liquid flow rate, the recording error of the liquid collecting time, and the error of liquid volume measurement in the cells.

Eq. 4-14 is the general formula for propagating the error associated with several values [129].

$$\sigma_x = \sqrt{\sum \sigma_i^2} \qquad \text{Eq. 4-14}$$

where σ_x is the accumulated error, σ_i is the error of the associated parameters.

The error on liquid flow rate included the instrumental error, and the human error on the reading of the flow meter. The error from the flow meter was $\pm 2\%$. Liquid flow rate was read manually. The human error on this reading was approximately 5%. Therefore, the error on liquid flow rate was approximately $\pm 5.4\%$.

Liquid collecting time was recorded by using a watch. The approximate fluctuations on this reading were about ± 1 second due to the manual operation. The variations due to this on computing the relative liquid velocity (V/V_{av}) and maldistribution factor (M_f) could be ignored because they had little effect in light of the scale of other errors.

In addition, the liquid volume in a cell was obtained by measuring the water depth in the cell. It was calibrated by a measuring cylinder with an accuracy of ±1%. The error of this measurement approach was about 2%. Therefore, the error on liquid volume measurement was approximately ±2.2%.

Based on Eq. 4-14, the accumulated error resulting from the uncertainty in the liquid distribution measurement was about ±5.8%.

4.5.2. Uncertainty in MTM

In the local mass transfer coefficient measurement, besides the instrumental and reading error of liquid flow rate, the errors could also come from ionic migration, temperature, chemical analysis on ferricyanide concentration, and physical properties.

The error on liquid flow rate was approximately ±5.4%, as mentioned above.

Since the ferricyanide ions ($[Fe(CN)_6]^{3-}$) would be electrically repelled from the cathode, the current through the cell would be lowered by this repelling force acting on the ferricyanide ions. The repulsive effect of ionic migration can be seen from Fig. 2-3. In the condition of the present study, the error was 0.36%.

The fluctuation of temperature in the system is always a critical factor, which need to be concerned. Although the temperatures in the column and electrolyte tank were maintained at a constant value by a cooling coil, the error caused by the J thermocouples should be considered. Based on Table B-1, the J thermocouple has an accuracy of 1% by hand calibration against a mercury thermometer. For electrolyte temperature 20 °C, the variation of temperature was 0.2 °C. Berger and Ziai [88] proposed that the test error in the

limiting current was less than 1% with the variation of temperature in ± 0.2 °C. It can also be seen from Fig. 2-2.

The most important factor influencing uncertainty on the data was the determination of the ferricyanide concentration. The determination error included the error of lab instruments (e.g. pipette, burette) and the error of titrant preparation. The pipette used was 25 ml in volume with an uncertainty of 0.02 ml. The burette was 50 ml with an uncertainty of 0.1 ml. The titrant was 0.020 M $Na_2S_2O_3$ with an uncertainty of 0.0001 M. Based on Eq. 4-14, the accumulated error resulting from the uncertainty in the titration process is 0.6%.

Determination of the physical properties of a system is critical because they will be used to calculate the dimensionless groups. In the present study, the viscosity and diffusivity of the solution were estimated by the correlations obtained from the experimental data. The errors for diffusivity and viscosity were less than 2% and 2.5%, respectively, as mentioned in Section 3.3.2.

Overall, the accumulated error for local mass transfer coefficient measurement was approximately $\pm 6.4\%$.

5. Conclusions and Recommendations

5.1. Conclusions

The objective of the present study was to investigate the liquid distribution and the variation of local mass transfer coefficients as liquid flows downwards in a random packed column of 0.3 m diameter. The data was obtained at the various spatial positions, initial liquid distributions and fluid flow rates. By analysis and discussion on the findings obtained in the present study, the conclusions can be drawn as follows:

- Design of liquid distributor is critical for liquid distribution in a random packed column. The equilibrium liquid flow pattern was established at x/D = 4.92 for LLD and x/D = 6.56 for CLD. However, for SPLD, the liquid flow pattern did not reach equilibrium even at x/D = 6.56 (2 m below the liquid distributor level). The more uniform the initial liquid distribution, the less the packing height needed to reach the equilibrium liquid flow pattern.

- The values of V/V_{av} in the bulk region were closer to 1.0 with increases in liquid flow rate. However, the effect of liquid flow rate on liquid distribution was insignificant. For instance, the value of V/V_{av} obtained from LLD at r/R = 0.25 and x/D = 3.28 decreased approximately 6.3% from 1.59 (at Re = 97) to 1.49 (at Re = 291).

- Due to the weak interaction between gas and liquid phases, no influence of gas flow rate on liquid distribution and mass transfer process was found at the experimental gas flow rate (i.e. 0.9 kg $m^{-2} s^{-1}$), which was much lower than the loading point (i.e. 2.2 kg $m^{-2} s^{-1}$).

- Liquid maldistribution still existed even when an equilibrium liquid flow was established. The liquid maldistribution factor (M_f) decreased along the packing height and appeared to reach a relatively constant value at a certain x/D. For instance, for CLD, M_f decreased from 0.18 (at x/D = 1.64) to 0.14 (at x/D = 4.92) and appeared to level out at x/D = 6.56 with the value of 0.13.

- A rise in the mass transfer coefficient just below the liquid distributor followed by a decline was observed. For example, for SPLD, the value of $Sh/Sc^{0.33}$ peaked at x/D = 2.0 for Re = 291. It was attributed to the liquid spread-out over the packing at that height and then the decrease in liquid velocity due to liquid momentum loss by friction as liquid flowed over packings.

- With increase in the uniformity of the initial liquid distribution, the mass transfer maldistribution factor (MT_{VAR}) deceased from 0.48 (for SPLD) to 0.22 (for LLD). The more uniform the initial liquid distribution, the less the mass transfer maldistribution factor, and hence, the higher the overall mass transfer coefficient in the bed. This behavior is attributed to the higher mass transfer efficiency obtained in the column by more uniform liquid distribution provided by LLD.

- For multiple liquid distributors (i.e. CLD and LLD), MT_{VAR} showed little dependency on liquid flow rate. However, for SPLD, MT_{VAR} was higher for lower Reynolds numbers (i.e. 97), especially at the upper packed section. For example, within the range of Reynolds numbers from 97 to 485 the value of MT_{VAR} fluctuated at 0.22 for LLD and 0.26 for CLD. However, for SPLD, the value of MT_{VAR} decreased from 0.55 (at Re = 97) to 0.48 (at Re = 194) and remained at 0.48 with increase in Reynolds number.

- The angular effect of liquid-distributor configurations on local mass transfer coefficients depended on the design of liquid distributors. Compared with the values of MT_{VAR} at the 0° and 45° configuration, the deviation of MT_{VAR} at x/D = 0.5 was 96% and 67% for CLD and LLD, respectively.

- Good agreement was observed on the relation of the maldistribution factors M_f and MT_{VAR}. The higher M_f values (e.g. 0.21 for SPLD) corresponded to the higher MT_{VAR} values (e.g. 0.48 for SPLD).

5.2. Recommendations

Although the present study has achieved all the anticipated goals and objectives, more efforts are needed to further expand this work. Considering the complexity of the random packed column, the following should be considered:

- The use of the different packing sizes and types in the investigation of mass transfer and liquid distribution is recommended and introduced into mass transfer correlations in the form of the packing factor.

- The change in the ratios of column diameter over packing size allows observation of the scale-up effect of the column. It is important in design and scale-up based on the experimental data or empirical models.

References

[1]. Hoek, P. J., J. A. Wesselingh and F. J. Zuiderweg, *Small scale and large scale liquid maldistribution in packed columns.* Chem. Eng. Res. Des., 1986. **64**: p. 431 – 449.

[2]. Wang, Y. F., Z. S. Mao and J. Chen, *Scale and variance of radial liquid maldistribution in trickle beds.* Chemical Engineering Science, 1998. **53**(6): p. 1153 – 1162.

[3]. Albright, M. A., *Packed tower distributors tested.* Hydrocarbon Processing, 1984. **63**(9): p. 173 – 177.

[4]. Wang, Y. F., Z. S. Mao and J. Y. Chen, *A new instrumentation for measuring the small scale maldistribution of liquid flow in trickle beds.* Chem. Eng. Commun., 1998. **163**: p. 233 – 244.

[5]. Melli, T. R., J. M. de Santos, W. R. Kolb and L. E. Scriven, *Cocurrent downflow in networks of passages. Microscale roots of Macroscale flow regimes.* Ind. Engng. Chem. Res., **29**: p. 2367 – 2379.

[6]. Kumar, S., S. N. Upadhyay and V. K. Mathur, *Low Reynolds number mass transfer in packed beds of cylindrical particles.* Ind. Eng. Chem. Process Des. Dev., 1977. **16**(1): p. 1 – 8.

[7]. Kouri, R.J. and J. Sohlo, *Liquid and gas flow patterns in random packings.* The Chemical Engineering Journal, 1996. **61**: p. 95 – 105.

[8]. Stanek, V. and V. Kolar, *A model of the effect of the distribution on liquid holdup in a packed bed and new concept of static hold-up.* Chem. Eng. J. 1973. **5**: p. 51 – 60.

[9]. Stanek, V. and N. Kolev, *A study of the dependence of radial spread of liquid in random beds on local conditions of irrigation.* Chemical Engineering Science, 1978. **33**(8): p. 1049 – 1053.

[10]. Farid, M. M., and D. J. Gunn, *Liquid distribution and redistribution in packed columns--II. Experimental.* Chemical Engineering Science,

1978. **33**(9): p. 1221 – 1231.

[11]. Kunjummen, B., T. S. Prasad and P. S. T. Sai, *Radial liquid distribution in gas-liquid concurrent downflow through packed beds.* Bioprocess Engineering, 2000. **22**: p.471 – 475.

[12]. Yin, F., Z. Wang, A. Afacan, K. Nandakumar and K. T. Chuang, *Experimental studies of liquid flow maldistribution in a random packed column.* The Canadian Journal of Chemical Engineering, 2000. **78**: p. 449 – 457.

[13]. Guo, G. and K. E. Thompson, *Experimental analysis of local mass transfer in packed beds.* Chemical Engineering Science, 2001. **56**(1): p. 121 – 132.

[14]. Yin, F. H., A. Afacan, K. Nandakumar and K. T. Chuang, *CFD simulation and experimental study of liquid dispersion in randomly packed metal pall rings.* Trans IChemE, 2002. **80**(Part A): p. 135 – 144.

[15]. Macias-Salinas, R. and J. R. Fair, *Axial mixing in modern packings, gas and Liquid phases: I. Single-phase flow.* AIChE Journal, 1999. **45**(2): p. 222 – 239.

[16]. Macias-Salinas, R. and J. R. Fair, *Axial mixing in modern packings, gas and liquid phases: II. Two-phase flow.* AIChE Journal, 2000. **46**(1): p. 79 – 91.

[17]. Bennett, A., and F. Goodridge, *Hydrodynamic and mass transfer studies in packed absorption column. Part I: Axial liquid dispersion.* Trans. Inst. Chem. Engrs, 1970. **48**: p. T232 – T240.

[18]. Van Bate, J. M., J. Ellenberger and R. Krishna, *Radial and axial dispersion of the liquid phase within a KATAPAK-S structure: experimental vs. CFD simulations.* Chemical Engineering Science, 2001. **56**(3): p. 813 – 821.

[19]. Tsochatzidia, N. A., A. J. Karabelas, D. Giakoumakis and G. A. Huff, *An investigation of liquid maldistribution in trickle beds.* Chemical

Engineering Science, 2002. **57**(17): p. 3543 – 3555.

[20]. Tsochatzidia, N. A., A. J. Karabelas, M. Kostoglou and A. J. Karabelas, *A conductance probe for measuring liquid fraction in pipes and packed beds.* International Journal of Multiphase Flow, 1992. **18**: p. 653 – 667.

[21]. Loser, T., G. Petritsch, D. Mewes, *Investigation of the two-phase countercurrent flow in structured packings using capacitance tomography*, Proc. of the 1st World Congress on Industrial Process Tomography, Buxtion, Greater Manchester, April 14-17, 1999. p. 354-361.

[22]. Marchot, P., D. Toye, M. Crine, A-M. Pelsser and G. L'Homme, *Investigation of liquid maldistribution in packed columns by X-ray tomography.* Trans IChemE, 1999. **77**(Part A): p. 511 – 518.

[23]. Reinecke, N. and D. Mewes, *Investigation of the two-phase flow in trickle-bed reactors using capacitance tomography.* Chemical Engineering Science, 1997. **52**(13): p. 2111 – 2127.

[24]. Reinecke, N., G. Petristsch, D. Schmitz and D. Mewes, *Tomographic measurement techniques – visualization of multiphase flows.* Chem. Eng. Tech., 1998. **21**(1): p. 7 – 18.

[25]. Al-Samadi, R.A., C.M. Evan, G.M. Cameron, M.E. Fayed and M. Leva, *A study of liquid distribution in an industrial scale packed tower.* AIChE Meeting Preprint, Houston, TX, April 1989.

[26]. Gunn, D. J., *Liquid distribution and redistribution in packed columns – I Theoretical.* Chemical Engineering Science, 1978. **33**(9): p. 1211 – 1219.

[27]. Baker, T., T.H. Chilton and H.C. Vernon, *The course of liquor flow in packed towers.* Trans. AIChE, 1935. **31**: p.296 – 313.

[28]. Veer, K. J. R. T., H. W. Van Der Klooster and A. A. H. Drinkenburg, *The influence of the initial liquid distribution on the efficiency of a packed column.* Chemical Engineering Science, 1980. **35**(3): p. 759 – 761.

[29]. Billet, R., *Packed Towers in Processing and Environmental Technology.* 1st ed. 1995, New York: VCH Publisher, Inc. 382.

[30]. Sun, C.G., F.H. Yin, A. Afacan, K. Nandakumar and K.T. Chuang, *Modeling and simulation of flow maldistribution in random packed columns with gas-liquid countercurrent flow*, Chem. Eng. Research and Design, 2000. **78**(Part A): p. 378 – 388.

[31]. Song, M., F. H. Yin, K. Nandakumar and K. T. Chuang, *A three-dimensional model for simulating the maldistribution of liquid flow in random packed beds.* The Canadian Journal of Chemical Engineering, 1998. **76**: p. 161 – 166.

[32]. Klemas, L. and J. A. Bonilla, *Accurately assess packed-column efficiency.* Chemical Engineering Progress, 1995. July: p. 27 – 44.

[33]. Semkov, K.R., *Liquid flow distribution in packed beds by multipoint liquid distributors.* Chemical Engineering Science, 1991. **46**(5/6): p. 1393 – 1399.

[34]. Schultes, M., *Influence of Liquid Redistributors on the Mass-Transfer Efficiency of Packed Columns.* Industrial & Engineering Chemistry Research. 2000, **39**(5): p.1381 – 1389.

[35]. Kister, H. Z., *Distillation Operation*; McGraw-Hill: New York, 1990.

[36]. Raschig. *Tower Packings/Internals.* Raschig GmbH: Ludwigshafen, Germany, 1997.

[37]. Eckert, J. S., *Design of Packed Columns.* In Handbook of Separation Techniques for Chemical Engineers, Schweitzer, P. A., Ed.; McGraw-Hill: New York, 1997.

[38]. Striggle, R. F. Jr., *Random Packings and Packed Towers.* Gulf Publishing: Houston, TX, 1987.

[39]. Stikkelman, R. M., J. de Graauw, Z. Olujic, H. Teeuw and J. A. Wesselingh, *A study of gas and liquid distributions in structured packings.* Chemical Engineering and Technology, 1989. **12**: p. 445 –

449.

[40]. Stoter, F., Z. Olujic and J. de Graauw, *Modelling and measurement of gas flow distribution in corrugated sheet structured packings.* Chemical Engineering Journal, 1993. **53**: p. 55 – 66.

[41]. Petrova, T., K. Semkov and C. Dodev, *Mathematical modeling of gas distribution in packed columns.* Chemical engineering and Processing, 2003. **42**: p. 931 – 937.

[42]. Bemer, G. G. and F. J. Zuiderweg, *Radial liquid spread and maldistribution in packed columns under different wetting conditions.* Chemical Engineering Science, 1978. **33**(12): p. 1637 – 1643.

[43]. Badr El-Din, A. A., M. M. El-Halwagi and M. A. Saleh, *Liquid flow distribution in a two-phase countercurrent packed column.* Chemical Engineering Science, 1977. **32**(3): p. 343 – 345.

[44]. Xiong, T. Y., Z. S. Mao and J. Y. Chen, *A study of the external wetting efficiency in a trickle-bed reactor.* Huagong Yejin, 1995. **16**: p. 47 – 53. (in Chinese)

[45]. Herskowitz, M. and J. M. Smith, *Liquid distribution in trickle-bed reactors, Part I, Flow measurements.* A.I.Ch.E. J., 1978. **24**: p. 439 – 450.

[46]. Borda, M. and J. F. Gabitto, *Radial liquid distribution in a trickle bed reactor.* Chem. Eng. Commun., 1987. **60**: p. 243 – 252.

[47]. Onda, K., H. Takeuchi, Y. Maeda and N. Takeuchi, *Liquid distribution in a packed column.* Chemical Engineering Science, 1973. **28**(9): p. 1677 – 1683.

[48]. Kramers, H. and G. Alberda, *Frequency response analysis of continuous flow systems.* Chemical Engineering Science, 1953. **2**(4): p. 173 – 181.

[49]. Macias-Salinas, R. *Gas and liquid-phase axial dispersion through random and structured packings.* Ph. D. Dissertation, The University of

Texas at Austin, U.S.A., 1995.

[50]. Mak, A. N. S., P. J. Hamersma and J. M. H. Fortuin, *Solids holdup and axial dispersion during countercurrent solids-liquid contacting in a pulsed packed column containing structured packing.* Chemical Engineering Science, 1992. **47**(3): p. 565 – 577.

[51]. Ebach, E. A., and R.R. White, *Mixing of fluids flowing through beds of packed solids.* AIChE J., 1958. **4**(2): p. 161.

[52]. Kunugita, E., T. Otake and K. Yoshu, *Holdup and mixing coefficients of liquid flowing through irrigated packed beds.* Chemical Engineering (Japan). 1962. **26**(6): p. 672.

[53]. Miller, S. F. and C. J. King, *Axial dispersion in liquid flow through packed beds.* AIChE J., 1966. **12**(4): p. 767.

[54]. Liles, A.W., and C. J. Geankoplis, *Axial diffusion of liquids in packed beds and end effects.* AIChE J., 1960. **6**(4): p. 591.

[55]. Tan, C.S. and D. C. Liou, *Axial dispersion of supercritical carbon dioxide in packed beds.* Ind. Eng. Chem. Res., 1989. **28**: p. 1246.

[56]. Kumar, S., S. N. Upadhyay and V. K. Mathur, *Low Reynolds number mass transfer in packed beds of cylindrical particles.* Ind. Eng. Chem. Process Des. Dev., 1977. **16**(1): p. 1 – 8.

[57]. Noseir, S. A., A. El-Kayar, H. A. Farag, and G. H. Sedahmed, *Forced convection solid-liquid mass transfer at a fixed bed of Raschig rings.* International Communications in Heat and Mass Transfer, 1995. **22**(1): p. 111 – 122.

[58]. Sedahmed, G. H., A. M. El-Kayar, H. A. Farag and S. A. Noseir, *Liquid-solid mass transfer in packed beds of Raschig rings with upward two-phase (gas-liquid) flow.* The Chemical Engineering Journal, 1996. **62**: p. 61 – 65.

[59]. Rexwinkel, G., A. B. M. Heesink, and W. P. M. van Swaaij, *Mass transfer in packed beds at low Peclet numbers - wrong experiments or*

wrong interpretations?. Chemical Engineering Science, 1997. **52**: p. 3995 – 4003.

[60]. Williamson, J. E., K. E. Bazaire, and C. J. Geankoplis, *Liquid-phase mass transfer at low Reynolds numbers*. Industrial and Engineering Chemistry, Fundamentals, 1963. **2**: p. 126 – 129.

[61]. Gostick, J., *Measurement of local mass transfer coefficient in a packed bed of Pall rings using the electrochemical technique*. M. A. Sc. Thesis, Department of Chemical Engineering, University of Waterloo, Ontario, Canada, 2002.

[62]. Gostick, J., H. D. Doan, A. Lohi and M. Pritzker, *Investigation of local mass transfer in a packed bed using a limiting current technique*. Ind. Eng. Chem. Res., 2002. **42**(15): p. 3626 – 3634.

[63]. Gostick, J., M. Pritzker, A. Lohi and H. D. Doan, *Mass transfer variation within a packed bed and its relation to liquid distribution.* Chemical Engineering Journal, 2004. **100**(1-3): p. 33 – 41.

[64]. Tasat, A. I., O. N. Cavatorta and U. Bohm, *Electrochemical mass transfer to regular packings in a bubble column*. Journal of Applied Electrochemistry, 1995. **25**: p. 273 – 278.

[65]. Seguin, D., A. Montillet, D. Brunjail and J. Comiti, *Liquid-solid mass transfer in packed beds of variously shaped particles at low Reynolds numbers: experiments and model.* The Chemical Engineering Journal, 1996. **63**: p. 1 – 9.

[66]. Comiti, J and M. Renaud, *Liquid-solid mass transfer in packed beds of parallelepipedal particles: energetic correlation.* Chemical Engineering Science, 1991. **46**(1): p. 143 – 154.

[67]. Cavatorta, O. N., U. Bohm and A. M. C. D. Del Giorgio, *Fluid-dynamic and mass transfer behavior of static mixers and regular packings.* AIChE Journal, 1999. **45**(5): p. 938 – 948.

[68]. Legrand, J., P. Legentilhomme, S. Farias Neto and H. Aouabed, *Mass*

transfer in developing flows. Electrochimica Acta, 1997. **42**: p. 805 – 811.

[69]. Yang, J. D., A. Shehata, V. Modi and A. C. West, *Mass-transfer to a channel wall downstream of a cylinder.* Int. Journal Heat mass transfer, 1997. **40**(18): p. 4263 – 4271.

[70]. Del Giorgio, A. C. D., O. N. Cavatorta, and U. Bohm, *Local mass transfer for tube banks in two-phase flow.* The Canadian Journal of Chemical Engineering, 1994. **72**: p. 50 – 55.

[71]. Tsochatzidis N.A. and A.J. Karabelas, *Solid-liquid mass transfer in cocurrent gas-liquid flow through packed beds.* Proceedings of the 3rd Intern. Workshop on Electrodiffusion Diagnostics of Flow, Dourdan, France. 1993.

[72]. Benadda, B., M. Otterbein, K. Kafoufi and M. Prost, *Influence of pressure on the gas/liquid interfacial area a and the coefficient k_La in a counter-current packed column.* Chemical Engineering and Processing, 1996. **35**(4): p. 247 – 253.

[73]. Aroonwilas, A., A. Chakma, P. Tontiwachwuthikul and A. Veawab, *Mathematical modeling of mass-transfer and hydrodynamics in CO2 absorbers packed with structured packings.* Chemical Engineering Science, 2003. **58**(18): p. 4037 – 4053.

[74]. Aroonwilas, A. and P. Tontiwachwuthikul, *Mass transfer studies of high performance structured packing for CO2 separation processes.* Energy Convers. Mgmt., 1997. **38**: p. S75 – S80.

[75]. Linek, V., T. Moucha and F. J. Rejl, *Hydraulic and mass transfer characteristics of packings for absorption and distillation columns. Rauschert-Metall-Sattel-Rings.* Trans. Inst. Chem. Engrs, 2001. **79**(Part A): p. 725 – 732.

[76]. Pandya, J. D., *Adiabatic gas absorption and stripping with chemical reaction in packed towers.* Chemical Engineering Communications,

1983. **19**(4–6): p. 343 – 361.

[77]. Glasscock, D. A., J. E. Critchfield, and G. T. Rochelle, *CO_2 absorption / desorption in mixtures of methyldiethanolamine with mono-ethanolamine or diethanolamine.* Chemical Engineering Science, 1991. **46**(11): p. 2829 – 2845.

[78]. Viviani, E., A. Paglianti, and G. Nardini, *A new model to design structured packing columns. Absorption of inorganic acid gases.* I. Chem. E. Research Event / First European Conference, 1995. **1**: p. 435 – 437.

[79]. Akehata, T. and K. Sato, *Flow distribution in packed beds.* Kagaku Kogaku, 1958.

[80]. Levec, J. and A. Lakota, *Liquid-solid mass transfer in packed beds with concurrent downward two-phase flow.* In M. Quintard, & M. Todorovic, Heat and mass transfer in porous media, 1992. p. 663 – 672.

[81]. Satterfield, C. N., N. W. Van Eek and G. S. Bliss, *Liquid-solid mass transfer in packed beds with downward concurrent gas-liquid flow.* The American Institute of Chemical Engineers Journal, 1978. **24**: p.709 – 717.

[82]. Rao, V. G. and A. A. H. Drinkenburg, *Solid-liquid mass transfer in packed beds with cocurrent gas-liquid downflow.* The American Institute of Chemical Engineers Journal, 1985. **31**: p. 1059 – 1068.

[83]. Stichlmair, J. and A. Stemmer, *Influence of maldistribution on mass transfer in packed columns.* Institution of Chemical Engineers Symposium Series, 1987. **104**: p. B213 – B224.

[84]. Marcandelli, C., G. Wild, A. S. Lamine and J. R. Bernard, *Measurement of local particle-fluid heat transfer coefficient in trickle-bed reactors.* Chemical Engineering Science, 1999. **54**(21): p. 4997 – 5002.

[85]. Levich V.G., *Physicochemical hydrodynamics.* 1962. Prentice Hall, U.S.A.

[86]. Tobias, C. W., M. Eisenberg and C. R. Wilke, *Diffusion and convection in electrolysis – A theoretical review.* Journal of the Electrochemical Society, 1952. **99**(12): p. 359C.

[87]. Mizushina, T., *The electrochemical method in transport phenomena.* Advances in Heat and Mass Transfer, 1971. **7**: p. 87 – 161.

[88]. Berger, F. P. and A. Ziai, *Optimization of experimental conditions for electrochemical mass transfer measurements.* Chemical Engineering Research and Design, 1983. **61**(6): p. 377 – 382.

[89]. Wragg, A. A., *Application of the limiting diffusion current technique in chemical engineering.* The Chemical Engineer, 1977 January: p. 39 – 44.

[90]. Grassmann P. P., *Applications of the electrolytic method – I: Advantages and disadvantages, mass transfer between a falling film and the wall.* International Journal of Heat and Mass Transfer, 1978. **22**: p. 795 – 798.

[91]. Lin, C. S., E. B. Denton, H. S. Gaskill, and G. L. Putnam, *Diffusion controlled electrode reactions.* Industrial & Engineering Chemistry, 1951. **43**(9): p. 2136 – 2143.

[92]. Newman, J. S., *Electrochemical Systems.* 2nd ed. 1991, Englewood Cliffs: Prentice – Hall. 560.

[93]. Arvia, A. J., S. L. Marchiano, and J. J. Podesta, *The diffusion of ferrocyanide and ferricyanide ions in aqueous solutions of potassium hydroxide.* Electrochimica Acta, 1967. **12**: p.259 – 266.

[94]. Arvia, A. J., J. C. Bazan, and J. S. W. Carrozza, *The diffusion of ferro- and ferricyanide ions in aqueous potassium chloride solutions and in solutions containing carboxymethlcellulose sodium salt.* Electrochimica Acta, 1968. **13**: p. 81 – 90.

[95]. Dawson, D. A., *Mass transfer in rough pipes.* In Chemical Engineering, 1968. University of Toronto.

[96]. Moggi, L., F. Bolletta, V. Balzani, and F. Scandola, *Photochemistry of coordination compounds – XV: cyanide complexes.* Journal of Inorganic and Nuclear Chemistry, 1966. **28**: p. 2589 – 2597.

[97]. Kolthoff, I. M. and E. A. Pearson, *Stability of potassium ferrocyanide solutions.* Industrial & Engineering Chemistry: Analytical Edition, 1931. **3**(4): p. 381 – 382.

[98]. Young, C.A. and T.S. Jordan, *Cyanide remediation: current and past technologies.* In 10th Annual Conference on Hazardous Waste research, 1995. Manhattan, Kansas.

[99]. Burdick, G. E. and M. Lipschuetz, *Toxicity of ferro- and ferricyanide solutions to fish, and the determination of the cause of mortality.* Transactions of the American Fisheries Society, 1948. **78**: p. 192 – 202.

[100]. Aggarwal, J. K. and L. Talbot, *Electrochemical measurements of mass transfer in semi-cylindrical hollow.* International Journal of Heat and Mass Transfer, 1979. **22**: p. 61 – 75.

[101]. Sutey, A. M. and J. G. Knudsen, *Effect of dissolved oxygen on the redox method for measurements of mass transfer coefficients.* Industrial & Engineering Chemistry Fundamentals, 1967. **6**(1): p. 132 – 139.

[102]. Eisenberg, M., C.W. Tobias, and C.R. Wilke, *Selected physical properties of ternary electrolytes employed in ionic mass transfer studies.* Journal of the Electrochemical Society, 1956. **103**(7): p. 413.

[103]. Jameson, G. J., *A model for liquid distribution in packed columns and trickle-bed reactors.* Trans. Inst. Chem. Engrs., 1966. **44**: p. 198 – 206.

[104]. Templeman, J. J. and K. E. Porter, *Experimental determinations of wall flow in packed columns.* Chemical Engineering Science, 1965. **20**: p. 1139 – 1140.

[105]. Porter, K. E. and J. J. Templeman, *Liquid flow in packed columns. Part III: Wall flow.* Trans. Inst. Chem. Engrs. 1968. **46**: T86 – T94.

[106]. Porter, K. E., V. D. Barnett and J. J. Templeman, *Liquid flow in packed columns. Part II: The spread of liquid over random packings.* Trans. Inst. Chem. Engrs. 1968. **46**: T74 – T85.

[107]. Dutkai, E. and E. Ruckenstein, *Liquid distribution in packed columns.* Chemical Engineering Science, 1968. **23**: p. 1365 – 1373.

[108]. Dutkai, E. and E. Ruckenstein, *New experiments concerning the distribution of a liquid in a packed column.* Chemical Engineering Science, 1970. **25**: p. 483 – 488.

[109]. Sutton, F., *A systematic handbook of volumetric analysis.* London: Butterworths Scientific Publications, 1955. p. 331 – 336.

[110]. Bazan, J.C. and A.J. Arvia, *The diffusion of ferro- and ferricyanide ion in aqueous solutions of sodium hydroxide.* Electrochimica Acta, 1965. **10**: p. 1025 – 1032.

[111]. Hiraoka, S., I. Yamada, H. Ikeno, H. Asano, S. Nomura, T. Okada, and H. Nakamura, *Measurement of diffusivities of ferricyanide and ferrocyanide ions in dilute-solution with KOH supporting electrolyte.* Journal of Chemical Engineering of Japan, 1981. **14**(5): P. 345 – 351.

[112]. Gabitto, J. F., and N. O. Lemcoff, *Local solid-liquid mass transfer coefficients in a trickle bed reactor.* Chemical Engineering Journal, 1987. **35**: p. 69.

[113]. Robbins, L. A., *Improve pressure drop prediction with a new correlation.* Chemical Engineering Progress, 1991. **87**: p. 87 – 91.

[114]. Leva, M., *Reconsider packed-tower pressure-drop correlations.* Chemical Engineering Progress, 1992. January: p. 65 – 72.

[115]. Delaunay, C. B., A. Storck, A. Laurent and J. C. Charpentier, *Electrochemical determination of liquid-solid mass transfer in a fixed-bed irrigated gas-liquid reactor with downward cocurrent flow.* International Chemical Engineering, 1982. **22**(2): p. 244 – 251.

[116]. Bartelmus, G., *Local solid-liquid mass transfer coefficients in a*

three-phase fixed bed reactor. Chemical Engineering and Processing, 1989. **26**: p. 111 – 120.

[117]. Groenhof, H.C., *Scaling-up of packed columns. Part I.* Chemical Engineering Journal, 1977. **14**: p. 181 – 191.

[118]. Groenhof, H.C., *Scaling-up of packed columns. Part II.* Chemical Engineering Journal, 1977. **14**: p. 193 – 203.

[119]. Senol, A., *Mass transfer efficiency of randomly-packed column: modeling considerations.* Chemical Engineering and Processing, 2001. **40**: p. 41 – 48.

[120]. Beg, S. A., M. M. Hassan and M. S. M. Naqvi, *Hydrodynamics and mass transfer in a concurrent packed column: A theoretical study.* The Chemical Engineering Journal, 1996. **63**: p. 93 – 103.

[121]. Doan, H. D. and M. E. Fayed, *Dispersion-concentric model for mass transfer in a packed bed with a countercurrent flow of gas and liquid.* Ind. Eng. Chem. Res., 2001. **40**: p. 4673 – 4680.

[122]. Guedes de Carvalho, J. R. F., and J. M. P. Q. Delgado, *Mass transfer from a large sphere buried in a packed bed along which liquid flows.* Chemical Engineering Science, 1999. **54**: p. 1121 – 1129.

[123]. Kawase, Y. and J. Ulbrecht, *A new approach for heat and mass transfer in granular beds based on the capillary model.* Ind. Eng. Chem. Fundam., 1985. **24**: p. 115.

[124]. Wen, X., A. Afacan, K. Nandakumar and K. T. Chuang, *Geometry based model for predicting mass transfer in packed columns.* Ind. Eng. Chem. Res., 2003. **42**: p. 5373.

[125]. Schlichting, H. *Boundary Layer Theory.* 6th ed. 1968, New York: McGraw – Hill. 748.

[126]. Olive, H. and G. Lacoste, *Application of volumetric electrodes to the recuperation of metals in industrial effluents – I. Mass transfer in fixed beds of spherical conductive par.* Electrochim. Acta, 1979. **24**: p.1109.

[127]. Wilson J.E. and C. J. Geankoplis, *Liquid phase mass transfer at very low Reynolds numbers in packed beds.* Ind. Eng. Chem. Fundam., 1966. **5**: p. 9.

[128]. Nelder, J. A. and R. Mead, *A simplex method for function minimization.* Computer Journal, 1965. **7**: p. 308 – 313.

[129]. Holman, J. P., *Experimental Methods for Engineers*, 5th ed. 1989, New York: McGraw – Hill. 549.

Appendix A. Nomenclature

A1. Variables and Parameters

A	cathode area	[m^2]
A_0 - A_{14}, B_0 - B_{14}	regression coefficients	
a, b	coefficients	
C_0 - C_2, $C_0^{'}$ - $C_2^{'}$	correlation coefficients	
C_∞	bulk concentration of ferricyanide	[mol m^{-3}]
C_i^B	bulk concentration of ferricyanide	[mol m^{-3}]
C_{NaOH}^B	bulk concentration of sodium hydroxide	[mol m^{-3}]
D	column diameter	[m]
D_e	axial dispersion coefficient	[m^2 s^{-1}]
D_v	diffusion coefficient of ferricyanide in solution	[m^2 s^{-1}]
d_p	equivalent diameter of packing – diameter of a sphere having the same surface area as the packing	[m]
F	Faraday constant (96,487)	[C mol^{-1}]
G	gas flow rate	[kg m^{-2} s^{-1}]
H	packing height	[m]
I_L	current due to diffusion only	[A]
I_D	measured current	[A]
I_{mig}	current due to ion migration	[A]
I_i	measured current	[A]
i_L	limiting current for ferricyanide reduction	[A]
k_L	liquid-phase mass transfer coefficient	[m s^{-1}]
L	liquid flow rate	[kg m^{-2} s^{-1}]
M_f	liquid maldistribution factor	

MT_{VAR}	mass transfer maldistribution factor	
n	total number of collectors or sampling electrodes in column	
N	mass transfer rate	[kmol m^{-2} s^{-1}]
Q_i	volumetric flow rate to i^{th} collector cell	[m^3 s^{-1}]
Q_{av}	average volumetric flow rate for n collector cells	[m^3 s^{-1}]
$(Sh/Sc^{0.33})_i$	value for the i^{th} sampling cathode in a bed	
$(Sh/Sc^{0.33})_{av}$	mean value for all sampling cathodes in the packed bed	
$(Sh/Sc^{0.33})_r$	mean value for all sampling cathodes at the same radial position in a certain layer	
T	Temperature	[°C]
r_a	surface reaction rate	[kmol m^{-2} s^{-1}]
r'	ratio of supporting electrolyte to total electrolyte	
r/R	ratio of radial position to column radius	
U	superficial velocity of liquid through column	[m s^{-1}]
U	liquid velocity	[m s^{-1}]
V	average liquid volumetric flow rate of the collecting cells with the same radius in the bed cross section	[m^3 s^{-1}]
V_{av}	average liquid volumetric flow rate of all collecting cells at a certain packing height	[m^3 s^{-1}]
W	volumetric flow rate of wall flow	[m^3 s^{-1}]
W_{tot}	total volumetric flow rate for all collecting cells and wall flow at a certain packing height	[m^3 s^{-1}]
x/D	ratio of axial position to column diameter	
Z	number of electrons exchanged	

A2. Greek Symbols

μ	dynamic viscosity	[kg m^{-1} s^{-1}]
v	kinematic viscosity of solution	[m^2 s^{-1}]
ρ	density	[kg m^{-3}]
ε	void fraction	
δ_w	width of wall region	[mm]
σ_i	errors needed to be associated	
σ_x	accumulated error	
| |	absolute value of function	

A3. Dimensionless Numbers

Bo	Bodenstein number	$Bo = \frac{U \cdot l}{D_e}$
Pe	Peclet number for mass transfer - the ratio of convective and diffusive transport	$Pe = \frac{U \cdot d_p}{D_v}$
Re	Reynolds number - the ratio of inertial force and viscous force	$\mathrm{Re} = \frac{U \cdot d_p \cdot \rho}{\mu}$
Sc	Schmidt number - the ratio of kinetic viscosity and molecular diffusivity	$Sc = \frac{\mu}{\rho \cdot D_v}$
Sh	Sherwood number - the ratio of mass diffusivity and molecular diffusivity	$Sh = \frac{k_L \cdot d_p}{D_v}$

Appendix B. Instrumental Error and Sample Calculations

B.1. Error in Instrumentation

Several instruments were used in this study. The error from each instrument is tabulated in Table B-1.

Table B-1. Instruments and their errors in parameter measurement.

Instrument Name	Accuracy	Application
Omega FP7001 paddlewheel flow sensor	2%	Liquid flow rate
Omega HHF710 Hydro-thermo Anemometer	1%	Gas flow rate
Type J thermocouples	1%	Temperature
Daytronic Model 10S-ACFG DAS	0.02%	Voltage drop

B.2. Sample Calculations on Uncertainty Analysis

B.2.1. Error on liquid distribution measurement (LDM)

Human error on the liquid flow rate reading

For example: Expected value: 4.5 gpm

Reading value: 4.4 – 4.6 gpm

Error: 100%*|4.4 - 4.5|/4.5 + 100*|4.6 - 4.5|/4.5 = 4.4%

Error on liquid flow rate

$$\sigma_{la} = \sqrt{\sum \sigma_i^2} = \sqrt{\left(\frac{2}{100}\right)^2 + \left(\frac{5}{100}\right)^2} = 5.4\%$$

where σ_{la} is the error on liquid flow rate, σ_1 is the instrumental error on liquid flow rate and σ_2 is the human error on the liquid flow rate reading.

Error on liquid colleting time

For example: for cell C01, L = 7.8 9 kg m^{-2} s^{-1}, G = 0.9 kg m^{-2} s^{-1} and SPLD:

t_1 = 5 s, V_1/V_{av1} = 5.63; M_f = 0.24

t_2 = 5-1 = 4 s, V_2/V_{av2} = 5.64; M_f = 0.24

t_3 = 5+1 = 6 s, V_3/V_{av3} = 5.63; M_f = 0.24

Error on V/V_{av}: 100%*|5.64-5.63|/5.63 + 100%*|5.63-5.63|/5.63 = 0.18%

Error on M_f: 100%*|0.24-0.24|/0.24 + 100%*|0.24-0.24|/0.24 = 0

Error on liquid volume measurement

$$\sigma_{lb} = \sqrt{\sum \sigma_i^2} = \sqrt{\left(\frac{1}{100}\right)^2 + \left(\frac{2}{100}\right)^2} = 2.2\%$$

where σ_{lb} is the error on liquid volume measurement, σ_1 is the instrumental error on liquid volume measurement and σ_2 is the error on measurement approach.

Accumulated error in liquid distribution measurement

$$\sigma_{lx} = \sqrt{\sum \sigma_i^2} = \sqrt{\left(\frac{5.4}{100}\right)^2 + \left(\frac{2.2}{100}\right)^2} = 5.8\%$$

where σ_{lx} is the accumulated error, σ_{la} is the error on liquid flow rate, σ_{lb} is the error on liquid volume measurement and σ_{lc} is the error on the liquid loss during liquid collection process.

B.2.2. Error on mass transfer measurement (MTM)

Error from ionic migration

For example: C^B_{ferri} = 3.6 mol m^{-3}, C^B_{NaOH} = 500 mol m^{-3}

Based on Eq. 2-7,

$$I_{mig} = \frac{1}{2}\frac{C^B_{ferri}}{C^B_{NaOH}} I_i = \frac{1}{2} \times \frac{3.6}{500} I_i = 0.0036 I_i \quad \text{or} \quad \frac{I_{mig}}{I_i} = 0.36\%$$

where I_{mig} is the current due to ion migration (A); I_i is the measured current (A); C^B_{ferri} is the bulk concentration of ferricyanide (mol m^{-3}); and C^B_{NaOH} is the bulk concentration of supporting electrolyte (mol m^{-3}).

Error on the determination of ferricyanide concentration

$$\sigma_{mf} = \sqrt{\sum \sigma_i^2} = \sqrt{\left(\frac{0.08}{100}\right)^2 + \left(\frac{0.2}{100}\right)^2 + \left(\frac{0.5}{100}\right)^2} = 0.6\%$$

where σ_{mf} is the error on the determination of ferricyanide concentration, σ_1 is the error from the pipette ($\sigma_1 = \frac{0.02}{25} \times 100\% = 0.08\%$), σ_2 is the error from the burette ($\sigma_2 = \frac{0.1}{50} \times 100\% = 0.2\%$) and σ_3 is the error from titration ($\sigma_3 = \frac{0.0001}{0.020} \times 100\% = 0.5\%$).

Accumulated error in local mass transfer measurement

$$\sigma_{mx} = \sqrt{\sum \sigma_i^2} = \sqrt{\left(\frac{5.4}{100}\right)^2 + \left(\frac{0.36}{100}\right)^2 + \left(\frac{1}{100}\right)^2 + \left(\frac{0.6}{100}\right)^2 + \left(\frac{2}{100}\right)^2 + \left(\frac{2.5}{100}\right)^2} = 6.4\%$$

where σ_{mx} is the accumulated error, σ_1 is the error on liquid flow rate, σ_2 is the error from ionic migration, σ_3 is the error from the temperature, σ_4 is the error on the determination of the ferricyanide concentration, σ_5 is the error on diffusivity and σ_6 is the error on viscosity.

Appendix C. Additional Figures

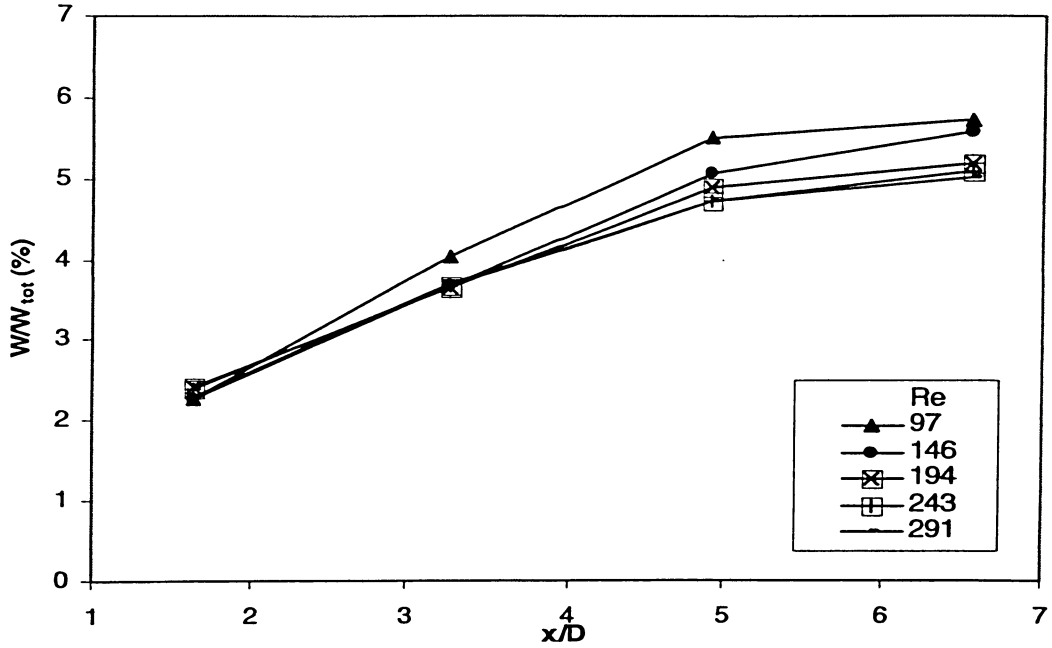

Fig. C-1. Effect of liquid flow rate on wall flow development along packing height, CLD.

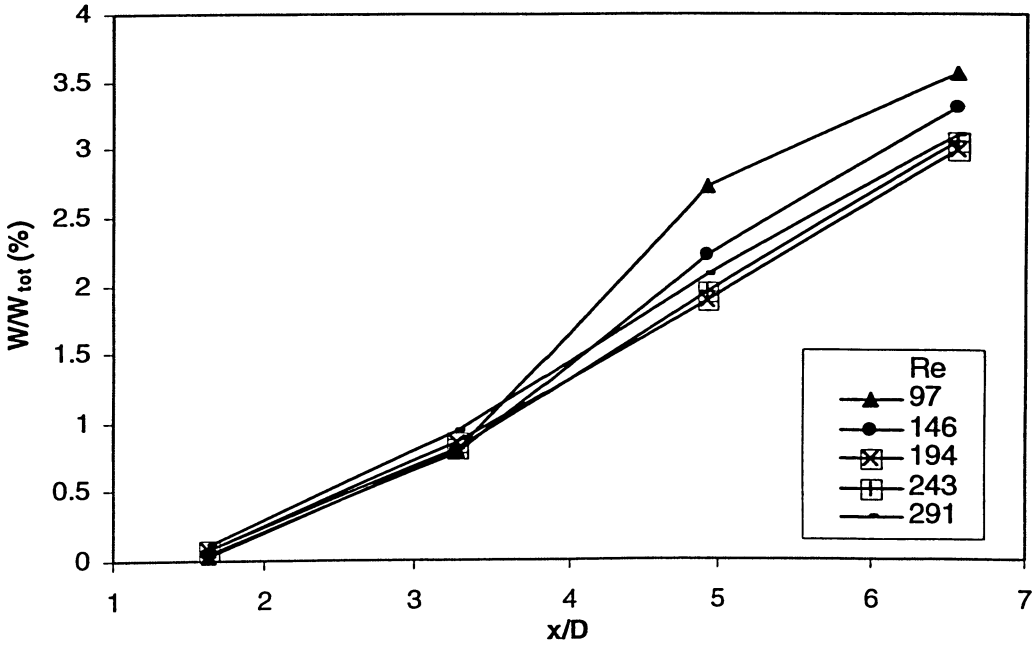

Fig. C-2. Effect of liquid flow rate on wall flow development along packing height, SPLD.

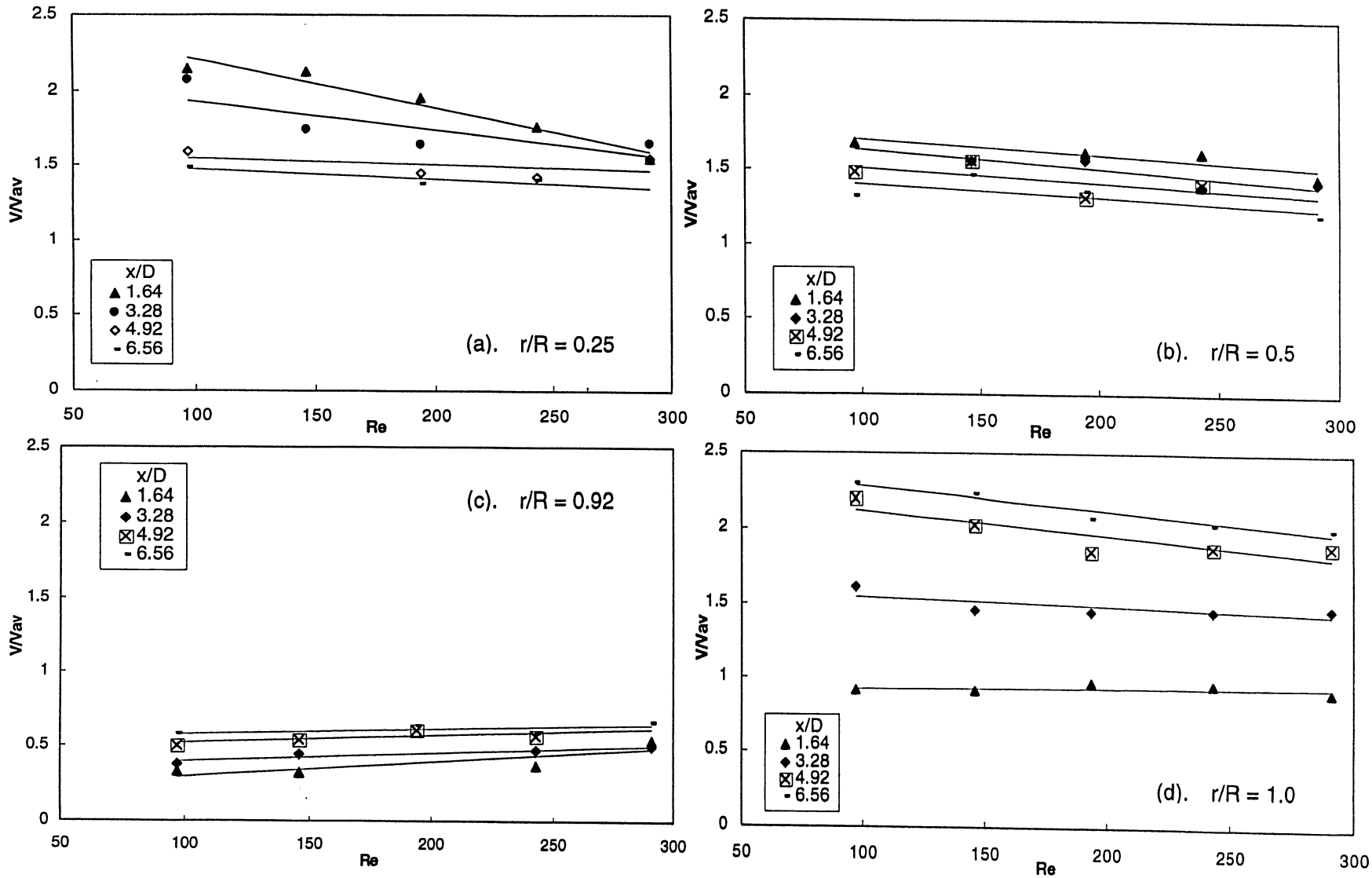

Fig. C-3. Effect of liquid flow rate on relative liquid velocity along packing height at four radial positions, CLD.

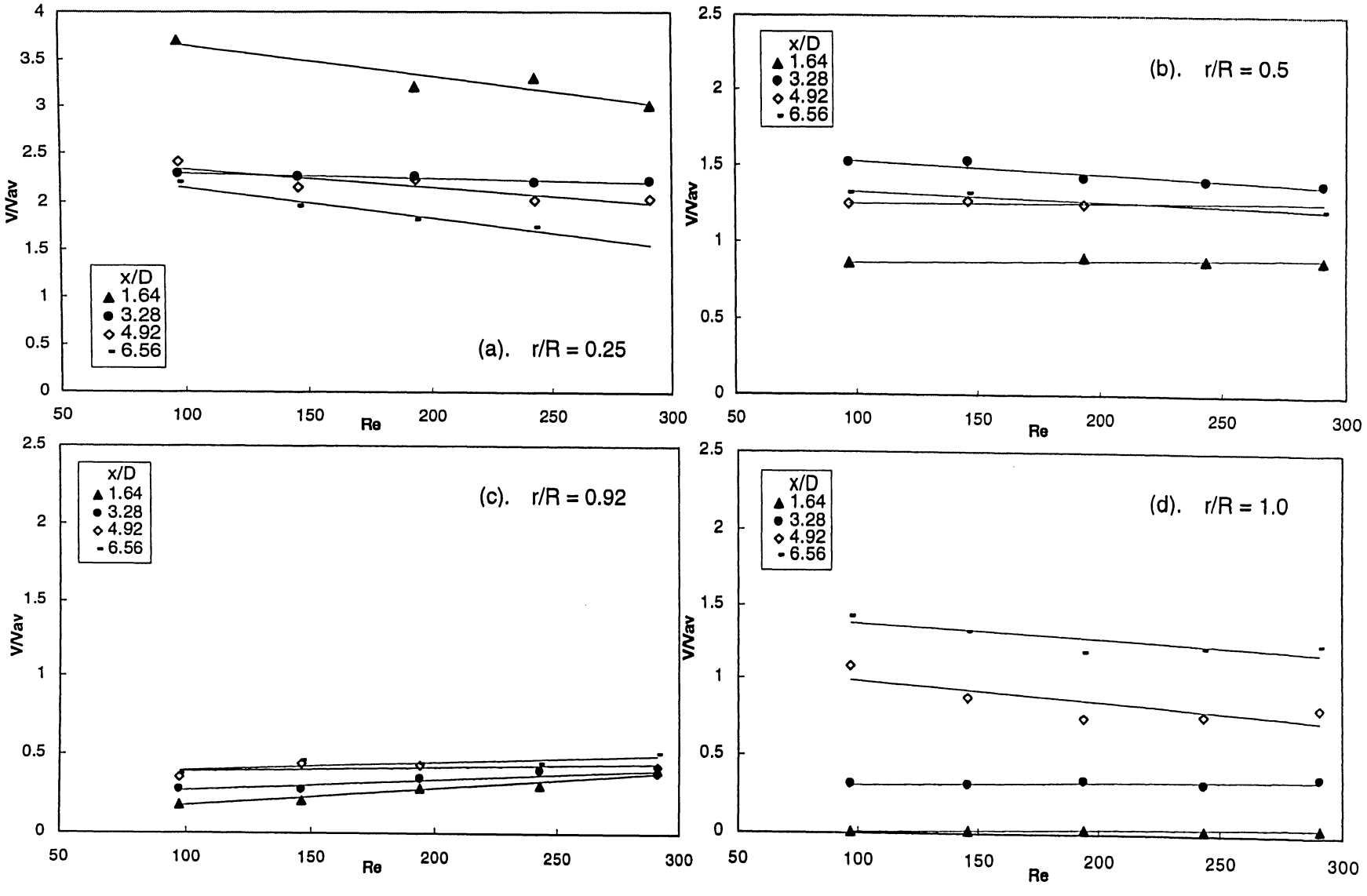

Fig. C-4. Effect of liquid flow rate on relative liquid velocity along packing height at four radial positions, SPLD.

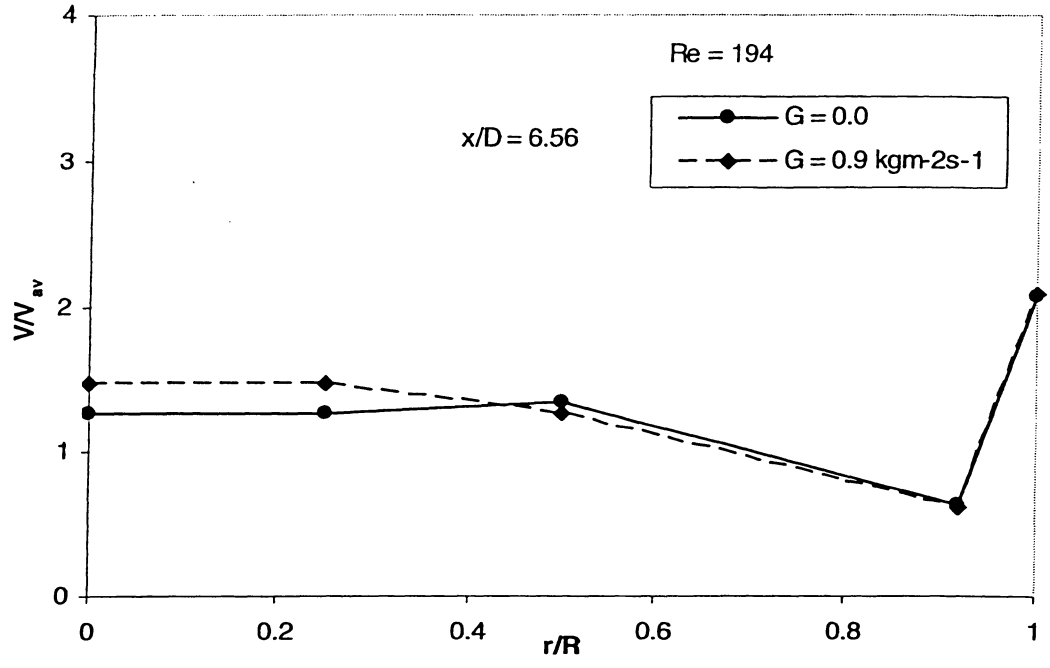

Fig. C-5. Effect of gas flow rate on liquid radial distribution, CLD, x/D = 6.56 and Re = 194.

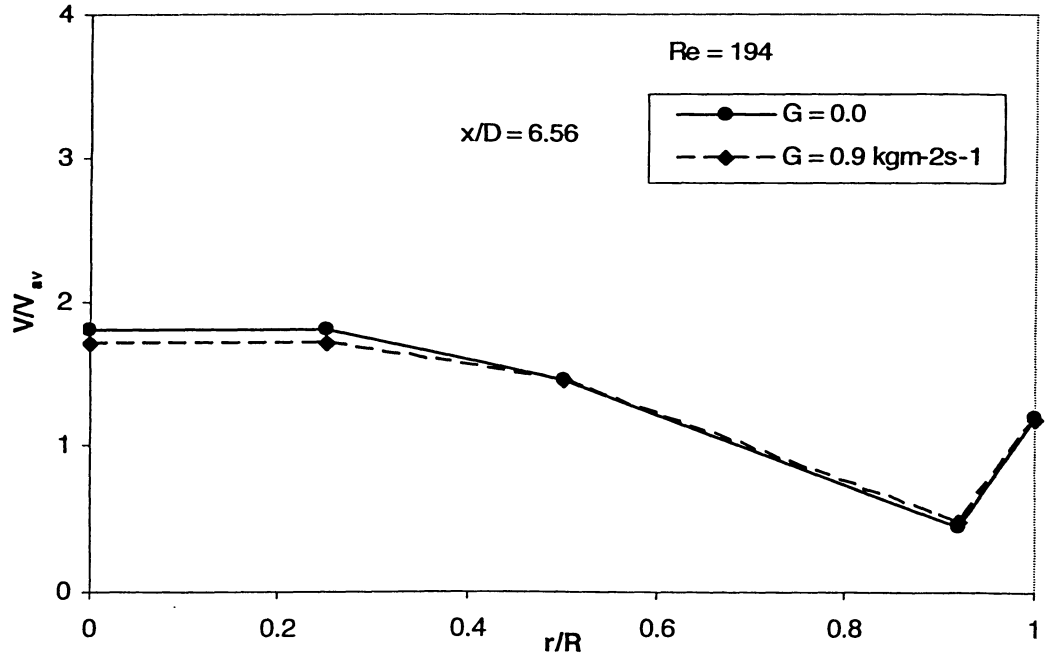

Fig. C-6. Effect of gas flow rate on liquid radial distribution, SPLD, x/D = 6.56 and Re = 194.

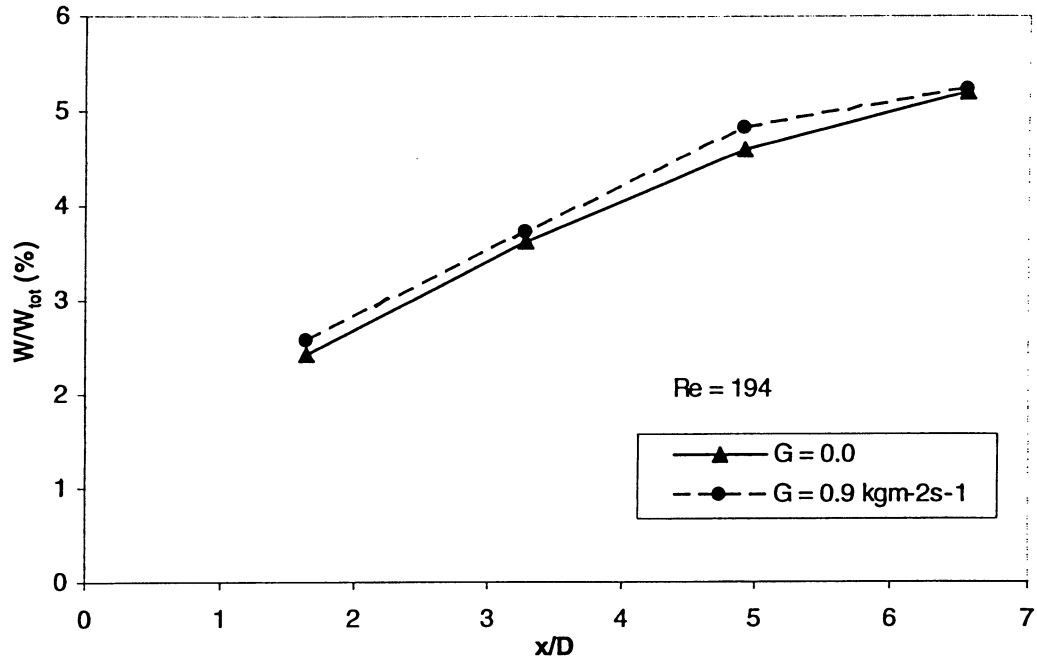

Fig. C-7. Effect of gas flow rate on liquid wall flow development, CLD and Re = 194.

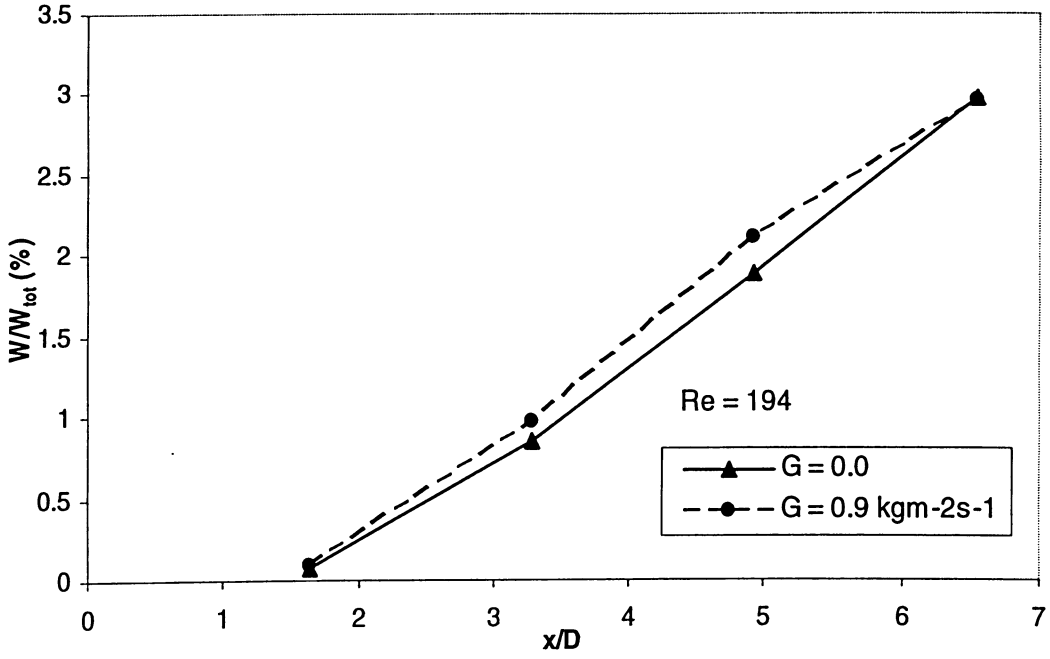

Fig. C-8. Effect of gas flow rate on liquid wall flow development, SPLD and Re = 194.

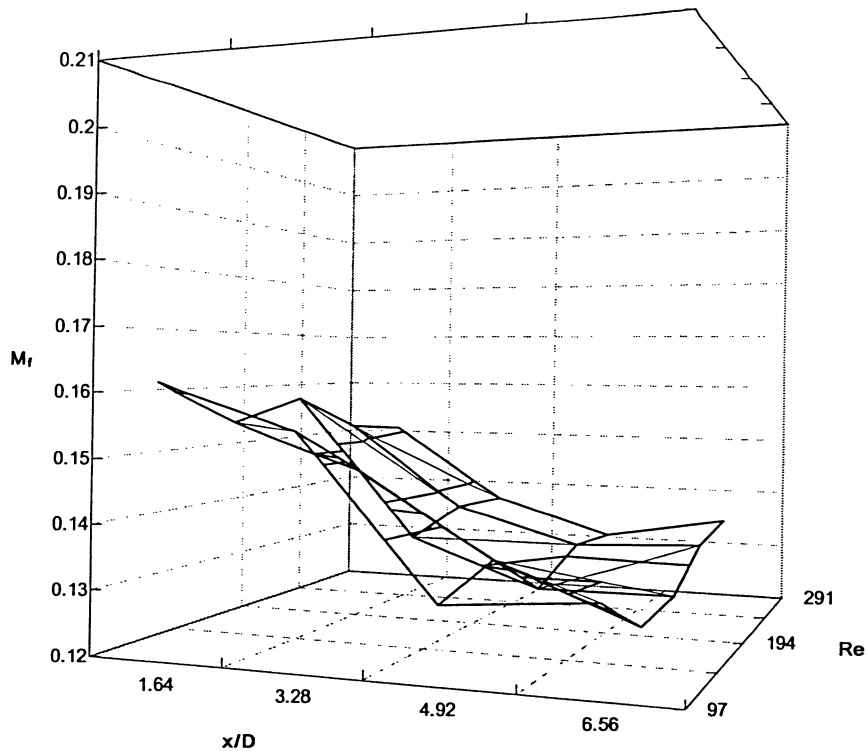

Fig. C-9. The trend of M_f at various x/D and Re for LLD, G = 0.

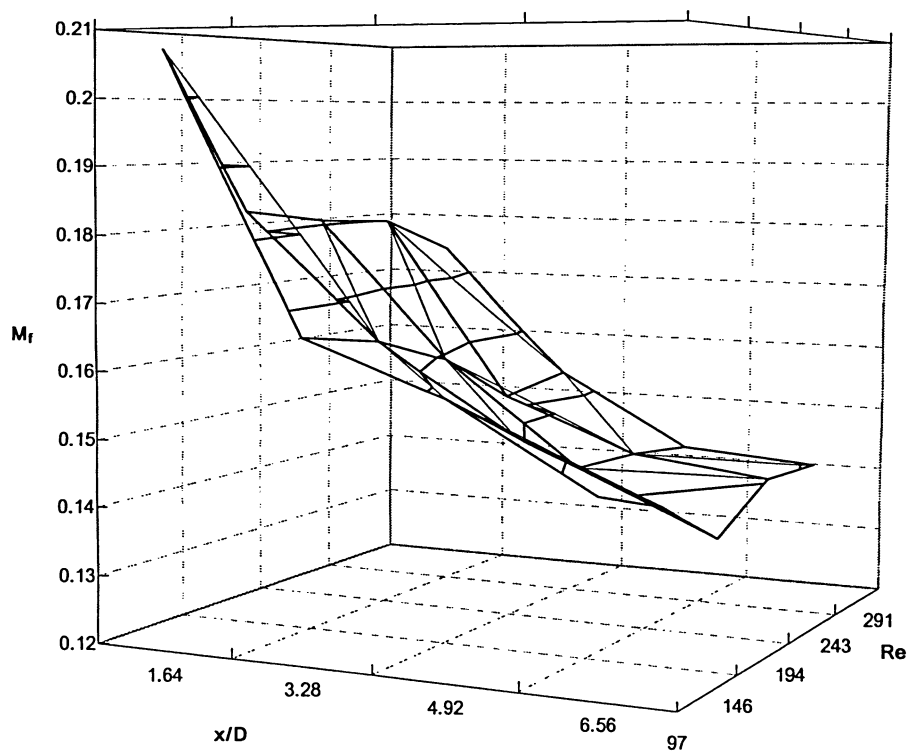

Fig. C-10. The trend of M_f at various x/D and Re for CLD, G = 0.

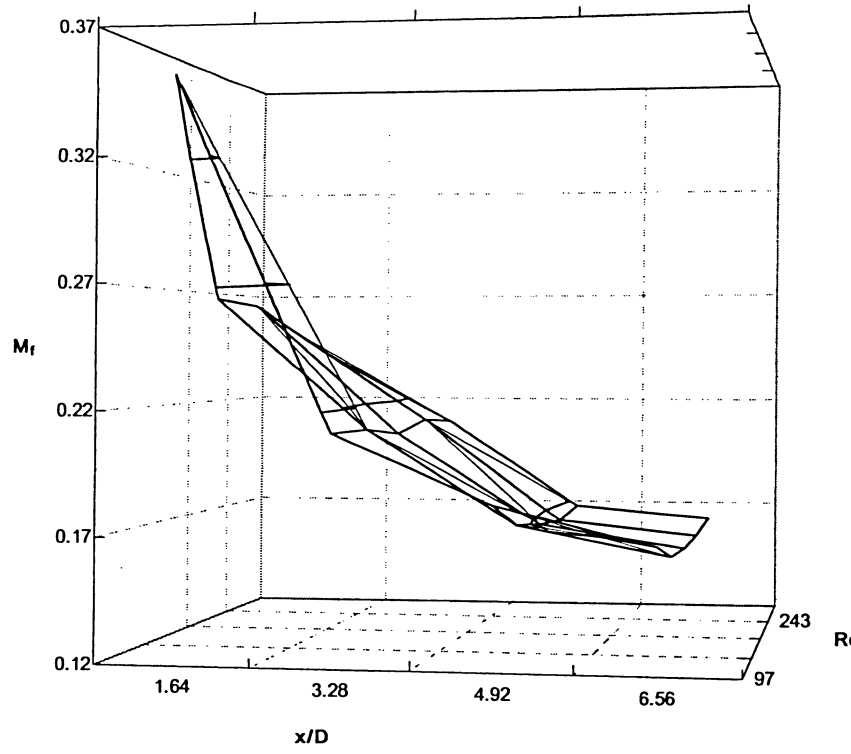

Fig. C-11. The trend of M_f at various x/D and Re for SPLD, G = 0.

Appendix D. Tabulated Data for LDM

D1. Notation

H	packing height	[m]
L	liquid flow rate	[kg m^{-2} s^{-1}]
G	gas flow rate	[kg m^{-2} s^{-1}]
t	liquid collecting time	[s]
V	liquid volume calculated by the depth of liquid in the cell, the cross-sectional area of the cell and the liquid collecting time	[ml min^{-1}]

D2. Experimental Data Tables

Table D-1. Summary table for LDM by SPLD.

H	L	G	t	H	L	G	t	H	L	G	t	H	L	G	t
0.5	2.6	0	7	1.0	2.6	0	15	1.5	2.6	0	19	2.0	2.6	0	22
		0.9	7			0.9	15			0.9	19			0.9	22
	3.9	0	7		3.9	0	10		3.9	0	12		3.9	0	15
		0.9	7			0.9	10			0.9	12			0.9	15
	5.2	0	7		5.2	0	8		5.2	0	11		5.2	0	11
		0.9	7			0.9	8			0.9	11			0.9	11
	6.5	0	6		6.5	0	5		6.5	0	8		6.5	0	9
		0.9	7			0.9	5			0.9	7			0.9	8
	7.8	0	5		7.8	0	5		7.8	0	6		7.8	0	7
		0.9	5			0.9	5			0.9	6			0.9	7

Table D-2. Summary table for LDM by CLD.

H	L	G	t	H	L	G	t	H	L	G	t	H	L	G	t
0.5	2.6	0	15	1.0	2.6	0	20	1.5	2.6	0	21	2.0	2.6	0	21
		0.9	15			0.9	20			0.9	21			0.9	21
	3.9	0	12		3.9	0	15		3.9	0	15		3.9	0	15
		0.9	12			0.9	15			0.9	16			0.9	16
	5.2	0	8		5.2	0	10		5.2	0	11		5.2	0	11
		0.9	8			0.9	10			0.9	11			0.9	11
	6.5	0	7		6.5	0	10		6.5	0	10		6.5	0	10
		0.9	7			0.9	10			0.9	10			0.9	10
	7.8	0	7		7.8	0	7		7.8	0	7		7.8	0	9
		0.9	7			0.9	7			0.9	7			0.9	8

Table D-3. Summary table for LDM by LLD.

H	L	G	t	H	L	G	t	H	L	G	t	H	L	G	t
0.5	2.6	0	24	1.0	2.6	0	26	1.5	2.6	0	25	2.0	2.6	0	25
		0.9	24			0.9	26			0.9	25			0.9	25
	3.9	0	15		3.9	0	17		3.9	0	18		3.9	0	15
		0.9	16			0.9	17			0.9	18			0.9	17
	5.2	0	12		5.2	0	12		5.2	0	12		5.2	0	12
		0.9	11			0.9	12			0.9	12			0.9	13
	6.5	0	10		6.5	0	10		6.5	0	11		6.5	0	11
		0.9	10			0.9	11			0.9	11			0.9	10
	7.8	0	7		7.8	0	7		7.8	0	7		7.8	0	7
		0.9	7			0.9	8			0.9	10			0.9	8

Table D–4. Data of liquid volume (V) in the cells for SPLD without gas.

	H = 0.5 m						H = 1 m				
L	2.6	3.9	5.2	6.5	7.8	L	2.6	3.9	5.2	6.5	7.8
C01	129.1	15.9	1044.9	1132	1663	*C01*	37.9	67.1	96.8	222.1	439
I02	822.7	389.3	536.33	751.2	754	*I02*	482	702.4	374.4	1477	1363
I03	114.4	552.2	194.67	211.3	464.8	*I03*	60.3	116.2	271.1	129.1	211.8
I04	1014	250.3	1203.8	1291	1549	*I04*	439	606.9	790.8	1224	1116
I05	40.58	1136.2	27.8	70.4	206.6	*I05*	77.5	108.5	481	232.4	346
I06	169.7	11.9	147	690.2	377	*I06*	327.1	405.4	529.4	624.9	955.5
I07	84.9	282.1	560.2	967.2	733.4	*I07*	96.4	178.2	74.2	93	82.6
O08	11.1	437	123.2	201.9	222.1	*O08*	60.3	56.8	77.5	320.2	124
O09	129.1	51.6	158.9	47	351.2	*O09*	337.4	340.9	422.9	263.4	320.2
O10	302.5	206.6	893.9	1042	1012	*O10*	132.6	273.7	497.1	702.4	707.6
O11	110.7	774.7	309.9	42.3	273.7	*O11*	74	333.1	706.9	976.1	1260
O12	3.7	182.8	19.9	14.1	72.3	*O12*	25.8	51.6	67.8	98.1	129.1
O13	55.3	15.9	47.7	47	98.1	*O13*	55.09	100.7	45.2	185.9	46.5
O14	221.3	91.4	488.7	239.5	284.1	*O14*	437.3	746.3	648.8	945.1	960.6
O15	3.7	353.6	107.3	253.5	258.2	*O15*	111.9	144.6	32.3	330.5	841.8
O16	3.7	83.4	11.9	23.5	15.5	*O16*	43	23.2	35.5	77.5	67.1
O17	70.1	11.9	31.8	211.3	129.1	*O17*	210	160.1	161.4	170.4	253.1
O18	11.1	99.3	55.6	93.9	77.5	*O18*	132.6	103.3	48.4	87.8	51.7
O19	18.45	47.7	63.6	108	82.6	*O19*	111.9	204	71	103.3	82.6
U20	3.7	43.7	31.8	4.7	5.2	*U20*	37.9	105.9	25.8	98.1	165.3
U21	3.7	31.8	19.9	47	25.8	*U21*	5.2	7.7	9.7	46.5	15.5
U22	3.7	11.9	123.2	497.7	671.4	*U22*	13.8	23.2	87.2	98.1	294.4
U23	44.3	91.4	99.3	136.2	160.1	*U23*	27.5	43.9	96.8	67.1	93
U24	136.5	55.6	476.7	521.2	1074	*U24*	146.3	178.2	397	635.3	909
U25	3.7	198.6	31.8	4.7	15.5	*U25*	5.2	7.7	9.7	20.7	15.5
U26	3.7	4	11.9	14.1	15.5	*U26*	37.9	72.3	87.2	196.3	108.5
U27	36.9	4	47.7	42.3	51.7	*U27*	55.1	100.7	64.6	129.1	134.3
U28	3.7	47. 7	4	4.7	25.8	*U28*	8.6	33.6	100	201.4	154.9
U29	3.7	4	4	4.7	41.3	*U29*	51.7	56.8	113	72.3	56.8
U30	59	4	115.2	23.5	46.5	*U30*	34.4	33.6	25.8	232.4	15.5
U31	3.7	59.6	4	4.7	5.2	*U31*	20.7	25.8	22.6	31	31
U32	3.7	4	4	4.7	5.2	*U32*	5.2	7.7	9.7	31	31
U33	3.7	4	4	4.7	5.2	*U33*	8.6	7.7	9.7	62	41.3
U34	3.7	4	4	4.7	5.2	*U34*	8.6	7.747	9.7	15.5	15.5
U35	3.7	4	4	4.7	5.2	*U35*	24.1	23.2	32.3	46.5	67.1
U36	3.7	4	4	4.7	5.2	*U36*	8.6	7.7	9.7	15.5	15.5
U37	3.7	4	4	4.7	5.2	*U37*	13.8	7.7	9.7	15.5	15.5
U38	3.7	4	4	4.7	5.2	*U38*	8.6	7.7	9.7	15.5	15.5
U39	3.7	4	4	4.7	5.2	*U39*	5.2	7.7	9.7	15.5	20.7
W40	21	64	124	164	290	*W40*	715	1026	1342	1985	2580

Table D–4. Data of liquid volume (V) in the cells for SPLD without gas. (...)

	H = 1.5 m						H = 2 m				
L	2.6	3.9	5.2	6.5	7.8	L	2.6	3.9	5.2	6.5	7.8
C01	47.6	75.3	201.7	158.7	90.6	*C01*	41.1	42.7	107.6	218.7	199.2
I02	333	436.8	543.5	777.8	1092	*I02*	297	397.1	511.7	732.2	645.6
I03	50.3	96.8	179.5	342.2	280.9	*I03*	76.3	156.7	71.7	106.3	88.5
I04	421.3	710.1	811.6	734.3	1142	*I04*	355.7	578.8	779.4	799	1217
I05	61.16	73.2	61.5	90.2	199.3	*I05*	76.3	32.1	54.9	94.18	383.7
I06	265	340	651.7	628.5	1028	*I06*	219.5	317	561.9	583.3	922.3
I07	92.4	116.2	130.4	177.3	181.2	*I07*	191.3	151.3	150.6	230.9	129.1
O08	80.2	185.1	142.6	286.2	335.2	*O08*	54	85.4	114.8	154.9	121.7
O09	126.4	144.2	179.5	342.2	434.9	*O09*	347.4	336.6	299	628.9	317.3
O10	168.5	312	359.1	426.2	815.5	*O10*	125.6	245.8	487.8	601.5	605
O11	91.1	269	312.3	342.2	557.2	*O11*	119.7	219	220	434.4	649.3
O12	25.8	45.2	59	49.8	68	*O12*	27	35.6	57.4	54.68	77.5
O13	44.9	96.8	167.2	105.8	135.9	*O13*	91.6	65.9	110	76	62.7
O14	131.8	137.7	474.7	668.9	792.8	*O14*	119.7	249.3	487.8	571.2	442.7
O15	92.4	96.8	231.2	575.6	480.2	*O15*	156.1	302.7	485.3	817.2	590.2
O16	28.5	127	103.3	158.7	203.9	*O16*	57.5	55.2	145.8	139.7	147.6
O17	146.8	290.5	223.8	395.1	489.3	*O17*	47	151.3	334.7	276.5	309.9
O18	96.5	96.8	137.7	155.6	240.1	*O18*	111.5	138.9	203.2	139.7	280.4
O19	95.1	83.9	83.6	127.6	117.8	*O19*	38.7	51.6	117.1	145.8	77.4
U20	84.3	77.5	159.9	62.2	122.3	*U20*	65.7	58.8	121.9	288.6	136.5
U21	10.9	17.2	14.8	21.8	18.1	*U21*	8.2	48.1	35.9	9.1	11.1
U22	19	15.1	7.4	9.3	90.6	*U22*	5.9	26.7	28.7	15.19	11.1
U23	21.75	40.9	51.6	49.8	108.7	*U23*	29.3	23.2	52.6	76	73.8
U24	77.5	137.7	250.9	364	448.5	*U24*	65.7	156.7	179.3	279.5	239.8
U25	20.4	73.2	61.5	9.3	36.2	*U25*	3.5	12.466	7.2	15.19	11.1
U26	42.1	90.4	93.5	80.9	154	*U26*	50.5	58.8	100.4	182.3	158.6
U27	61.2	96.8	98.4	43.6	317.1	*U27*	50.5	220.8	110	91.14	154.9
U28	6.8	53.8	68.9	40.45	262.8	*U28*	50.5	101.5	93.3	258.2	442.7
U29	10.9	107.6	91	146.2	126.9	*U29*	49.3	69.5	67	106.3	92.2
U30	16.3	17.2	29.5	118.2	27.2	*U30*	5.9	5.3	33.5	69.9	114.4
U31	9.5	21.5	32	28	122.3	*U31*	31.7	28.5	71.7	69.8	99.6
U32	4.1	6.5	49.2	6.2	9.1	*U32*	3.5	17.8	50.2	66.8	66.4
U33	12.2	25.8	36.9	12.4	27.2	*U33*	23.5	28.5	47.8	45.6	110.7
U34	15	105.5	103.3	59.1	163.1	*U34*	34	37.4	200.9	106.3	88.5
U35	74.8	114.1	145.1	342.2	199.3	*U35*	88	106.9	133.9	115.4	210.3
U36	12.2	10.8	34.4	74.7	77	*U36*	12.9	32.1	102.8	15.19	36.9
U37	12.2	15.1	49.2	59.1	49.8	*U37*	8.2	23.2	50.2	36.46	365.2
U38	17.7	43	39.4	15.6	31.7	*U38*	15.2	42.7	33.5	106.3	125.4
U39	9.5	21.5	24.6	15.6	27.2	*U39*	5.8	32	40.6	76	25.8
W40	1956	2590	2965	3810	5611	*W40*	2770	3853	5020	6610	7500

Table D–5. Data of liquid volume (V) in the cells for SPLD with gas.

	H = 0.5 m						H = 1 m				
L	2.6	3.9	5.2	6.5	7.8	L	2.6	3.9	5.2	6.5	7.8
C01	139	301.9	591.9	969	1523.6	*C01*	60.3	85.2	161.4	273	361.5
I02	1080.6	1013	1108	1005	1224	*I02*	516.5	609.4	361.5	1376	1239.5
I03	162.9	43.7	95.4	453	299.6	*I03*	37.9	56.8	245.3	219	72.3
I04	731	1148	1243	1089	1317	*I04*	439	818.6	774.7	1043	1265.3
I05	59.6	91.4	103.3	159	62	*I05*	93	160.1	193.7	209	511.3
I06	131.1	111.2	321.8	354	325.4	*I06*	292.7	426.1	522.9	611	909
I07	63.6	508.5	321.8	520	387.3	*I07*	185.9	175.6	158.2	209	134.3
O08	43.7	83.4	111.2	135	206.6	*O08*	86.1	77.5	122.7	243	170.4
O09	154.9	218.5	274.1	318	330.5	*O09*	289.2	351.2	125.9	422	356.4
O10	369.5	790.6	1021	1037	1224	*O10*	120.5	157.5	409.9	646	878
O11	190.7	151	143	401	154.9	*O11*	84.4	364.1	765	884	1058.8
O12	4	31.8	19.9	11.9	77.5	*O12*	41.3	31	48.4	54.6	108.5
O13	43.7	47.7	31.8	147	160.1	*O13*	103.3	149.8	71	169	103.3
O14	166.9	218.5	508.5	560	1007.1	*O14*	430.4	573.3	632.7	804	867.7
O15	11.9	11.9	99.3	596	934.8	*O15*	94.7	111	100.1	144	635.3
O16	11.9	11.9	11.9	47.7	51.6	*O16*	43	23.2	87.2	49.7	170.4
O17	95.3	75.5	202.6	167	211.8	*O17*	160.1	183.3	564.9	263	315
O18	11.9	39.7	63.6	67.5	77.5	*O18*	67.1	93	87.2	129	62
O19	11.9	59.6	115.2	83.4	77.5	*O19*	86.1	154.9	87.2	144	139.4
U20	4	4	43.7	43.7	56.8	*U20*	56.8	82.6	58.1	124	139.4
U21	11.9	11.9	19.9	35.8	41.3	*U21*	27.5	31	12.9	49.7	25.8
U22	11.9	11.9	107.3	99.3	160.1	*U22*	91.2	72.3	113	457	196.3
U23	35.8	91.4	147	123	108.5	*U23*	32.7	31	67.8	104	93
U24	83.4	250.3	544.3	628	449.3	*U24*	65.4	201.4	390.6	566	872.8
U25	4	4	19.9	4	5.2	*U25*	8.6	7.7	9.7	14.9	124
U26	4	4	11.9	4	25.8	*U26*	43	43.9	93.6	94.4	129.1
U27	11.9	27.8	39.7	35.8	51.6	*U27*	58.5	121.4	71	184	227.2
U28	4	4	4	4	41.3	*U28*	8.6	56.8	48.4	59.6	191.1
U29	4	4	4	23.8	98.1	*U29*	34.4	41.3	58.1	79.5	82.6
U30	19.9	31.8	43.7	91.4	25.8	*U30*	43	67.1	29.1	367	25.8
U31	4	4	4	4	41.3	*U31*	20.7	20.7	16.1	34.8	25.8
U32	4	4	4	4	5.2	*U32*	5.2	12.9	9.7	14.9	25.8
U33	4	4	4	4	5.2	*U33*	8.6	7.7	9.7	14.9	25.8
U34	4	4	4	4	5.2	*U34*	8.6	12.9	9.7	14.9	25.8
U35	4	4	4	4	5.2	*U35*	25.8	20.7	45.2	44.7	46.5
U36	4	4	4	4	5.2	*U36*	5.2	20.7	9.7	14.9	15.5
U37	4	4	4	4	5.2	*U37*	13.8	25.8	9.7	14.9	15.5
U38	4	4	4	4	5.2	*U38*	5.2	7.7	9.7	14.9	15.5
U39	4	4	4	4	5.2	*U39*	5.2	7.7	9.7	14.9	25.8
W40	49	68	147	184	490	*W40*	863	1150	1542	2057	3094

Table D–5. Data of liquid volume (V) in the cells for SPLD with gas. (...)

	H = 1.5 m						H = 2 m				
L	2.6	3.9	5.2	6.5	7.8	L	2.6	3.9	5.2	6.5	7.8
C01	59.8	109.7	184.5	192	126.9	*C01*	52.8	98	114.8	161	75.5
I02	304.4	454.1	634.5	844	1005.8	*I02*	291.1	391.8	521.2	694	695.2
I03	57.1	81.8	135.3	314	194.8	*I03*	69.3	114	98	174	79.5
I04	417.3	639.1	730.4	810	1114.5	*I04*	346.3	475.5	781.9	830	897.9
I05	81.5	32.3	140.2	157	258.2	*I05*	88	49.9	47.8	74.2	178.8
I06	247.4	294.8	405.8	792	1137.1	*I06*	234.8	406	430.4	710	1032.9
I07	122.3	150.6	159.9	220	212.9	*I07*	167.9	151.4	138.7	229	147
O08	65.2	170	93.5	209	199.3	*O08*	91.6	206.6	174.5	274	317.8
O09	172.6	228.1	273	447	493.8	*O09*	334.5	325.9	176.9	152	337.7
O10	131.8	223.8	157.4	447	756.6	*O10*	100.9	151.4	420.8	139	333.7
O11	62.5	200.1	150	338	516.5	*O11*	93.9	115.8	208	265	286
O12	27.2	49.5	66.4	66.3	81.5	*O12*	30.5	57	43	80.7	75.5
O13	54.4	120.5	366.4	223	194.8	*O13*	71.6	62.3	186.5	96.8	99.3
O14	153.6	189.4	614.8	838	901.6	*O14*	144.4	283.2	569.1	775	901.8
O15	103.3	118.4	346.8	694	511.9	*O15*	144.4	329.5	416	733	270.2
O16	35.3	146.3	154.9	199	231.1	*O16*	68.1	85.5	126.7	200	206.6
O17	156.3	314.2	263.2	359	421.3	*O17*	51.6	187	373	297	381.4
O18	76.1	58.1	73.8	140	154	*O18*	103.3	99.7	275	207	190.7
O19	81.5	58.1	34.4	154	90.6	*O19*	73.9	98	138.7	168	166.9
U20	76.1	56	120.5	69.8	99.7	*U20*	51.6	80.1	186.5	242	87.4
U21	6.8	15.1	12.3	27.9	18.1	*U21*	21.1	65.9	62.2	22.6	11.9
U22	29.9	28	36.9	27.9	117.8	*U22*	8.2	30.3	52.6	42	27.8
U23	16.3	32.3	36.9	45.4	104.2	*U23*	36.4	26.7	59.8	87.2	83.4
U24	54.4	66.7	142.6	168	389.6	*U24*	72.8	89.1	121.9	96.8	111.2
U25	24.5	49.5	7.4	10.5	58.9	*U25*	5.9	21.4	7.2	38.7	19.9
U26	35.3	83.9	91	80.3	167.6	*U26*	55.2	62.3	45.4	155	107.3
U27	61.2	187.2	228.7	73.3	348.8	*U27*	69.3	112.2	176.9	184	135.1
U28	6.8	64.6	236.1	73.3	312.6	*U28*	54	39.2	62.2	194	409.2
U29	10.9	101.1	86.1	154	117.8	*U29*	64.6	44.5	88.5	110	143
U30	20.4	32.3	46.7	199	27.2	*U30*	12.9	8.9	71.7	96.8	317.8
U31	12.2	28	34.4	38.4	135.9	*U31*	20	41	71.7	74.2	95.3
U32	4.1	2.2	22.1	14	9.1	*U32*	5.9	24.9	40.7	110	79.5
U33	12.2	30.1	39.4	27.9	27.2	*U33*	24.6	41	55	58.1	123.2
U34	13.6	99	36.9	101	190.3	*U34*	27	44.5	102.8	145	198.6
U35	81.5	111.9	115.6	290	163.1	*U35*	103.3	92.6	229.5	152	329.7
U36	15	17.2	66.4	97.7	81.5	*U36*	17.6	42.7	50.2	51.6	47.7
U37	13.6	23.7	61.5	73.3	49.8	*U37*	15.3	42.7	59.8	51.6	643.6
U38	12.2	28	12.3	38.4	27.2	*U38*	24.6	44.5	107.6	210	115.2
U39	9.5	25.8	29.5	27.9	40.8	*U39*	9.4	35.6	55	113	43.7
W40	1940	2734	3300	4700	5700	*W40*	2790	3870	5036	6140	7314

Table D–6. Data of liquid volume (V) in the cells for CLD without gas.

	H = 0.5 m						H = 1 m				
L	2.6	3.9	5.2	6.5	7.8	L	2.6	3.9	5.2	6.5	7.8
C01	44.8	65	187.2	198.6	87.4	*C01*	87.4	162	164.6	142	234.4
I02	518	648	439	885.9	1005	*I02*	338	425	394.9	689.5	786.6
I03	89.5	125	151.7	63.6	222.5	*I03*	29.1	29	81	80.1	91.4
I04	425	710	955.5	1017	1192	*I04*	362	546	640.5	694.6	651.5
I05	89.5	118	113	147	162.9	*I05*	87.4	114	58.2	173	198.6
I06	115	517	406.7	603.9	591.9	*I06*	150	179	387.3	736	838.3
I07	74	146	119.4	182.7	79.5	*I07*	147	119	227.9	229.8	262.2
O08	134	187	529.4	361.5	91.4	*O08*	129	327	397.5	224.7	258.2
O09	415	411	529.4	361.5	552.2	*O09*	274	591	582.3	565.5	643.6
O10	122	209	309.9	405.2	810.5	*O10*	175	126	331.7	470	536.3
O11	72.3	228	267.9	361.5	882	*O11*	27.8	98	106.3	201.4	230.4
O12	31	54	38.7	43.7	43.7	*O12*	54.3	28	63.3	69.7	79.5
O13	74	67	61.3	115.2	67.5	*O13*	98	81	179.8	160.1	182.7
O14	331	506	413.2	933.6	719.1	*O14*	234	188	676	841.8	1251
O15	141	226	487.4	1017	1073	*O15*	105	193	182.3	258.2	294
O16	44.8	39	87.2	166.9	91.4	*O16*	42.4	117	124.1	154.9	178.8
O17	62	138	148.5	452.9	445	*O17*	23.8	312	73.4	382.2	437
O18	105	265	242.1	528.4	301.9	*O18*	134	126	334.2	149.8	170.8
O19	58.5	256	264.7	135.1	286	*O19*	63.6	91	146.8	235	270.2
U20	31	105	58.1	115.2	95.3	*U20*	95.3	145	225.3	302.1	345.6
U21	13.8	22	29.1	11.9	15.9	*U21*	14.6	14	40.5	38.7	43.7
U22	8.6	26	32.3	39.7	707.2	*U22*	14.6	52	35.4	67.1	75.5
U23	56.8	60	38.7	115.2	87.4	*U23*	23.8	50	101.3	206.6	234.4
U24	43	73	135.6	206.6	738.9	*U24*	50.3	76	76	90.4	103.3
U25	5.2	8.6	9.7	11.9	15.9	*U25*	27.8	10	50.6	23.2	27.8
U26	25.8	34	25.8	35.8	23.8	*U26*	30.5	121	83.5	100.7	115.2
U27	62	88	116.2	83.4	186.7	*U27*	66.2	102	232.9	229.8	262.2
U28	13.8	22	58.1	43.7	143	*U28*	18.5	55	35.4	28.4	31.8
U29	18.9	93	45.2	43.7	47.7	*U29*	49	79	91.1	276.3	313.9
U30	43	22	12.9	19.9	115.2	*U30*	5.3	81	17.7	250.5	286
U31	13.8	26	12.9	59.6	147	*U31*	21.2	26	38	18.1	19.9
U32	8.6	22	25.8	75.5	75.5	*U32*	26.5	10	27.8	31	35.8
U33	17.2	22	9.7	11.9	43.7	*U33*	14.6	14	35.4	67.1	75.5
U34	25.8	13	12.9	27.8	15.9	*U34*	23.8	22	43	28.4	31.8
U35	20.7	32	42	59.6	99.3	*U35*	79.5	131	124.1	87.8	218.5
U36	8.6	22	25.8	11.9	15.9	*U36*	4	38	38	18.1	19.9
U37	77.5	93	132.3	210.6	47.7	*U37*	14.6	45	48.1	90.4	139
U38	39.6	82	180.8	560.2	667.4	*U38*	27.8	29	45.6	108.5	151
U39	48.2	80	25.8	103.3	23.8	*U39*	15.9	43	17.7	38.7	119.2
W40	1960	3250	4020	5740	6720	*W40*	3190	4520	5890	7750	9370

Table D–6. Data of liquid volume (V) in the cells for CLD without gas. (...)

	H = 1.5 m						H = 2 m				
L	2.6	3.9	5.2	6.5	7.8	L	2.6	3.9	5.2	6.5	7.8
C01	61.7	65	123	54.2	107.9	*C01*	45.5	71	77.5	46.2	83.2
I02	260	341	494.3	624.9	447.1	*I02*	175	324	478.9	524.6	596.8
I03	27.7	26	73.8	98.1	30.8	*I03*	20.9	43	56.3	38.1	40.2
I04	197	274	147.6	697.2	678.3	*I04*	232	334	223	473	820.6
I05	56.7	55	154.9	100.7	239	*I05*	43	155	169	176.7	166.4
I06	121	110	432.8	149.8	651.4	*I06*	153	282	223	617	616.9
I07	60.5	60	123	105.9	269.8	*I07*	77.5	76	190.2	190.3	149.2
O08	171	284	169.7	281.5	212	*O08*	75	164	79.8	307.2	74.6
O09	320	405	578	655.9	782.4	*O09*	199	284	392	258.2	167.9
O10	132	155	91	309.9	543.4	*O10*	79.9	246	335.7	551.8	352.9
O11	41.6	86	120.5	284.1	212	*O11*	30.7	134	136.2	231.1	352.9
O12	39	24	73.8	80.1	80.9	*O12*	20.9	81	21.1	48.9	113.3
O13	80.6	72	110.7	131.7	185	*O13*	38.1	47	131.5	127.8	74.6
O14	142	193	275.4	247.9	258.2	*O14*	117	134	201.9	236.5	545.2
O15	86.9	277	319.7	180.8	678.3	*O15*	219	398	455.4	709.5	522.2
O16	21.4	102	110.7	183.3	161.9	*O16*	24.6	40	115	116.9	172.2
O17	51.6	274	309.9	157.5	408.5	*O17*	138	231	314.6	386	439
O18	15.1	110	123	276.3	354.6	*O18*	151	127	251.2	258.2	264
O19	56.7	79	137.7	338.3	235.1	*O19*	46.7	83	152.6	212	186.5
U20	92	277	356.6	284.1	173.4	*U20*	177	45	373.3	233.8	654.2
U21	26.5	12	17.2	31	15.4	*U21*	27.1	19	25.8	24.5	8.6
U22	16.4	21	36.9	351.2	165.7	*U22*	18.4	21	75.1	95.1	103.3
U23	18.9	38	32	64.6	73.2	*U23*	29.5	40	51.6	48.9	68.9
U24	6.3	67	214	224.7	138.8	*U24*	30.7	117	98.6	149.5	215.2
U25	36.5	10	19.7	10.3	15.4	*U25*	18.4	16	28.2	21.7	2.9
U26	35.3	74	41.8	85.2	131	*U26*	39.3	91	93.9	163.1	66
U27	110	148	297.6	160.1	100.2	*U27*	18.4	72	352.1	130.5	154.9
U28	25.2	50	63.9	87.8	123.3	*U28*	28.3	40	35.2	318	223.8
U29	10.1	21	76.2	149.8	127.2	*U29*	32	60	89.2	29.9	34.4
U30	74.3	152	115.6	103.3	27	*U30*	14.8	21	11.7	57.1	80.3
U31	16.4	22	19.7	25.8	23.1	*U31*	19.7	48	28.2	40.8	63.1
U32	23.9	10	27.1	10.3	15.4	*U32*	22.1	16	11.7	19	100.4
U33	8.8	12	27.1	41.3	92.5	*U33*	28.3	29	58.7	32.6	94.7
U34	15.1	19	36.9	41.3	115.6	*U34*	38.1	50	61	95.1	172.2
U35	111	164	297.6	121.4	173.4	*U35*	192	136	382.7	149.5	510.7
U36	8.8	12	36.9	100.7	123.3	*U36*	14.8	36	21.1	100.6	160.7
U37	22.7	40	61.5	90.4	215.8	*U37*	27.1	43	152.6	127.8	109
U38	18.9	28	36.9	46.5	61.7	*U38*	28.3	40	44.6	68	114.8
U39	29	21	49.2	56.8	88.6	*U39*	19.7	41	28.2	46.2	111.9
W40	3670	5330	6684	8300	10100	*W40*	3920	5940	7860	9540	11050

Table D–7. Data of liquid volume (V) in the cells for CLD with gas.

	H = 0.5 m						H = 1 m				
L	2.6	3.9	5.2	6.5	7.8	L	2.6	3.9	5.2	6.5	7.8
C01	43	92.5	149	238	190.7	*C01*	77.5	136	119	235	266.2
I02	522	654.2	484	775	965.4	*I02*	316	501	509	746	806.5
I03	94.7	118.4	83.9	199	214.5	*I03*	38.7	39.6	145	67.1	75.5
I04	405	675.7	972	858	1053	*I04*	316	556.1	615	573	591.9
I05	94.7	142	149	151	218.5	*I05*	72.3	118.8	129	204	218.5
I06	169	355.1	365	568	429.1	*I06*	182	253.1	333	436	735
I07	67.1	234.6	210	219	214.5	*I07*	107	125.7	207	217	286
O08	99.9	303.4	181	354	317.8	*O08*	186	239.3	199	413	635.7
O09	398	378.7	565	640	611.8	*O09*	297	377	374	648	508.5
O10	103	221.6	255	719	643.6	*O10*	155	365	400	630	258.2
O11	110	148.5	213	397	1001	*O11*	49.1	129.1	129	222	270.2
O12	29.3	58.1	42	47.7	47.7	*O12*	29.7	68.9	59.4	119	131.1
O13	99.9	92.5	103	143	143	*O13*	109	82.6	209	142	182.7
O14	296	611.2	536	818	866.1	*O14*	200	332.3	656	865	1148
O15	133	241	336	886	953.5	*O15*	85.2	170.4	325	294	389.3
O16	79.2	83.9	77.5	103	190.7	*O16*	58.1	77.5	132	134	131.1
O17	89.5	210.9	242	417	437	*O17*	42.6	177.3	134	305	492.6
O18	96.4	249.6	345	334	286	*O18*	156	108.5	323	186	286
O19	43	198	129	215	413.2	*O19*	69.7	137.7	158	238	158.9
U20	17.2	66.7	96.8	119	115.2	*U20*	106	80.9	114	139	226.5
U21	8.6	25.8	32.3	31.8	23.8	*U21*	19.4	8.6	12.9	18.1	27.8
U22	18.9	49.5	35.5	83.4	564.1	*U22*	16.8	36.2	38.7	62	35.8
U23	43	79.6	58.1	91.4	182.7	*U23*	29.7	34.4	77.5	59.4	166.9
U24	29.3	45.2	132	215	389.3	*U24*	34.9	115.3	129	199	194.7
U25	5.2	8.6	9.7	11.9	15.9	*U25*	24.5	10.3	7.7	38.7	27.8
U26	27.5	25.8	25.8	23.8	23.8	*U26*	40	65.4	43.9	114	154.9
U27	70.6	94.7	126	99.3	119.2	*U27*	85.2	72.3	114	124	214.5
U28	22.4	45.2	61.3	63.6	79.5	*U28*	16.8	25.8	41.3	43.9	55.6
U29	25.8	68.9	42	79.5	123.2	*U29*	33.6	154.9	116	274	234.4
U30	58.5	25.8	16.1	47.7	95.3	*U30*	6.5	34.4	173	59.4	441
U31	18.9	34.4	16.1	35.8	67.5	*U31*	18.1	41.3	59.4	72.3	27.8
U32	13.8	21.5	71	27.8	99.3	*U32*	12.9	5.2	18.1	31	23.8
U33	20.7	21.5	9.7	15.9	15.9	*U33*	16.8	15.5	25.8	25.8	43.7
U34	13.8	21.5	9.7	43.7	23.8	*U34*	19.4	32.7	95.5	56.8	47.7
U35	34.4	47.3	61.3	63.6	95.3	*U35*	58.1	120.5	142	207	234.4
U36	17.2	12.9	29.1	23.8	15.9	*U36*	18.1	17.2	25.8	28.4	31.8
U37	80.9	38.7	136	75.5	67.5	*U37*	15.5	48.2	85.2	82.6	87.4
U38	43	92.5	187	473	742.9	*U38*	20.7	41.3	67.1	72.3	83.4
U39	5.2	8.6	107	127	31.8	*U39*	9	12.1	18.1	59.4	250.3
W40	2130	3380	4220	5860	6910	*W40*	3260	4700	6020	7940	9460

Table D–7. Data of liquid volume (V) in the cells for CLD with gas. (...)

	H = 1.5 m						H = 2 m				
L	2.6	3.9	5.2	6.5	7.8	L	2.6	3.9	5.2	6.5	7.8
C01	23.9	75	128	62.6	119.2	*C01*	71.8	78.3	106	116	93.6
I02	212	313.2	433	558	528.4	*I02*	169	386.5	448	491	713.4
I03	41.6	35	36.9	54.8	115.2	*I03*	31.5	36.7	47	33.6	154.9
I04	202	238.2	221	329	738.9	*I04*	170	276.6	357	788	568.1
I05	52.9	75	140	263	246.3	*I05*	68	83.3	225	204	54.9
I06	34	269.9	507	652	258.2	*I06*	179	203.3	406	457	858.6
I07	55.4	81.6	148	133	274.1	*I07*	94.5	105	72.8	191	261.5
O08	111	229.9	406	337	278.1	*O08*	155	266.6	289	447	242.1
O09	241	374.9	485	563	1041	*O09*	179	296.6	282	251	261.5
O10	60.5	116.6	155	344	198.6	*O10*	59.2	208.3	369	416	593.9
O11	57.9	106.6	123	157	321.8	*O11*	37.8	76.6	91.6	253	432.5
O12	18.9	25	34.4	65.2	95.3	*O12*	25.2	43.3	35.2	87.8	96.8
O13	51.6	58.3	101	67.8	238.4	*O13*	18.9	55	58.7	82.6	96.8
O14	199	241.6	234	211	198.6	*O14*	78.1	158.3	115	305	129.1
O15	199	243.2	239	485	246.3	*O15*	213	374.9	437	292	119.4
O16	54.2	60	86.1	154	270.2	*O16*	50.4	95	132	173	206.6
O17	113	278.2	386	383	413.2	*O17*	183	271.6	329	364	374.4
O18	31.5	75	155	292	222.5	*O18*	92	120	117	258	142
O19	66.8	146.6	113	224	321.8	*O19*	113	80	193	230	216.3
U20	199	254.9	239	227	301.9	*U20*	192	133.3	195	506	493.9
U21	3.8	15	17.2	13	31.8	*U21*	30.2	25	35.2	18.1	16.1
U22	59.2	16.7	51.6	57.4	55.6	*U22*	18.9	25	49.3	43.9	48.4
U23	21.4	41.7	61.5	54.8	43.7	*U23*	29	20	58.7	43.9	42
U24	35.3	20	226	151	151	*U24*	18.9	76.6	91.6	98.1	316.3
U25	1.3	11.7	12.3	20.9	35.8	*U25*	25.2	25	51.6	7.7	9.7
U26	44.1	70	61.5	96.5	115.2	*U26*	18.9	56.6	82.2	80.1	109.7
U27	29	174.9	125	93.9	139	*U27*	11.3	66.6	362	106	271.1
U28	46.6	25	68.9	49.6	194.7	*U28*	26.5	40	42.3	67.1	387.3
U29	23.9	31.7	98.4	144	158.9	*U29*	27.7	71.6	122	72.3	9.7
U30	141	183.3	101	13	63.6	*U30*	11.3	33.3	25.8	12.9	277.6
U31	35.3	13.3	32	36.5	67.5	*U31*	17.6	63.3	30.5	36.2	106.5
U32	12.6	15	12.3	15.7	67.5	*U32*	21.4	18.3	35.2	31	38.7
U33	8.8	18.3	17.2	44.3	135.1	*U33*	15.1	41.7	37.6	62	54.9
U34	18.9	21.7	27.1	39.1	39.7	*U34*	15.1	43.3	32.9	103	193.7
U35	20.2	146.6	332	164	182.7	*U35*	178	108.3	289	318	98.5
U36	6.3	20	46.7	136	27.8	*U36*	18.9	20	103	111	22.6
U37	22.7	31.7	56.6	117	75.5	*U37*	25.2	56.6	216	87.8	226
U38	37.8	15	36.9	117	313.9	*U38*	25.2	61.6	61	220	458.4
U39	16.4	25	54.1	75.6	47.7	*U39*	13.9	71.6	68.1	64.6	61.3
W40	3700	5430	7000	8500	10500	*W40*	3980	6060	7990	9650	11210

Table D–8. Data of liquid volume (V) in the cells for LLD without gas.

	H = 0.5 m						H = 1 m				
L	2.6	3.9	5.2	6.5	7.8	L	2.6	3.9	5.2	6.5	7.8
C01	44.1	63.7	125	250.5	140.5	*C01*	40.5	48.5	53.8	35.4	147.6
I02	313	568.1	374	392.5	740.5	*I02*	172	256.7	263	574.7	575.5
I03	28	106.7	99	139.4	98.7	*I03*	45.6	51.6	73.2	35.4	132.8
I04	326	359.8	646	702.4	569.6	*I04*	311	422.6	626	787.4	767.3
I05	48.4	98.1	136	198.8	110.1	*I05*	40.5	100.2	131	45.6	114.4
I06	209	406.3	338	754	846.9	*I06*	165	244.1	439	524.1	686.2
I07	144	110.2	123	167.9	186.1	*I07*	56.7	51.6	79.6	98.7	140.2
O08	174	146.3	121	167.9	87.3	*O08*	26.3	195.6	387	91.1	527.5
O09	264	397.7	245	596.5	474.7	*O09*	112	231.6	220	562	619.8
O10	230	185.9	611	797.9	474.7	*O10*	282	414.7	383	430.4	269.3
O11	164	98.1	544	266	512.7	*O11*	251	79.8	235	270.9	461.1
O12	34.4	75.7	151	56.8	57	*O12*	9.1	48.5	127	68.4	88.5
O13	48.4	56.8	133	126.5	292.4	*O13*	43.5	89.2	88.2	81	269.3
O14	252	177.3	280	470	600	*O14*	147	244.1	476	384.8	870.6
O15	179	272	411	539.7	1044.3	*O15*	190	95.5	185	308.9	346.8
O16	130	199.7	183	237.6	125.3	*O16*	84.1	106.4	127	88.6	166
O17	60.3	184.2	159	532	463.3	*O17*	73.9	117.4	211	298.7	261.9
O18	180	146.3	424	209.2	357	*O18*	187	162.8	170	308.9	357.8
O19	132	117.1	123	126.5	265.8	*O19*	45.6	87.6	217	53.2	339.4
U20	28	98.1	269	211.8	413.9	*U20*	124	137.7	146	98.7	129.1
U21	15.1	29.3	17.2	7.7	19	*U21*	6.1	7.8	10.8	88.6	70.1
U22	19.4	20.7	40.9	46.5	170.9	*U22*	28.4	21.9	36.6	106.3	177.1
U23	21.5	48.2	83.9	98.1	76	*U23*	45.6	42.3	60.3	111.4	73.8
U24	112	179	96.8	297	113.9	*U24*	44.6	118.9	211	260.8	118
U25	5.4	13.8	17.2	7.7	19	*U25*	12.2	15.7	10.8	2.5	11.1
U26	16.1	58.5	64.6	178.2	178.5	*U26*	30.4	37.6	198	149.4	129.1
U27	32.3	53.4	64.6	152.4	212.7	*U27*	30.4	89.2	88.2	167.1	202.9
U28	3.2	29.3	45.2	229.8	178.5	*U28*	20.3	61	250	313.9	140.2
U29	29.1	46.5	56	139.4	170.9	*U29*	25.3	175.3	127	124.1	114.4
U30	20.4	46.5	58.1	62	64.6	*U30*	119	4.7	43	215.2	22.1
U31	18.3	117.1	32.3	46.5	30.4	*U31*	54.7	73.6	19.4	438	125.4
U32	16.1	39.6	10.8	7.7	45.6	*U32*	5.1	11	15.1	7.6	11.1
U33	23.7	29.3	23.7	51.6	49.4	*U33*	25.3	32.9	38.7	40.5	92.2
U34	29.1	39.6	49.5	12.9	106.3	*U34*	23.3	28.2	28	174.7	107
U35	94.7	154.9	146	204	189.9	*U35*	67.8	192.5	60.3	136.7	298.8
U36	19.4	29.3	25.8	23.2	151.9	*U36*	8.1	11	10.8	63.3	92.2
U37	12.9	15.5	43	41.3	38	*U37*	34.4	18.8	177	364.6	210.3
U38	19.4	32.7	45.2	41.3	144.3	*U38*	35.4	25	243	43	48
U39	1.1	5.2	12.9	7.7	11.4	*U39*	12.2	17.2	49.5	68.4	110.7
W40	2450	3470	4470	6140	7000	*W40*	3500	4750	7020	8730	9870

Table D–8. Data of liquid volume (V) in the cells for LLD without gas. (...)

	H = 1.5 m						H = 2 m				
L	2.6	3.9	5.2	6.5	7.8	L	2.6	3.9	5.2	6.5	7.8
C01	39.3	71.7	112	113.4	92.2	*C01*	38.2	60.3	74.1	63.9	55.3
I02	173	226.7	366	533.4	557	*I02*	174	237.6	307	472.2	498
I03	26.9	64.6	73.2	53.1	121.7	*I03*	31	48.2	95.2	86.1	125.4
I04	189	266.8	422	494.7	730.4	*I04*	157	268.6	377	582.9	815.3
I05	62	124.8	68.9	154.5	140.2	*I05*	13.4	24.1	80.4	39.3	66.4
I06	95	121.9	142	359.6	527.5	*I06*	96.1	203.1	186	462.4	494.3
I07	152	84.6	64.6	149.6	169.7	*I07*	136	93	133	98.4	121.7
O08	134	165	136	178.6	173.4	*O08*	115	175.6	322	127.9	501.7
O09	182	225.2	101	296.8	726.7	*O09*	230	289.2	286	356.6	147.6
O10	52.7	176.5	267	494.7	313.6	*O10*	82.6	151.5	112	354.1	560.7
O11	41.3	64.6	116	197.9	306.2	*O11*	55.8	55.1	114	241	191.8
O12	44.4	33	49.5	50.7	103.3	*O12*	31	46.5	50.8	44.3	73.8
O13	72.3	180.8	220	465.8	228.7	*O13*	41.3	43	74.1	73.8	140.2
O14	80.6	304.1	379	562.3	678.8	*O14*	113	177.3	254	437.8	678.8
O15	98.1	104.7	258	318.6	265.6	*O15*	157	185.9	201	413.2	280.4
O16	28.9	51.6	159	161.7	173.4	*O16*	35.1	94.7	59.3	81.2	99.6
O17	124	200.8	207	289.6	129.1	*O17*	43.4	167	212	472.2	490.6
O18	117	248.2	314	246.2	228.7	*O18*	44.4	213.5	286	329.6	173.4
O19	52.7	51.6	81.8	125.5	210.3	*O19*	52.7	144.6	203	137.7	121.7
U20	173	255.4	523	325.8	586.6	*U20*	125	249.6	343	528.8	579.2
U21	12.4	7.2	19.4	19.3	51.6	*U21*	3.1	20.7	6.3	68.9	11.1
U22	23.8	21.5	58.1	29	121.7	*U22*	9.3	12.1	14.8	59	92.2
U23	37.2	35.9	71	77.2	103.3	*U23*	16.5	58.5	31.7	59	51.6
U24	95	104.7	241	255.8	236.1	*U24*	33.1	146.3	84.7	91	475.9
U25	5.2	7.2	23.7	14.5	33.2	*U25*	15.5	15.5	33.9	24.6	55.3
U26	23.8	31.6	114	183.4	114.4	*U26*	99.2	167	50.8	61.5	99.6
U27	169	235.3	288	234.1	169.7	*U27*	136	74	307	88.5	95.9
U28	30	50.2	301	176.2	575.5	*U28*	26.9	22.4	182	386.1	560.7
U29	43.4	68.9	129	50.7	162.3	*U29*	44.4	60.3	188	332	121.7
U30	5.2	7.2	32.3	38.6	309.9	*U30*	11.4	17.2	6.3	86.1	66.4
U31	6.2	30.1	83.9	21.7	92.2	*U31*	95	101.6	265	39.3	616.1
U32	5.2	10	32.3	16.9	44.3	*U32*	11.4	15.5	14.8	22.1	36.9
U33	19.6	23	43	16.9	73.8	*U33*	32	24.1	27.5	39.3	92.2
U34	30	17.2	68.9	74.8	103.3	*U34*	36.2	55.1	40.2	307.4	118
U35	150	218.1	129	149.6	121.7	*U35*	150	230.7	246	307.4	509.1
U36	5.2	11.5	43	62.7	114.4	*U36*	15.5	27.5	10.6	36.9	306.2
U37	13.4	63.1	64.6	82.1	73.8	*U37*	39.3	41.3	82.5	282.8	140.2
U38	32	30.1	92.5	132.7	166	*U38*	22.7	34.4	21.2	49.2	125.4
U39	25.8	15.8	32.3	21.7	25.8	*U39*	9.3	8.6	6.3	49.2	77.5
W40	3720	5420	7920	8920	11180	*W40*	3980	6020	7430	9600	12290

Table D–9. Data of liquid volume (V) in the cells for LLD with gas.

	H = 0.5 m						H = 1 m				
L	2.6	3.9	5.2	6.5	7.8	L	2.6	3.9	5.2	6.5	7.8
C01	56	88.8	129.1	162.7	179.6	*C01*	55.7	68.9	75.3	136.3	122.5
I02	308.8	484.2	469.5	516.5	707.3	*I02*	165.1	233.2	198	382.6	509.8
I03	39.8	77.5	119.7	118.8	142.2	*I03*	52.7	39.1	122.7	100.4	76.1
I04	299.1	361.5	683.1	743.7	479	*I04*	291.7	400.7	626.2	557.1	913.7
I05	59.2	104.9	100.9	139.4	127.2	*I05*	52.7	112.7	139.9	131.5	205.3
I06	152.8	392.2	251.2	617.2	804.6	*I06*	132.7	156.5	329.2	693.4	397.3
I07	212	164.6	152.6	253.1	179.6	*I07*	49.6	76.7	53.8	124.3	324.4
O08	181.8	248.5	145.5	333.1	134.7	*O08*	26.3	189.4	378.7	547.5	675.4
O09	272.2	234	241.8	467.4	714.8	*O09*	109.4	234.8	120.5	633.6	744.9
O10	184	127.5	176.1	333.1	363	*O10*	221.8	399.1	340	289.3	397.3
O11	185.1	138.8	556.4	325.4	542.7	*O11*	269.4	106.4	260.4	215.2	155.6
O12	40.9	46.8	77.5	77.5	112.3	*O12*	7.1	45.4	107.6	83.7	149
O13	56	98.5	244.1	216.9	254.5	*O13*	43.5	154.9	75.3	255.8	271.5
O14	235.6	224.3	316.9	668.8	654.9	*O14*	136.7	314.6	460.5	411.3	374.1
O15	175.4	472.9	493	648.2	920.7	*O15*	169.1	140.9	107.6	428	122.5
O16	123.7	124.3	178.4	245.3	262	*O16*	84.1	129.9	200.1	193.7	182.1
O17	99	177.5	157.3	495.8	336.8	*O17*	100.3	175.3	90.4	205.6	314.5
O18	166.8	159.8	199.5	369.3	168.4	*O18*	164.1	140.9	148.5	160.2	569.4
O19	68.9	151.7	216	188.5	168.4	*O19*	32.4	68.9	286.2	174.5	473.4
U20	35.5	43.6	140.9	152.4	280.7	*U20*	93.2	112.7	238.9	76.5	350.9
U21	31.2	42	25.8	38.7	33.7	*U21*	6.1	7.8	40.9	69.3	43
U22	25.8	40.3	37.6	64.6	67.4	*U22*	21.3	34.4	40.9	186.5	53
U23	32.3	67.8	65.7	95.5	101	*U23*	72.9	81.4	71	69.3	168.8
U24	45.2	125.9	270	178.2	74.9	*U24*	68.9	65.7	25.8	126.7	172.2
U25	16.1	17.8	7	7.7	33.7	*U25*	15.2	18.8	15.1	21.5	115.9
U26	26.9	69.4	133.8	82.6	168.4	*U26*	42.5	45.4	241	162.6	115.9
U27	48.4	80.7	105.6	108.5	217.1	*U27*	42.5	70.4	133.4	143.5	314.5
U28	12.9	30.7	65.7	64.6	190.9	*U28*	15.2	68.9	260.4	90.9	69.5
U29	31.2	53.3	119.7	105.9	202.1	*U29*	35.4	134.6	154.9	126.7	92.7
U30	24.7	27.4	147.9	74.9	108.5	*U30*	125.6	4.7	200.1	344.3	23.2
U31	26.9	46.8	14.1	41.3	138.5	*U31*	66.8	25	32.3	102.8	46.3
U32	20.4	17.8	21.1	7.7	63.6	*U32*	9.1	14.1	12.9	12	46.3
U33	26.9	19.4	30.5	38.7	93.6	*U33*	31.4	37.6	51.6	55	69.5
U34	26.9	45.2	58.7	28.4	93.6	*U34*	15.2	28.2	34.4	83.7	79.5
U35	106.5	164.6	169	276.3	205.8	*U35*	73.9	153.4	64.6	377.8	304.6
U36	14	33.9	25.8	54.2	153.4	*U36*	15.2	14.1	15.1	57.4	69.5
U37	16.1	19.4	21.1	72.3	134.7	*U37*	62.8	31.3	208.7	74.1	69.5
U38	26.9	33.9	25.8	180.8	59.9	*U38*	35.4	28.2	247.5	59.8	109.3
U39	8.6	4.8	18.8	7.7	18.7	*U39*	12.2	36	75.3	64.6	105.9
W40	2520	3600	4560	6230	7100	*W40*	3590	4960	7230	8800	9950

Table D–9. Data of liquid volume (V) in the cells for LLD with gas. (...)

	H = 1.5 m						H = 2 m				
L	2.6	3.9	5.2	6.5	7.8	L	2.6	3.9	5.2	6.5	7.8
C01	46.5	93.3	96.8	145.5	89.7	*C01*	47.4	63.8	96.8	45.6	106.5
I02	161.1	279.8	327.1	462.5	502.9	*I02*	168.6	220.3	302.6	536.7	503.6
I03	23.8	28.7	99	44.6	187.6	*I03*	22.1	30.4	100.9	111.4	135.6
I04	200.4	297	320.6	436.6	557.2	*I04*	159.2	255.2	357.1	589.9	742.4
I05	76.4	129.1	90.4	105.6	138.6	*I05*	15.8	21.3	72.6	45.6	67.8
I06	101.2	97.6	114.1	368.6	638.8	*I06*	112.8	214.2	117	546.8	629.4
I07	109.5	150.6	99	164.3	225.6	*I07*	117	92.7	90.8	129.1	129.1
O08	142.5	187.9	329.2	197.2	165.8	*O08*	157	229.4	314.7	270.9	477.7
O09	165.3	179.3	284.1	187.8	345.2	*O09*	214	287.1	288.5	430.4	161.4
O10	69.2	137.7	213	528.2	530.1	*O10*	52.7	147.3	50.4	313.9	610.1
O11	40.3	74.6	131.3	201.9	375.1	*O11*	47.4	74.4	125.1	415.2	468
O12	41.3	23	56	84.5	89.7	*O12*	42.2	53.2	52.5	108.9	83.9
O13	87.8	150.6	193.7	356.8	231.1	*O13*	47.4	51.6	98.9	83.5	145.3
O14	144.6	274	329.2	410.8	769.3	*O14*	44.3	244.6	262.3	511.4	684.3
O15	83.7	199.4	161.4	293.4	448.5	*O15*	152.8	196	292.5	476	503.6
O16	56.8	81.8	120.5	140.9	195.7	*O16*	39	65.3	78.7	116.5	132.3
O17	44.4	177.9	99	199.5	261	*O17*	131.8	138.2	302.6	432.9	403.5
O18	88.8	117.6	269	293.4	108.7	*O18*	51.6	164.1	282.4	225.3	216.3
O19	110.5	63.1	118.4	154.9	163.1	*O19*	60.1	56.2	119	151.9	129.1
U20	183.9	238.1	475.6	385	456.7	*U20*	139.1	215.7	288.5	445.6	167.9
U21	19.6	17.2	75.3	21.1	27.2	*U21*	3.2	19.7	18.2	30.4	29.1
U22	21.7	28.7	56	35.2	48.9	*U22*	12.6	27.3	24.2	78.5	113
U23	35.1	44.5	75.3	58.7	65.2	*U23*	13.7	66.8	40.3	70.9	48.4
U24	31	53.1	350.8	312.2	149.5	*U24*	35.8	115.4	50.4	124.1	222.7
U25	14.5	4.3	32.3	16.4	32.6	*U25*	21.1	16.7	52.5	17.7	80.7
U26	25.8	30.1	38.7	126.8	176.7	*U26*	107.5	177.7	70.6	91.1	119.4
U27	172.5	210.9	335.7	293.4	111.4	*U27*	95.9	83.5	280.4	139.2	106.5
U28	23.8	43	327.1	82.2	168.5	*U28*	34.8	24.3	219.9	126.6	619.8
U29	50.6	84.6	25.8	16.4	152.2	*U29*	52.7	60.8	177.5	248.1	113
U30	12.4	10	28	47	622.5	*U30*	12.6	22.8	10.1	113.9	74.2
U31	10.3	14.3	71	28.2	103.3	*U31*	108.6	101.8	268.3	96.2	548.7
U32	3.1	12.9	23.7	21.1	32.6	*U32*	10.5	16.7	16.1	30.4	80.7
U33	24.8	25.8	38.7	21.1	46.2	*U33*	24.2	28.9	46.4	40.5	71
U34	31	30.1	58.1	82.2	100.6	*U34*	45.3	53.2	66.6	76	113
U35	161.1	249.6	297	340.4	122.3	*U35*	142.3	237	240.1	291.1	539.1
U36	10.3	34.4	10.8	51.6	114.2	*U36*	22.1	42.5	10.1	45.6	255
U37	12.4	146.3	71	75.1	538.2	*U37*	36.9	53.2	84.7	101.3	119.4
U38	20.7	28.7	47.3	136.2	100.6	*U38*	26.4	39.5	24.2	65.8	135.6
U39	13.4	21.5	34.4	32.9	40.8	*U39*	11.6	19.7	14.1	63.3	83.9
W40	3800	5560	8030	9050	11400	*W40*	4050	6080	7540	10236	12488

Appendix E. Tabulated Data for MTM

Table E–1. Data of the dimensionless group for SPLD.

x/D	L	Re	$Sh/Sc^{0.33}$								
	$kgm^{-2}s^{-1}$		C01	I02	I03	I04	I05	O06	O07	O08	O09
0.5	2.6	97	60.12	22.86	16.25	24.56	18.96	0	0	0	0
0.5	3.9	146	68.45	25.61	29.78	22.86	32.87	0.1	0.1	0.1	0.1
0.5	5.2	194	80.15	43.05	46.21	45.98	38.95	0.52	0.52	0.52	0.52
0.5	6.5	243	82.06	43.15	49.65	46.59	40.69	0.52	0.52	0.52	0.52
0.5	7.8	291	83.48	46.4	47.26	45.68	46.43	0.93	0.93	0.93	0.93
0.5	10.4	388	85.48	48.89	52.36	45.65	46.69	1.24	1.24	1.24	1.24
0.5	13	485	86.59	68.15	39.65	46.02	45.55	1.55	1.76	1.54	1.35
1	2.6	97	53.97	27.01	34.59	22.15	40.05	0	0	0	0
1	3.9	146	61.92	46.15	53.21	50.08	43.68	0.1	0.1	0.1	0.1
1	5.2	194	78.84	61.38	63.76	50.56	65.45	0.83	0.83	0.83	0.83
1	6.5	243	79.26	61.8	63.65	54.68	64.58	0.93	0.93	0.93	0.93
1	7.8	291	80.29	62.15	65.84	62.65	62.05	1.14	1.14	1.14	1.14
1	10.4	388	81.01	63.19	66.98	63.58	67.56	2.37	2.84	2.16	2.1
1	13	485	81.63	68.12	59.65	72.69	69.55	2.68	2.26	3.26	2.56
2	2.6	97	56.76	37.12	43.65	30.46	41.48	0.83	0.83	0.83	0.83
2	3.9	146	66.46	60.19	58.15	41.06	55.64	1.55	1.55	1.55	1.55
2	5.2	194	77.3	69.05	66.15	58.86	68.02	5.21	8.24	9.15	4.68
2	6.5	243	78.22	69.26	70.65	63.15	67.35	8.56	6.89	8.56	5.76
2	7.8	291	78.95	69.97	74.56	66.98	68.45	8.46	8.46	8.46	8.46
2	10.4	388	79.98	71.26	75.64	67.54	69.89	10.02	9.49	9.59	9.26
2	13	485	81.11	70.69	72.16	76.12	75.02	10.5	10.9	9.54	11.32
2.5	2.6	97	53.97	43.46	29.58	46.32	45.74	2.27	2.27	2.27	2.27
2.5	3.9	146	65.53	38.79	58.78	43.16	51.28	2.48	5.48	2.36	4.15
2.5	5.2	194	73.79	62.85	64.19	55.49	65.19	10.45	5.76	14.69	8.69
2.5	6.5	243	75.54	63.02	65.15	66.45	58.45	10.9	13.68	9.75	12.38
2.5	7.8	291	76.88	67.02	57.59	67.48	65.48	12.7	13.5	11.6	13.5
2.5	10.4	388	79.15	68.23	69.12	54.68	70.86	15.89	14.65	13.89	15.62
2.5	13	485	80.29	70.15	72.36	57.04	75.36	15.86	15.63	16.02	16.45
3	2.6	97	50.46	47.96	31.06	49.68	44.56	4.58	4.13	6.95	4.98
3	3.9	146	60.47	57.64	39.46	51.24	53.12	7.68	9.89	5.69	6.48
3	5.2	194	67.49	55.86	55.02	53.26	57.89	15.69	11.45	13.56	9.69
3	6.5	243	68.94	57.87	53.65	54.67	60.71	16.89	18.54	13.56	15.49
3	7.8	291	70.07	58.62	63.65	47.63	64.58	18.2	17.45	19.35	18.32
3	10.4	388	71.93	59.62	65.65	56.56	64.59	19	18.26	21.36	17.45
3	13	485	74.61	66.54	53.43	65.65	68.59	21.54	25.48	20.85	16.23

Table E–1. Data of the dimensionless group for SPLD. (...)

x/D	L	Re	$Sh/Sc^{0.33}$								
	$kgm^{-2}s^{-1}$		CC01	IC02	IC03	IC04	IC05	OC06	OC07	OC08	OC09
3.5	2.6	97	49.23	54.02	31.24	51.26	41.02	5.89	9.56	5.26	8.15
3.5	3.9	146	56.35	58.69	48.69	43.65	41.36	8.45	6.15	13.46	9.08
3.5	5.2	194	65.53	47.26	53.65	50.36	54.68	14.89	13.95	12.68	15.69
3.5	6.5	243	67.08	52.54	53.65	49.96	58.48	17.05	17.87	15.09	13.95
3.5	7.8	291	68.83	56.84	54.68	57.86	55.71	17.15	18.86	16.54	15.89
3.5	10.4	388	71.1	57.79	62.36	54.65	56.35	16.86	17.65	19.43	20.15
3.5	13	485	72.55	67.86	50.36	50.68	69.54	21.54	15.46	24.75	20.21
4	2.6	97	48.19	49.68	35.62	52.81	45.61	9.02	15.05	7.06	10.01
4	3.9	146	54.7	57.26	45.69	47.26	51.66	15.16	14.19	13.76	14.59
4	5.2	194	62.44	46.98	54.06	55.26	50.19	21.86	18.69	23.54	20.94
4	6.5	243	63.67	53.16	52.15	50.41	57.26	23.68	19.05	24.65	22.49
4	7.8	291	64.81	50.43	53.65	49.96	60.89	25.34	26.02	22.68	22.26
4	10.4	388	66.25	59.56	60.05	44.65	58.65	25.5	26.87	28.12	25.46
4	13	485	67.7	62.12	51.26	62.56	53.16	30.18	24.66	34.37	22.89
5	2.6	97	48.19	41.26	32.36	49.21	36.05	12.26	20.19	13.25	14.26
5	3.9	146	53.66	41.08	29.58	42.31	36.05	20.49	30.59	23.68	26.05
5	5.2	194	56.86	41.29	38.94	35.23	38.07	27.51	22.96	24.85	27.06
5	6.5	243	58.2	38.21	43.25	37.68	40.26	24.12	31.86	23.15	27.31
5	7.8	291	59.34	40.14	42.56	39.45	38.45	28.06	26.56	27.05	28.19
5	10.4	388	59.96	39.65	60.89	30.25	34.65	26.86	29.02	30.15	26.84
5	13	485	61.92	48.26	38.56	39.46	47.96	30.42	28.47	31.16	27.54
5.5	2.6	97	49.33	29.16	40.38	33.87	30.69	17.69	25.46	16.25	22.59
5.5	3.9	146	51.91	33.09	33.13	30.46	40.05	24.28	28.19	22.39	20.74
5.5	5.2	194	54.18	34.26	35.29	34.43	36.45	33.86	35.26	28.87	31.25
5.5	6.5	243	55.31	37.11	35.41	34.65	37.65	31.56	34.25	28.56	29.21
5.5	7.8	291	56.55	36.78	37.26	38.56	35.65	33.1	31.89	33.35	34.02
5.5	10.4	388	58.51	37.46	26.78	36.95	48.65	33.68	34.25	31.56	34.56
5.5	13	485	59.03	48.56	36.54	34.68	34.59	47.96	24.32	35.65	26.42

Table E–2. Data of the dimensionless group for CLD.

x/D	L	Re	$Sh/Sc^{0.33}$								
	$kgm^{-2}s^{-1}$		CC01	IC02	IC03	IC04	IC05	OC06	OC07	OC08	OC09
0.5	2.6	97	37.56	53.12	58.23	31.32	53.78	39.67	55.16	25.38	30.15
0.5	3.9	146	41.28	57.75	66.15	35.18	62.15	48.67	57.21	32.48	30.15
0.5	5.2	194	47.88	76.98	45.26	77.56	47.45	26.45	56.02	60.03	30.15
0.5	6.5	243	50.15	70.26	65.46	71.26	44.05	34.59	52.64	60.25	31.26
0.5	7.8	291	51.6	70.16	68.87	70.59	44.56	36.68	56.56	32.46	62.03
0.5	10.4	388	53.46	71.29	71.39	71.26	44.45	64.07	34.02	65.08	32.76
0.5	13	485	54.9	72.31	72.34	74.69	46.89	67.42	36.97	64.23	35.26
1	2.6	97	38.7	54.56	63.49	29.48	58.46	32.45	50.12	28.16	43.56
1	3.9	146	43.55	61.02	64.38	45.15	59.86	52.64	56.15	29.45	27.02
1	5.2	194	47.68	78.16	75.16	53.36	50.16	32.26	46.45	65.45	35.45
1	6.5	243	48.3	65.84	70.34	64.68	62.56	36.89	55.89	59.13	32.56
1	7.8	291	50.15	66.77	70.26	64.89	65.15	40.05	55.56	34.02	59.79
1	10.4	388	53.87	67.56	69.45	70.56	68.12	63.25	34.35	64.02	35.26
1	13	485	56.76	73.56	73.45	70.31	66.64	63.15	38.54	64.65	39.65
2	2.6	97	40.66	52.01	62.15	32.02	50.16	32.15	60.15	33.45	32.89
2	3.9	146	44.69	72.03	68.48	39.56	45.67	35.26	56.9	31.64	50.48
2	5.2	194	47.99	76.56	44.15	78.56	45.26	35.26	56.48	59.15	30.15
2	6.5	243	48.71	70.54	66.48	65.62	45.4	29.56	62.2	63.15	30.7
2	7.8	291	51.29	68.56	70.02	47.02	68.69	35.69	58.96	35.95	59.26
2	10.4	388	53.25	71.05	72.65	69.89	48.65	68.53	32.65	66.59	32.65
2	13	485	56.24	68.15	69.25	64.58	66.65	67.89	66.89	36.54	37.86
2.5	2.6	97	37.87	48.66	62.15	31.26	30.48	45.68	63.7	26.01	32.15
2.5	3.9	146	42.62	61.56	64.56	35.15	40.15	30.45	61.78	55.15	31.05
2.5	5.2	194	48.61	57.36	65.02	67.04	33.48	31	65.56	56.26	32.02
2.5	6.5	243	49.43	66.35	65.45	60.54	34.58	31.05	62.54	30.2	64.38
2.5	7.8	291	51.5	64.02	66.89	65.48	34.01	65.89	66.95	34.26	34.26
2.5	10.4	388	53.46	63.65	69.68	69.54	33.64	68.52	35.53	65.65	37.59
2.5	13	485	55.31	68.36	68.56	68.54	35.64	67.98	39.22	38.35	69.86
3	2.6	97	36.64	41.49	61.28	29.45	34.12	41.28	68.26	28.01	28.56
3	3.9	146	42.52	30.15	56.38	62.15	30.02	30.15	56.89	58.45	31.56
3	5.2	194	48.09	63.29	64.52	34.09	35.1	59.99	62.15	33.16	30.45
3	6.5	243	49.74	35.15	67.89	63.15	37.65	31.56	63.58	31.25	61.02
3	7.8	291	50.77	41.02	67.23	67.18	33.86	65.39	66.59	35.68	32.54
3	10.4	388	52.94	69.78	70.39	38.98	39.65	67.56	35.65	64.59	38.25
3	13	485	55.21	65.26	66.56	63.76	35.62	68.25	37.88	37.99	68.25

Table E–2. Data of the dimensionless group for CLD. (...)

x/D	L	Re	$Sh/Sc^{0.33}$								
	$kgm^{-2}s^{-1}$		CC01	IC02	IC03	IC04	IC05	OC06	OC07	OC08	OC09
3.5	2.6	97	35.71	45.62	59.15	26.34	28.56	45.64	58.46	30.15	33.16
3.5	3.9	146	41.9	28.62	56.59	56.45	29.23	33.95	56.43	56.02	29.45
3.5	5.2	194	47.57	31.26	54.99	30.45	63.18	32.01	62.15	31.15	59.56
3.5	6.5	243	48.92	30.12	68.15	27.18	59.45	63.58	31.99	65.48	31.26
3.5	7.8	291	51.5	31.25	63.05	62.12	33.04	36.12	64.23	63.5	33.05
3.5	10.4	388	52.53	62.39	65.48	31.26	32.35	66.69	35.76	64.25	34.63
3.5	13	485	54.18	35.02	60.32	66.45	34.63	68.25	36.89	37.12	67.78
4	2.6	97	36.53	33.45	29.45	22.26	57.12	48.91	57.12	30.02	29.45
4	3.9	146	42.62	26.03	63.15	34.02	25.48	43.26	53.45	55.26	25.6
4	5.2	194	48.4	30.26	62.56	31.38	35.56	61.89	65.72	28.26	27.05
4	6.5	243	50.05	29.18	64.89	32.18	38.48	59.83	64.89	32.56	30.15
4	7.8	291	51.5	35.23	66.12	39.14	32.16	36.56	62.15	33.26	60.25
4	10.4	388	53.77	34.56	68.57	36.98	38.65	68.57	31.05	66.45	31.56
4	13	485	55.11	31.08	61.58	30.09	63.01	63.52	35.41	36.32	66.89
5	2.6	97	35.91	39.45	23.02	22.13	52.78	45.26	52.72	28.15	30.18
5	3.9	146	42.83	32.15	55.02	35.26	26.15	26.15	62.15	26.78	50.62
5	5.2	194	49.12	29.56	31.56	62.95	31.59	57.04	28.66	59.48	29.01
5	6.5	243	50.46	33.12	61.45	32.14	32.15	59.78	62.25	26.18	29.23
5	7.8	291	53.25	37.23	60.56	32.63	30.15	35.89	59.56	30.45	57.06
5	10.4	388	54.39	32.26	67.98	33.65	33.26	60.12	33.65	61.36	32.15
5	13	485	56.24	33.65	42.35	33.56	64.56	36.25	59.68	34.39	60.35
5.5	2.6	97	41.28	36.45	22.02	51.03	23.15	45.6	51.49	25.68	27.86
5.5	3.9	146	45.41	26.15	56.02	26.02	32.15	45.89	53.15	26.45	30.15
5.5	5.2	194	48.81	30.15	28.65	61.45	30.48	35.59	33.65	61.58	33.45
5.5	6.5	243	50.26	32.15	59.15	26.26	34.29	41.49	61.02	33.26	30.15
5.5	7.8	291	51.5	32.56	58.12	30.86	33.26	36.12	40.26	35.02	56.63
5.5	10.4	388	53.56	32.48	63.45	32.15	31.25	56.89	32.16	54.68	30.45
5.5	13	485	55.01	35.23	35.42	35.25	58.69	36.58	60.25	38.59	41.26

Table E–3. Data of the dimensionless group for LLD.

x/D	L	Re	$Sh/Sc^{0.33}$								
	$kgm^{-2}s^{-1}$		CC01	IC02	IC03	IC04	IC05	OC06	OC07	OC08	OC09
0.5	2.6	97	39.63	48.02	54.48	69.45	28.69	38.15	29.13	39.48	53.45
0.5	3.9	146	44.58	57.12	37.65	65.34	56.88	38.23	38.56	60.15	34.45
0.5	5.2	194	49.33	62.36	61.34	38.23	63.56	39.56	37.65	63.56	39.63
0.5	6.5	243	51.08	63.25	64.32	39.65	62.66	41.25	38.65	63.78	39.65
0.5	7.8	291	52.32	65.25	66.56	64.31	38.35	43.65	39.87	65.86	41.25
0.5	10.4	388	54.28	66.38	65.32	43.98	66.69	63.54	63.68	35.68	38.12
0.5	13	485	55.01	68.15	69.45	42.01	68.45	63.54	39.56	65.36	38.76
1	2.6	97	44.99	52.21	36.01	49.26	68.92	43.21	63.56	28.48	34.78
1	3.9	146	48.09	61.32	59.65	62.54	35.12	40.99	58.14	32.54	39.85
1	5.2	194	51.7	64.56	64.02	39.85	63.56	55.62	34.65	35.62	61.88
1	6.5	243	52.53	62.35	64.21	42.36	64.35	39.89	40.02	40.72	65.89
1	7.8	291	57.28	65.68	66.31	66.54	44.12	42.35	66.35	41.75	41.05
1	10.4	388	57.28	66.84	66.84	68.25	45.36	63.99	38.45	64.65	35.98
1	13	485	58.62	70.86	70.68	41.78	70.15	66.45	40.36	66.36	46.32
2	2.6	97	45.41	52.12	74.25	34.87	42.26	46.12	65.15	25.56	41.45
2	3.9	146	49.33	57.84	35.52	57.66	63.56	53.62	66.25	29.74	38.66
2	5.2	194	52.43	62.12	39.33	57.56	63.02	62.13	38.87	64.25	36.21
2	6.5	243	52.94	62.35	60.66	40.26	62.56	65.56	37.56	38.45	65.64
2	7.8	291	55.83	64.32	64.36	40.35	65.34	67.56	39.68	68.64	40.03
2	10.4	388	56.55	65.36	64.56	38.89	68.54	67.89	68.89	43.69	43.65
2	13	485	55.11	68.56	67.54	40.15	66.56	64.59	66.56	35.45	66.56
2.5	2.6	97	47.99	49.44	68.26	48.01	31.52	45.23	31.21	66.47	40.29
2.5	3.9	146	49.85	53.66	61.35	29.36	59.87	39.46	59.68	59.42	33.73
2.5	5.2	194	52.63	60.36	35.63	58.63	60.45	61.36	38.26	38.22	65.24
2.5	6.5	243	53.25	53.64	67.21	66.57	38.65	65.32	39.12	64.87	40.41
2.5	7.8	291	55.83	68.56	43.69	43.65	69.02	66.86	42.36	42.5	66.98
2.5	10.4	388	56.86	70.02	45.36	45.46	70.26	68.69	70.12	43.65	44.05
2.5	13	485	57.79	66.89	66.78	35.56	68.21	66.48	68.65	34.59	67.56
3	2.6	97	45.3	44.23	62.12	29.98	43.23	46.78	68.63	40.27	32.56
3	3.9	146	48.5	38.26	62.23	30.15	56.36	61.36	34.65	65.65	35.68
3	5.2	194	52.53	57.96	63.25	35.65	36.98	64.65	41.36	36.78	63.54
3	6.5	243	52.84	62.02	37.45	62.06	36.65	41.03	40.65	65.56	64.56
3	7.8	291	56.24	65.78	41.36	40.36	64.68	67.65	42.88	41.69	68.65
3	10.4	388	56.76	63.78	42.36	66.36	40.84	71.65	39.87	70.65	43.21
3	13	485	58.51	47.56	70.66	34.59	70.15	66.12	66.87	35.12	66.78

Table E–3. Data of the dimensionless group for LLD. (...)

x/D	L	Re	$Sh/Sc^{0.33}$								
	$kgm^{-2}s^{-1}$		CC01	IC02	IC03	IC04	IC05	OC06	OC07	OC08	OC09
3.5	2.6	97	51.29	44.55	59.66	39.75	28.98	49.66	64.35	49.74	28.56
3.5	3.9	146	52.84	49.59	30.15	32.15	63.54	37.8	59.66	63.23	36.59
3.5	5.2	194	53.46	43.35	61.36	38.63	37.86	63.76	63.8	37.88	38.45
3.5	6.5	243	55.21	39.56	63.87	39.89	38.47	65.65	39.68	64.21	40.12
3.5	7.8	291	56.66	42.36	40.36	43.02	67.45	66.58	42.35	42.21	66.48
3.5	10.4	388	56.66	46.36	41.35	40.56	69.91	43.65	67.78	42.15	68.47
3.5	13	485	57.59	38.15	67.66	40.21	64.18	42.69	71.56	42.06	73.69
4	2.6	97	51.6	39.01	33.25	27.78	59.32	44.21	42.96	31.84	64.25
4	3.9	146	53.15	38.22	36.52	59.84	32.62	56.12	62.45	35.24	35.68
4	5.2	194	53.66	34.65	38.09	35.63	62.38	58.66	63.56	37.36	37.65
4	6.5	243	55.73	38.65	38.26	38.12	61.56	38.95	63.54	60.58	37.58
4	7.8	291	56.35	39.65	63.86	38.95	38.02	54.55	39.56	40.25	69.07
4	10.4	388	56.76	40.32	69.65	38.65	37.12	40.02	40.31	59.62	69.34
4	13	485	57.48	41.46	40.37	40.55	67.54	42.15	63.98	40.16	68.33
5	2.6	97	50.36	38.02	55.82	38.29	26.87	43.21	49.23	57.95	28.75
5	3.9	146	52.53	42.33	32.15	33.65	57.33	56.78	35.96	33.65	62.31
5	5.2	194	54.08	35.62	59.88	38.17	35.12	57.88	36.98	62.36	36.78
5	6.5	243	55.01	37.45	38.04	37.45	60.35	59.56	62.35	38.45	38.25
5	7.8	291	56.04	39.04	38.87	38.69	60.09	59.35	38.98	64.56	38.49
5	10.4	388	57.28	40.02	40.16	40.61	59.63	62.36	66.21	38.64	37.56
5	13	485	58.51	40.16	65.02	40.69	40.69	40.08	65.78	40.12	64.12
5.5	2.6	97	51.39	37.88	38.21	59.85	22.56	43.22	60.97	44.84	31.71
5.5	3.9	146	52.73	32.65	34.33	33.65	61.23	38.77	58.26	36.66	54.56
5.5	5.2	194	53.66	35.68	35.24	35.67	58.05	56.36	38.96	39.15	58.32
5.5	6.5	243	54.9	38.01	36.24	57.04	37.21	58.54	38.56	39.21	61.35
5.5	7.8	291	56.55	38.12	38.65	39.68	58.14	63.58	62.58	38.69	35.64
5.5	10.4	388	57.28	59.65	40.66	40.61	42.02	65.23	38.24	37.69	65.31
5.5	13	485	58.41	63.89	40.08	40.06	40.07	65.39	64.56	41.56	41.02